The Nucleation of Crystallisation in Some Fluoride-Containing Silicate Glasses.

A Thesis submitted for
the Degree of Doctor of Philosophy

in the
University of London
by

Peter Edwin Johnson

Department of Metallurgy
Royal School of Mines
Imperial College of Science & Technology.

February 1971.

ABSTRACT.

The kinetics of the nucleation of internal crystallisation in some glasses of the system Na_2O, CaO, Al_2O_3, SiO_2, CaF_2, have been investigated. These investigations have shown that the mechanism of nucleation may be described as a series of reversible first and second order polymerisation reactions from embryo nuclei whose concentration is a function of glass composition and melt conditions. It has also been found that the transition from sub-critical nuclei to critical nuclei may be regarded as a rate determining step, particularly at low and high nucleation temperatures and at long times for all temperatures. The activation energy for this step was found to be similar to that governing viscous flow.

The importance of melt structure and dynamics in determining crystallisatio phenomena is demonstrated. In this respect infra-red spectroscopy provides useful structural information concerning the glasses.

It is inferred that the embryo nuclei are complex silicate of alumino-silicate anions, possibly containing fluorine, the major role of fluorine lying in the reduction of the activation energy for viscous flow and the provision of suitable, easily crystallised molecular fragments, through structural reorganisation of the glass.

Evidence is presented showing that the mineral phase fluor-xonotlite $Ca_6 Si_6 O_{17} F_2$, occurs only in those glasses which display volume crystallisation.

Finally, no relationship was found between the number of droplets of a second glassy phase (glass-in-glass phase separation) and the number of crystallisation centres in these glasses.

Who the hoard's door
with a key's power can unlock,
that guards the riddle against rune-guessers,
holds its heart close, hides it loyally with
cunning bonds?

(The Exeter Book)

Table of Contents

			Page.
Chapter 1.			
	1.1.	Introductory Remarks.	6
	1.2.	The Physico-chemical Behaviour of Fluorine in Silicate Melts.	8
	1.3.	Fluorine Containing Glasses.	10
	1.4.	Rationale for Present Work.	11
		References to Chapter 1.	13
Chapter 2.			
	2.1.	Theoretical Studies.	14
	2.2.	Experimentally Derived Models.	16
	2.3.	Infra-red Spectroscopic Studies of the Vitreous State.	17
	2.4.	Experimental Studies of the Infra-red Spectra of Glasses.	19
	2.5.	Further Possibilities in Infra-red Spectroscopy.	26
		References to Chapter 2.	27
Chapter 3.			
	3.1.	Classical Theory of Nucleation as Applied to Glasses.	29
		Key to Figures 1 and 2.	39
		Figures 1 - 6.	40-43
		References to Chapter 3.	44
Chapter 4.			
	4.1.	Materials.	46
	4.2.	Glass Preparation.	46
	4.3.	Heat Treatment Procedure.	47
	4.4.	Optical Microscopy and Sample Preparation.	48
	4.5.	Counting Procedure.	48

		Page
4.6.	Technique for Electron Microscopy	49
4.7.	Technique for Scanning Electron Microscopy	50
4.8.	Technique for Infra-red Spectroscopy	50
4.9.	Results	50
	Tables 1-5	53
	Key to Figures 7-68	56
	Figures 7-68	60
	References to Chapter 4	101
Chapter 5		
5.1.	Phase Separation and Crystallisation	102
5.2.	The Kinetics of Nucleation	103
5.3.	The Probable Nature of the Nucleus	105
5.4.	Infra-red Spectra	107
5.5.	Thermal History Effects	109
5.6.	Miscellaneous Considerations	110
5.7.	X-ray Diffraction Data	112
	References to Chapter 5	113
Chapter 6		
6.1.	Conclusions	114
6.2.	Suggestions for Further Work	116
	References to Chapter 6	118
	Key to Plates	119
	Plates	121
	Appendix	129
	Acknowledgements	135

Chapter 1

1.1. Introductory Remarks

Since early times when the first tool-making cultures accidently used obsidian nodules for the production of implements, glass, in one form or another, must have been a familiar material to mankind.

The date and place of the discovery of synthetic glass must remain a matter for speculation although it was a recognised product in Egypt by about the middle of the third millennium B.C. However, during this time glass objects were a rarity and obviously regarded and treated as imitations of precious stones. No glass vessels have been found in Egypt earlier than circa 1500 B.C. but, by the mid-fourteenth century B.C., Egyptian factories at El-Amarna, Lisht, Gurob and elsewhere were producing glasses of many kinds and colours. During the second millennium some articles were shaped in clay moulds and cold cutting was common, but, the vast majority of glass vessels were fashioned by dipping a core of sand tied in a cloth bag into a crucible of glass and modelling on a flat stone bench. Decoration was by coloured glass applique or painting.

The materials of the Egyptian glass-makers were quartz-sand, calcium carbonate, natron (native sodium sesquicarbonate) or plant ash, and a typical eighteenth dynasty glass had the following composition 55-65%SiO_2 15-22%Na_2O, 1-3%K_2O,3-10%CaO,3-5%MgO,1-3% Al_2O_3 and 1-3% iron oxides.

The techniques of glass-making were rapidly disseminated and during the succeeding millenia the techniques of cutting, flame-polishing and a form of millefiori decoration were perfected whilst the centre of fine-art glass working shifted from the Nile to Phoenicia and back again. The important technique of glass-blowing was apparently discovered in Syria at the end of the first century B.C. and although mould-blowing was practised at first, free-blowing was soon brought to perfection in Rome. From that time all the important glass-making and working techniques have continued substantially unchanged.

Opaque, opalescent and opal glasses have been known for many centuries. Although many Pre-Roman and Roman opaque glasses are said to be so because of the presence of countless microscopic bubbles, many ancient glasses were quite clear and free from bubbles and materials such as $Pb_2Sb_2O_7$ were deliberately added as opacifiers. Moreover, an X-ray diffraction study of some opaque glasses by Werner and Binson[1] has shown that fluoride opals were being used in China as early as the Tzang period (A.D. 618-707). This use of CaF_2 preceeds its use in the West by several centuries. Such materials were popular in art glassware of the 18th and 19th centuries with factories such as W.H.B. and J. Richardson, Stevens and Williams, and Sowerby's Ellison Glassworks producing beautifully uniform coloured and white opal products, although it is not clear that the glassmakers appreciated any of the special physical properties which we have come to expect of these materials.

However, during this period experiments were being conducted in France and England into the nature of igneous magmas and Chinese porcelain. Réaumur (2,3,4) saw that the secret of Chinese porcelain lay in its being a very fine-grained infusible material in a vitreous matrix. One of the methods which he suggested for acheiving this effect was, in fact, the devitrification of ordinary glass. This topic must have a long history, possibly as long as that of glass itself, because devitrification occurs whenever glass is heated at a dull-red heat for about an hour. Glass-workers in antiquity can scarcely have failed to notice this change and must have dismissed it as a mere peccadillo, for no well documented observation appears until 1763 when Lewis[5] reported that Casper Neumann had attributed the porcelainous appearance of aglass retort used for distilling milk to the action of the milk and heat.

Réaumur produced his porcelain by heating glass packed in refractory powder. By careful control of the heat treatment he was able to produce a fine fibrous ware capable of striking sparks from steel, cutting glass and resistant to attack by acid and alkaline liquors. William Lewis discovered that when Reaumur porcelain

was overannealed the fibrous nature of the material was lost and was replaced by a mass of coarse crystals growing radially from the surface leading to a weak, friable product. Despite the praises of its properties Réaumur porcelain remained obscure and the development of glass-ceramic materials stagnated.

During this century devitrification of glasses has received new attention. This renewed interest has been due to the realisation that controlled devitrification may lead to products combining high mechanical strength and resistance to chemical attack and thermal shock with the refractory properties of more traditional materials. Moreover, such materials would be amenable to the well-proved manufacturing and forming techniques of the glass industry.

In order to obtain such properties as the above it was realised that the surface nucleated devitrification of Réaumur's material was not suitable and that the requisite mechanical strength could only be obtained by inducing internally nucleated crystal growth. To this end many substances have been employed such as colloidal metals, sulphides, metallic oxides and, more peculiar to the study in hand, several inorganic fluorides.

The efficient mineralising action of fluorides in "anhydrous" hydrothermal systems has been appreciated for many years and early work on the opalising action of fluoride additions to glass melts has led to the realisation that herein may lie a route to viable glass-ceramics based on normal commercial glass compositions.

1.2. The physico-chemical behaviour of fluorine in silicate melts.

It seems reasonable to preface a survey of fluoride glasses with a consideration of the small amount of work concerned with the behaviour of fluorine in silicate melts.

In general, there are three effects associated with the addition

of fluorine to silicate melts:

(1) lowering of melt visco ity

(2) depression of freezing point

(3) suppression of glass-forming tendencies on cooling.

Whether these effects are uniquely separable is somewhat open to question but, nevertheless, they form a convenient basis for classification.

P. Kozakevitch[6] has made the distinction between acid and basic melts in connection with these effects. An acid melt is considered to be one in which the ratio of silica to total alkali is greater than one, a basic melt has a ratio of less than one. Kozakevitch found that additions of fluoride to basic melts depressed their freezing points without a marked lowering of viscosity whilst equivalent additions to acid melts resulted in a great reduction in melt viscosity without a decrease in freezing point. These observations are supported by the work of Herty et al, Schwerin, Matsukawa, Shiraishi and Kumar et al[7-12]. Because F^- and O^{2-} have similar radii (1.33Å and 1.32Å) it is argued that fluorine might well substitute for oxygen in the silicate network. Such a substitution would lead to dead-end bonding, breaking up the silicate network. A mechanism of this kind would tend to reduce the size of flow units and consequently the viscosity. It is believed that the commonest structural unit in basic melts is the silicate tetrahedron in an isolated state, it is therefore obvious that the addition of depolymerising agents to such melts cannot cause a reduction in viscosity. Kozakevitch[6] proposes such a mechanism whilst emphasising that fluorine-silicon covalent bonding is not known to occur in the presence of silicon-oxygen bonding. Bockris and Lowe[13] support this argument without, unfortunately, adducing any experimental evidence of their own. Kumar et al[11,12] reported evidence for silicon-fluorine bonding from the infra-red spectra of fluoride containing melts but a subsequent analysis of these results by Mitchell showed that the absorption band so ascribed in fact belonged to a vibrational mode of the $Si_2O_7^{6-}$ ion. Baak and Olander[15] investigated the system CaF_2-$CaSiO_3$ and explained the low viscosity

of the melts by the breaking up of the strong electrostatic forces in the cyclo-trisilicate complex anion $(Si_3O_4)^{6-}$ by ion pairs CaF^+ added to these. Moreover, C. Brisi definitely excluded the existence of calcium fluorosilicates in the partial system $CaSiO_3$-CaF_2[16].

It is thus clear that considerable controversy surrounds this matter although there are considerations which lead to a mechanism somewhere between these two extremes. The properties of fluorine in this respect are not unique and are displayed as well by phosphates[6]. In this case no fortuitous coincidence of ionic sizes can be invoked to provide a mechanism and a more subtle depolymerisation mechanism must be postulated.

1.3. Fluorine Containing Glasses.

"A method as claimed in claims 1 and 2, characterised in that, after the transformation of the mixture of constituent materials into a vitreous fused mass, objects are formed from said mass according to any method and means known in glass technology, and these objects are, after solidification by cooling, subjected to the heat treatment giving rise to the crystallisation". This quote from a successful patent application for a fluoride glass-ceramic[17] establishes succinctly the reason for research in this field. There have been several investigations into glasses containing fluorides in the system SiO_2, Al_2O_3, RO, R_2O but there seem to be as many explanations for the phenomena observed as there are investigators.

Silvestrovich and Rabinovich[18] and Vaisfeld and Rabinovich[19] observed opalescence in the above glasses which was ascribed to crystals of alkaline and alkaline earth fluorides and to glass-in-glass phase separation. These observations are confirmed to some extent by the work of Banerjee[20] in the system NaF-SiO_2-Na_2O wherein the presence of alkali-fluoride crystals was established by x-ray diffraction methods. Rothwell[21] also discovered simple fluoride phases as the opacifier in simple ternary glass systems. However, Lungu and Popescu-Has[22,23]

failed to observe these simple fluorides when working in more complex glasses but found instead an x-ray diffraction pattern indicative of a mica-like structure. These investigators also observed the kinetics of crystallisation of these glasses, finding complex kinetics comprising an induction period, a period of linear growth, and an asymptotic approach to some limiting value. They concluded that the process involves the initial precipitation of a fluoride or oxyfluoride lattice which serves as a nucleus for the growth of crystals increasingly free of fluorine, the original lattice decomposing as this process proceeds. Vogel and Rehfeld[24] discovered that the addition of small amounts of fluorine to glasses in the system Na_2O-SiO_2 increased the tendency towards micro-heterogeneity and imply that subsequent crystallisation may be catalysed at the droplet-matrix interface thus produced. Lyng[25] investigating crystallisation of glasses in the system Na_2O-CaO-MgO-Al_2O_3-SiO_2, discovered that at least 3wt% of fluoride was required to induce volume nucleation. By a combination of electron-microscopy and x-ray diffraction techniques Lyng discovered that the crystallisation process involves the formation of a suspended phase, high in fluoride, which crystallises to a simple or complex fluoride. This is followed by further crystallisation of various silicates, mostly fluorine analogues of hydrous layer minerals. Furthermore all the glasses investigated displayed a microheterogeneous structure independent of fluorine content. Mukherjee and Rogers[26] studied these phenomena in the system Na_2O,CaO,Al_2O_3,SiO_2 and found that the rate and number of nuclei formed depended on the fluorine content of the glass. They also observed that fluorine promotes the formation of a secondary glassy phase which they concluded was the rate-controlling process. However, it is admitted here and in a further paper[27] that there is a great disparity between the volume distribution of droplets in this metastable liquid/liquid phase separation and the eventual number of crystal growth centres.

1.4. Rationale for Present Work

The work to hand is an extension of the studies of Mukherjee and Rogers[26] into the nucleation processes involved in the crystallisation of fluorine containing silicate glasses. It is necessary to establish the validity of the standard equations

of nucleation kinetics (vide infra) in the above connection, Rogers[27] has intimated some doubt as to their applicability in glasses. It is further necessary to establish the relationship (if any) of metastable phase separation to subsequent crystallisation behaviour and/or to establish a mechanism for the processes preceeding observable crystallisation.

In general it is known that the processes of nucleation and growth can be separated according to their respective efficiency at a particular temperature. Tammann[28] showed that the nucleation step is more efficient than crystal growth at some temperature below the temperature for maximum crystal growth. It is clear then, that the kinetics of nucleation may be followed by forming nuclei at a low temperature and growing them to observable dimensions by subsequent heat treatment at a higher temperature. This is the technique which will be adopted to establish the kinetics of the transformation. It is hoped that structural information of the process may be obtained through techniques to be described (vide infra) and by investigating the kinetic effects of glass composition through varying the proportions of the various batch components.

References to Chapter 1

(1) A.E. Werner, M. Binson, 'Advances in Glass Technology', 2, 303-5, New York (1963).

(2) R.A.F. de Réaumur, Mem.Acad.Sci., 165-203, (1727).

(3) R.A.F. de Réaumur, Mem.Acad.Sci., 325-44, (1729).

(4) R.A.F. de Réaumur, Mem.Acad.Sci., 370-88, (1739).

(5) W. Lewis, Commercium Philosophico-Techicum, London (1763).

(6) P. Kozakevitch, Rev.Met., 51, 559-587, (1954).

(7) C.H. Herty, F.A. Hartgon, G.L. Frear, M.B. Royer, U.S. Bur.Mines,(Rept. Investigation 3232),(1934).

(8) L. Schwerin, Metals and Alloys, 5, 61,118, (1934).

(9) T.Matsukawa, Suiyokai-Shi, 8, 245, (1933).

(10) Y. Shiraishi, T. Saito, Nippon Kinzoku Gakkaishi, 29, (6), 614-22,(1965).

(11) D. Kumar, R.G.Ward, D.J. Williams, Disc.Far.Soc. 32, 147, (1961).

(12) D. Kumar, R.G.Ward, D.J. Williams, Trans,Far.Soc., 61, 1850, (1966).

(13) J.O'M Bockris, D.C. Lowe, Proc.Roy.Soc., A. 226, 423-35, (1954).

(14) A. Mitchell, Trans,Far.Soc., 63, 1408-17, (1966).

(15) Tr.Baak, A. Olander, Acta.Chem.Scand., 9, 1350, (1955).

(16) C.Brisi, J.Am. Chem.Soc., 40, 174, (1957).

(17) St.N. Lungu, D. Popescu-Has, Pat.No.848, 447. (1960).

(18) S.I. Silvestrovich, E.M. Rabinovich, Zhur.Prik.Khim., 32, 1690, (1959).

(19) N.M. Vaisfeld, E.M. Rabinovich, Zhur.Prik.Khim., 35, 2393, (1962).

(20) B.K. Banerjee, Proc.Nat.Inst.Sci.India, 25A, 155, (1959).

(21) G. Rothwell, J.Am.Ceram.Soc. 39, 407, (1956).

(22) St. N. Lungu, D. Popescu-Has, Industria Usoara, 5, 63, (1958).

(23) St. N. Lungu, D. Popescu-Has, Silicates Industriels, 22, 391, (1958).

(24) W. Vogel, R. Rehfeld, Z.Chem., 7, 24, (1967).

(25) S. Lyng, Glass Technology, 9, 179, (1968).

(26) S.P. Mukherjee, P.S. Rogers, Phys.Chem.Glasses, 8, 81, (1967).

(27) P.S. Rogers, Min.Mag., 37, 741, (1970).

(28) G. Tammann, The States of Aggregation, (1926).

Chapter 2

Theoretical and Experimental Aspects of the Structure of Glasses and Melts.

2.1. Theoretical Studies

Although, in the past, extreme stances were adopted by workers seeking to describe the structure of glasses, as witnessed by the mutually exclusive network, crystallite and vitron theories[1-3], the consensus of opinion now occupies a comfortable middle ground. This "tempering the wind to the shorn lamb" has been occasioned by a more sceptical examination of the conclusions drawn from Warren's[4] x-ray diffraction studies, and the appreciation that a glass is a supercooled liquid. This latter realisation leads to the conclusion that those structural elements identified or postulated in the liquid state may persist in the glass to which this melt was the precursor.

The investigations into the structures of silicate melts divide, conveniently, into a priori and a posteriori approaches, both leading to much the same conclusions. It would be well to consider the a priori approaches prior to the experimentally derived models. Lacy[5] established a purely statistical model of polymerisation and depolymerisation in silicate melts by considering the mathematical probability that any particular silicon atom is surrounded by so many bridged and non-bridged oxygen atoms. Unfortunately, this approach does not admit of any dependence of structure on temperature and seems to become extremely involved for even a simple binary mixture.

Following a suggestion by Richardson[6] that the liquid silicates may contain an array of ions the distribution of which is governed by considerations of chemical equilibria, Toop and Samis[7] expressed the distribution in terms of an equilibrium constant involving singly bonded and doubly bonded oxygen atoms and free oxygen

ions. By limiting the discussion to basic melts Masson[8] extended this work to enable specific conclusions to be drawn concerning the concentrations of polyionic species. By considering equilibria containing the SiO_4^{4-} ion as follows

$$SiO_4^{4-} + SiO_4^{4-} \rightleftharpoons Si_2O_7^{6-} + O^{2-} \qquad (K_{1.1})$$

$$SiO_4^{4-} + Si_2O_7^{6-} \rightleftharpoons Si_3O_{10}^{8-} + O^{2-} \qquad (K_{1.2})$$

etc.

and making the assumption that the ion fraction of a silicate ion may be equated with its activity Masson was able to express the mole fraction of the species present as

$$N_{(Si_2O_7^{6-})} = \frac{K_{1.1} N_{(SiO_4^{4-})} \cdot N_{(SiO_4^{4-})}}{N_{(O^{2-})}} \quad \text{etc.}$$

Such an approach leads to the calculation of metal oxide activities in binary systems which are in good agreement with experiment. This approach is extended by adopting the formalism of polymer distribution studies embodying a stochastic treatment similar to that of Lacy[5]. The results of these calculations are also in good agreement with experiment[9,10,11]. However, this theory is only valid for binary melts in the basic region although it embodies features which would admit of further development albeit at some cost in computational effort.

These ideas lead, quite naturally, to the suggestion[12] that a silicate glass may be considered as a collection of polysilicates held together by van der Waals forces. These aggregate to form different sizes and types of polysilicic acids (or salts) according to the thermal history of the glass. The consequences of such ideas will be discussed later.

2.2. Experimentally Derived Models.

Techniques for the direct examination of polymeric distributions in silicates by chromatographic separations are only recently available[13] and have yet to be applied in a systematic way, but these techniques have already provided useful information about the more easily fractionated phosphates[14]. It has thus been experimentally established that the concentrations of phosphate ions may be related to one another by equilibrium products whose values are nearly independent of composition.

The greatest amount of information concerning melt structures has been obtained by classical studies of viscous flow and electrical conduction. When combined with thermodynamic data the results of these investigations confirm that the melts are ionic with small cations conferring electrical conduction and large anions determining viscosity. An extensive series of papers by Bockris and co-workers illustrate the methods and conclusions involved[15-21], and provide the most exhaustive collection of data in this field. The distribution of anions as a function of composition may be summarised as follows[22].

Composition.	Dominant Anions.
From 66% to 50% M_xO_y	Polymerisation of SiO_4^{4-} anions to $(O_3Si\text{-}O\text{-}SiO_3)^{6-}$ anions and chains.
At about 50% M_xO_y	Ring formation occurs due to the increase in chain length $(SiO_3)_3^{6-}$ and $(SiO_3)^{5-}$ rings.
From 50% to 33% M_xO_y	Larger ring anions are formed.
At about 33% M_xO_y	$(Si_6O_{15})^{6-}$ and $(Si_8O_{20})^{8-}$ anions dominate.
M_xO_y reduced below 33%	Further ring polymerisation occurs.

It should be understood that these species are the dominant anions in an idealised model. A short review of these topics has been prepared by Knapp[23].

If as shown above, the structure of melts and glasses are determined by ionic equilibria a mechanism for the reduction of viscosity by the addition of certain materials, notably fluorides, is suggested. In equilibria such as

$$SiO_4^{4-} + SiO_4^{4-} \rightleftarrows Si_2O_7^{6-} + O^{2-}$$

it is clear that the ionicity of the melt with respect to silicon decreases as the reaction proceeds from left to right, in that the proportion of ionic charge per silicon atom in the anion decreases. It is a well established principle of organic reaction kinetics that an increase in the dielectric constant of the medium will favour the production of more highly charged species. The introduction of a metallic fluoride or similar substance would tend to increase the ionicity of the medium and hence the dielectric constant. This would favour the production of smaller anions and would result in a reduced viscosity without the need for direct nucleophilic attack on the silicon atoms. The influence of metal oxides can also be explained in this way, for, by the Law of Mass Action, an equilibrium described by

$$K = \frac{[N_{(SiO_4^{4-})}]^2}{N_{(O^{2-})} N_{(Si_2O_7^{6-})}}$$

must be displaced so that the increase in $N_{O^{2-}}$ is matched by a decrease in $N_{Si_2O_7^{6-}}$ and an increase in $N_{SiO_4^{4-}}$.

2.3 Infra-red spectroscopic studies of the vitreous state.

A rational interpretation of the properties of solid substances is hardly possible without a knowledge of their structure on a molecular scale. The classical technique for such studies is x-ray crystallography which has a long history in this context.

On the other hand infra-red spectroscopy has registered numerous successes in different fields of physical chemistry in a fundamentally different way to x-ray crystallography. The x-ray pattern of a crystalline solid is determined primarily by the existence of a regular lattice of molecules, whilst the shape of the infra-red spectrum of the same solid is determined by the masses of its atoms, the interatomic forces and molecular geometry. Furthermore, x-ray crystallography is insensitive to isomorphous substitution involving atoms of similar ionic radii and atomic numbers which produce substantial alteration of the infra-red spectra. It is obvious from these considerations that, in principle at least, infra-red spectroscopy is capable of supplying structural information concerning glasses which is not available through other, more traditional techniques.

The cations occurring in inorganic glass systems are generally classified in three types.

1/ Network formers (e.g. Si,B,Ge,As) whose oxides have the capacity to form stable glasses on their own.

2/ Network modifiers (Ca,Sr,Ba,Na,K) whose oxides are susceptible to reaction with the network formers, modifying the properties of the glasses formed by these in a more or less profound manner, these changes generally corresponding to a weakening of the network.

3/ Intermediate oxides (Al,Te,Ti,Mg) which are incapable of forming a glass on their own, but which are capable of entering isomorphically into the glass structure network.

Because infra-red spectra depend primarily upon nearest-neighbour interactions, studies in this field should, in principle, be capable of establishing the local structure of glasses. Unfortunately, however, much controversy still attaches to the theory of the lattice dynamics of molecular crystals and the theory for simple ionic lattices is still in a parlous state. Thus it can be seen that, in the absence of a reliable theory of the lattice dynamics of glasses, no a priori predictions of the effects of various glass constituents can be made. It is perhaps possible that a closer examination of the spectra of simple glasses and the comparison of these with the

spectra of crystalline compounds of a similar nature may lead to some clues as to the basis of a sound theoretical treatment of the vibrational spectra of glasses. If the characteristic group frequencies for various silicate structures can be determined it may be possible to interpret the spectra in terms of mathematical distributions of these frequencies and hence give structural information in accord with modern theories of glass structure.

2.4. Experimental studies of the infra-red spectra of glasses.

The studies that have been made can be broadly classified under three headings.

(1) Comparative studies of the infra-red spectra of materials corresponding to definite chemical compositions in both the crystalline and vitreous states. One of the objectives of such research is to see whether or not the transition from the crystalline to the vitreous state is accompanied by the retention of parts of the original structure.

(2) Studies of the tetrahedral coordination of certain elements which can behave as both network formers and modifiers.

(3) Studies of the distributions of network formers in glasses containing several such elements.

2.41. The Structure of a glass corresponding to a definite chemical composition.

a) SiO_2 and GeO_2.

Vitreous silica has been extensively studied[20,28] and the authors agree on several points.

(i) One can find in the spectra of vitreous silica the same bonds that are common to the diverse varieties of crystalline silicates.

(ii) The width of these bands is not great which indicates a relatively well ordered structure.

These results suggest a strong analogy between the structure of vitreous silica and the crystalline forms of silica. The findings of Florinskaya in this field[29] diverge a little from the generally accepted ideas. According to this author, the infra-red spectra of vitreous silica sometimes give rise to fine details from which it is possible to prove the existence of crystallites of quartz, tridymite or cristobalite. However, certain of these details are represented by variations of transmission of less than 1% which are not reproducible and which have not been found by other investigators working with a resolution at least equal to that used by Florinskaya. However, it can be shown that when quartz is heated to a temperature slightly higher than its melting point, the liquid obtained shows spectra similar to quartz, and these fragments of structure are capable of lasting for a relatively long time and at temperatures higher than the melting point. Germania shows great similarities to SiO_2[26,27].

The theoretical treatments of such spectra have generally been undertaken in terms of the spectra of crystalline silicates[29,33]. All of these have attempted the interpretation by considering the basic SiO_4 tetrahedron as a free entity. Wadia and Balloomal[28] have attempted to introduce refinements of the SiO_4 unit linked to fixed walls. All such treatments have met with a certain amount of success, but, the absence of any really good agreement between theory and observation necessarily restricts the utility of such treatments.

b) Layer and chain structures.

The case of vitreous silica is probably the most simple to be encountered. For layer and chain silicates however, the intervention of a positive ion such as K^+, Na^+ or Ca^{2+} complicates the problem by making several different kinds of structures possible. In such a case one must enquire as to whether the fundamental elements of the crystalline sturcture are preserved in the vitreous state. Zarzycki and Naudin[27] have attempted to answer this question by comparing the spectra of a series of simple glasses with the theoretical spectra

derived from the theory of Stepanov and Prima[33]. This theory does not take account of torsional vibrations and is thereby limited to the region of fundamental frequencies (1200-900 cm^{-1}) which are more or less independent of deformation vibrations. In the case of disilicates $X_2Si_2O_5$ and digermanates $X_2Ge_2O_5$ (X = Li,Na,K,Rb,Cs) in the vitreous state, the agreement between theoretical and observed spectra is relatively satisfactory, and it seems that remnants of the characteristic sheets of the crystals persist in the corresponding glass.

The case of metasilicates and metagermanates is less clear for a number of reasons: the theoretical spectra are more complex than for disilicates; the observed bands are much more broad and, finally, the samples used contained a fair amount of carbonate which gave rise to spurious bands. The results in this case, whilst not excluding the presence of silicate chains, are ambiguous and are thus not capable of deciding the problem either way.

c) Other structures.

The case of alkali polysilicates is relatively simple. The alkali metal ions with their small charge and large atomic radii (apart from Li) produce a small electrostatic field and therefore do not greatly perturb the structure and vibrational frequencies of the silicate skeleton. This approximation, however, is probably insufficient when dealing with glasses containing more strongly polarising ions.

Experimental studies concerning this aspect of the problem are sadly lacking for the vitreous state; but such experimental studies that have been undertaken for crystalline compounds seem to confirm this point of view. In $MnSiO_3$ it is possible to replace nearly 25% of the Mn by Ca without changing the crystal structure[34] or the chain structure of the SiO_4 tetrahedra. Nevertheless such substitution leads to relatively important changes in the infra-red spectrum although the crystal structure remains the same; therefore, these changes must be due to a specific cation effect.

Because the theory does not take into account the interactions

due to the cations, the comparisons between theory and observation lo se much of their meaning when applied to cations other than the alkali metals. In even more complex silicate structures the passage from the crystalline to the vitreous state is accompanied by far more profound changes in the spectra and hence in the structural elements.

In conclusion the published results show that the structures of different glasses cannot be represented by a universal structure theory. For very simple glasses such as SiO_2 & $Na_2Si_2O_5$ the transition from the crystal to the glass preserves certain aspects of the crystal spectra and, from this it can be deduced that the glasses so formed are in the same way analogous to the crystals from which they arose. On the other hand the passage from the crystal to glass for more complex silicates is accompanied by a more or less profound change in structure. Even if such a glass contains certain ordered regions, the disposition of the atoms in these regions is very probably different to that in the crystal. As stated earlier, the structure of a glass is better related to the melt from which it came than to the compounds which its stoichiometry suggests, and it is in this light that an approach to interpretation should be undertaken.

1.4.2. Studies of the tetrahedral coordination of certain elements which can behave as both network formers and modifiers.

a. General Considerations.

The cation-oxygen vibrational frequencies of a coordinated group AO_n depend on the co-ordination number n of the cation, and several authors have applied this relation to the determination of cation co-ordination in glasses. However, these studies have generally been restricted to the so-called glass forming cations (B, Si, Ge), [34,25,36] and much less attention has been paid to the network modifiers. The infra-red spectra of solids of the type $A_xB_yO_z$ can sometimes be considered as the result of the vibrations of AO_p and BO_r co-ordinated groups. In general, however, a given oxygen atom is bonded to both A and B atoms, and thus there must be some interaction between the vibrations of the AO_p and BO_r groups. Strictly speaking, the vibrations are those of the whole unit cell, but in most cases a rigorous treatment is unthinkable because of the mathematical complexity of

such a treatment. If, however, vibrational interactions between AO_p and BO_r groups are negligible or weak, it is possible to assign the bands to either AO_p or BO_r groups, which are thus considered as vibrating independently. This concept of separate or independent group vibrations was put forward by Tarte[37], who found it to be fundamentally correct in a number of cases when the vibrational frequencies of the AO_p and BO_r groups are very different[38,39]. However, he also discovered that matters were complicated when some of the vibrational frequencies had similar values: in some cases the concept of separate vibrations was still found to be valid; in others severe vibrational interactions were observed, thus preventing the assignment of the bands to a definite coordinated group.

The factors influencing the vibrational frequencies of a coordinated group AO_n to which the above concept may be applied have been found to be:-

The chemical nature and the valency state of the cation A, the value of the coordination number n, the "isolated" or "condensed" state of the coordinated groups. The first factor requires no comment apart from the fact that highly ionic bonds have no specific infra-red frequencies and cannot be studied by these methods.

The influence of the coordination number n has first been observed with typical network formers such as boron and germanium [35,26,36] and with a few intermediate elements such as aluminium [40,41,42] the vibrational frequencies being higher the smaller the coordination number. This effect has been observed for a fairly large number of cations $\{Fe^{II}, Ca, Mg, Zn, Co, Ni, Fe^{III}, Li\}$[40,41] and so it seems that this variation of the vibrational frequencies with coordination number is quite general.

The relation between vibrational frequencies and coordination number is only an approximate one, first because there is always a more or less important influence of neighbouring groups and also because of a additional effect, namely the isolated or condensed nature of the coordinated groups under consideration.

This effect is well known in silicates (in orthosilicates with isolated SiO_4 tetrahedra, the strongest bands are generally observed near 900-950 cm^{-1}, in polysilicates with condensed tetrahedra, this absorption is extended to much higher frequencies, 1100 cm^{-1}).

The extension towards higher frequencies observed with condensed groups is particularly important for octahedral coordination and, for certain cations at least, there is some overlapping of the absorption ranges of isolated tetrahedra and condensed octahedra. Experimental studies on a number of different structures[39] have shown that, except for some cases of severe vibrational interactions, the frequencies of a given coordinated group are generally observed in a limited spectral range which is not too broad and may be considered as typical for the group under consideration. Moreover, the characteristic ranges for four-fold and six-fold coordination for a given cation seldom overlap. This latter is an essential condition for the applicability of these data to the determination of coordination numbers.

b. Application to Vitreous Systems.

The experimental determination of a characteristic frequency range is carried out on crystalline compounds of known structure. The transferability of these data to vitreous systems is generally taken for granted. However, certain considerations should be taken into account. The characteristic frequencies apply to coordinated groups in widely different environments and so it seems plausible to extend them to glassy systems. This however, is only valid in the absence of important vibrational couplings which can be checked for in crystals but not in glasses. Furthermore, the broadness of the infrared bands in glassy substances may prevent reliable assignments, particularly if two or more bands are superimposed in the same spectral range and blended into an ill-defined absorption.

c. Experimental studies on some glass systems.

Alumina-silica glasses have been found to have a moderately

strong band near 800-700 cm^{-1} [43,44]. This has been assigned to AlO_4 tetrahedra in agreement with other experimental data from molar refractivity and x-ray fluorescence studies [44,45]. The spectra further suggest that AlO_6 octahedra are missing or in fairly low concentration.

Much the same effect has been observed for magnesia-silica glasses where the change from a Na_2O-SiO_2 glass to a Na_2O-MgO-SiO_2 glass is characterised by the appearance of a diffuse absorption in the 600-550cm^{-1} range. Zinc-silica glasses are unfavourable for this kind of study because ZnO_4 tetrahedra absorb mainly in the 500-540 cm^{-1} range which is also the position of the most persistent of all bands in silica glasses. Titanium-silica glasses and crystalline solids have also been studied [46-49] together with lithia glasses.

From this it can be seen that infra-red spectroscopy is able to give direct, unequivocal proof of the structural role of certain cations in glasses where these are tetrahedrally coordinated. However, the detection of octahedral coordination in glasses is not easy for several reasons:-

(i) The characteristic frequency range is not so well defined as in the case of tetrahedral coordination.

(ii) These vibrations generally occur in the low frequency range which is difficult to study for instrumental reasons.

(iii) The bands corresponding to six-fold coordination have a fairly ionic character which means that their absorption bands will be fairly diffuse.

2.3. Studies of the distributions of network formers in glasses containing more than one network former.

Two a priori possibilities concerning this can be envisaged. In the first the network formers are distributed through the glass in a statistically random fashion, in the second the network formers are gathered in "micelles" containing only one kind of ion. From the point of view of infra-red studies the first case would lead to a

much greater dispersion of fundamental frequencies than the second because of the range of mixed vibrations of the type X-O-Y. Of the glasses containing several network formers only borosilicate glasses have been studied from a structural point of view. It is well established that such glasses exhibit a marked tendency towards phase separation which is easily demonstrated with the aid of the electron microscope[50]. Comparison of the spectra of such glasses with comparable, monophase glasses indicate that mixed vibrations do not occur. However, it has been demonstrated[51] that the diffuse bonds in high titanium glasses may be due to depolymerisation occasioned by the titanium rather than mixed vibrations. It is clear that infra-red spectra alone are incapable of supplying definitive evidence for phase separation.

2.5. Further possibilities in infra-red spectroscopy.

It has been suggested above that, with care, the infra-red spectra of glasses may be interpreted in the light of theories concerning the structure of melts. If a sufficient number of silicate minerals were studied it should be possible to establish a set of group vibrational frequencies for the various structures involved in the same manner as that adopted for the infra-red investigation of organic materials. If proper care is exercised in the preparation of specimens and execution of measurements a great deal of information can be extracted from the spectrum of a mineral. However, the bands in some minerals and in all glasses are difficult to observe using standard instruments. Furthermore, the maximum absorption of any particular band does not give a measure of the concentration of that resonating species for the intensity of such a band depends rather on the transition probability for such a resonance. The true measure of the concentration is given by the area under the curve minus certain corrections associated with background absorbances. It is suggested that great improvements may be effected in the study of silicate minerals through the technique of derivative infra-red spectroscopy[52,53] which permits the resolution of overlapping bands and an accurate measurement of optical density, facilitating the identification of polymeric species in the glass and the establishment of their proportions, one to another.

References to Chapter 2

(1) W.H. Zachariasen, J.Am.Chem.Soc., 54, 3841, (1932).

(2) J.T. Randall, H.P. Rooksby, B.S.Cooper, Z.Krist., 75, 196, (1930).

(3) L.W. Tilton, J.Res.Nat.Bur.Stand., 59, 139, (1957).

(4) B. Warren, Zts.Krist., 86, 349, (1933)., 89, 481, (1934).

(5) E.D. Lacy, Phys. Chem, Glasses, 6, 171, (1965).

(6) F.D. Richardson, 'The Vitreous State' p.63, Glass Delegacy of the University of Sheffield, (1955).

(7) G.W. Toop, C.S. Samis, Trans.Met.Soc. A.I.M.E., 224, 878, (1962).

(8) C.R. Masson, Proc.Roy.Soc., A287, 201, (1965).

(9) S.G. Whiteway, I.B. Smith, C.R. Masson, Can.J.Chem., 48, 33, (1970).

(10) S.G. Whiteway, I.B. Smith, C.R. Masson, Can.J. Chem., 48, 201, (1970).

(11) S.G. Whiteway, I.B. Smith, C.R. Masson, Can.J. Chem., 48, 1456, (1970).

(12) P. Beyersdorfer, Glass-Email-Keramo-Tech., 20, 417, (1969).

(13) F.F.H. Wu, J. Chromatog., 48, 515, (1970).

(14) A.E.R. Westman, P.A. Gartaganis, J.Am.Ceram.Soc., 40, 293, (1957).

(15) J.O'M. Bockris, J.A. Kitchener, S.Ignatowicz, J.W. Tomlinson, Trans. Far.Soc., 48, 75, (1952).

(16) J.O'M. Bockris, D.C. Lowe, Proc.Roy.Soc., 226A, 423, (1954).

(17) J.O'M. Bockris, J.A. Kitchener, S. Ignatowicz, J.W. Tomlinson, Disc. Far.Soc., 4, 265, (1948).

(18) J.O'M.Bockris, J.W. Tomlinson, J.L. White, Trans.Far.Soc., 52, 299, (1956).

(19) J.O'M.Bockris, J.A. Kitchener, A.E. Davies, Trans.Far.Soc., 48, 536, (1952).

(20) J.O'M.Bockris, J.A. Kitchener, J.D. Mackenzie, Trans.Far.Soc., 51, 173, (1955).

(21) J.O'M.Bockris, D.C. Lowe, J.Sci.Instr., 30, 403, (1953).

(22) H. Bloom, J.O'M. Bockris, 'Fused Salts', p.53, B.R. Sundheim Ed., New York (1964).

(23) W.J. Knapp, 'Topics in High Temperature Chemistry', (1961).

(24) I. Simon, H. McMahon, J.Chem.Phys., 21, 23, (1953).

(25) J. Reitzel, J.Chem. Phys. 23, 2407, (1955).

(26) E. Lippincott et al., J.Res.Nat. Bur. Standards, 61, 61, (1958).

(27) J. Zarzycki, F. Naudin, Verres et Refract., No. 3, (1960).

(28) W. Wadia, L.S.Balloomal, Phys.Chem.Glasses, 9, 115, (1968).

(29) V. Florinskaya, R. Pechenkina, 'Structure of Glass', p55, Symposium (1953).

(30) F. Matossi, J.Chem.Phys., 17, 679, (1949).

(31)B.D. Saksena,Proc.Indian Acad.Sci., 12, 93, (1940).

(32) J. Barriol, J.Phys.Radium, 7, 209, (1946).

(33) B.J. Stepanov, A.N. Prima, Optika. Spektrosk, 47, 34, (1958).

(34) F. Liebau, M. Sprung, E. Thilo,J.Am. Ceram.Soc., 41, 78, (1959).

(35) S. Anderson et al., J.Am. Ceram.Soc., 38, 370, (1955).

(36) F. Dachille, R. Roy, Z.Krist, 111, 462, (1959).

(37) P. Tarte, Spectrochim Acta., 18, 467, (1962).

(38) P. Tarte, Silicates Industriels, 28, 345, (1963).

(39) P. Tarte, 'These d'Aggregation de I'Enseignment Superieur', Leige (1965).
(40) P. Tarte, Silicates Industriels, 25, 171, (1960).
(41) P. Tarte, Nature, 191, 1002, (1961).
(42) V.A. Kolesova, Opt.i. Spektrosk., 6, 38, (1959).
(43) V.A. Kolesova, ' The Structure of Glass' Symposium (1953).
(44) D.E. Day, G.E. Rindone, J.Am. Ceram.Soc., 45, 489, (1962).
(45) D.E. Day, G.E. Rindone, J.Am. Ceram.Soc., 45, 579, (1962).
(46) M.D. Beals, J.H. Strimple, Glass.Ind, 44, 495, (1963).
(47) J.A. Bland, Acta. Cryst., 14, 875, (1961).
(48) H. Trap, J. Stevels, Phys.Chem. Glasses, 1, 181, (1960).
(49) P. Tarte, Spectrochim.Acta., 20, 238, (1964).
(50) W. Vogel, Glastech. Ber., 31, 15, (1958).
(51) P. Tarte, Spectrochim.Acta., 19, 59, (1963).
(52) G.L. Collier, F. Singleton, J.Appl.Chem., 6, 495, (1956).
(53) A.E. Martin, Conf. of European Mol.Spec.Group, Oxford, (1955).
(54) A.E. Martin, Nature, 180, 231, (1957).

Chapter 3

Nucleation Theory

3.1. Some aspects of homogeneous nucleation theory

It has been stated earlier that a glass may be considered, in many ways, as a supercooled liquid. This is true insofar that the structure of a glass would appear to be closer to that of a liquid than a crystalline solid, and no structural changes have been observed in association with the glass transition. However, glasses show important thermodynamic deviations from the behaviour of crystalline solids, liquids and supercooled liquids.

A phase transformation from the liquid to the solid is accompanied by an abrupt change in enthalpy and associated properties. This is referred to as a first order phase transformation. When foreign bodies are excluded, most liquids may be cooled below their characteristic freezing points. This supercooling is not accompanied by any abrupt changes in the trends of thermodynamic properties as functions of temperature. Liquids which are highly viscous at their freezing points, when supercooled, exhibit a change in the trend of their thermodynamic functions, which, although abrupt, is not so sharp as that associated with a standard phase transformation In complex liquids this takes place over a characteristic range of temperature rather that at a singular point. The region of temperature in which this occurs is rather loosely called the glass transition temperature, T_g. Williams, Landel and Ferry [1] have explained this phenomenon in terms of a free volume theory, the free volume becoming a very small characteristic volume at or very near the glass transition temperature. When this happens the motion of the atoms or molecules is no longer translational in a free volume as in a liquid, but vibrational as in a crystal, whilst the orientational entropy is still characteristic of a liquid-type structure. Because of this, relaxation times for the motions of molecules in a glass become much longer than the duration of most experiments, and phase transformations proceed very slowly. Some idea of this may be obtained by considering the existence of natural glasses whose ages are measured in millions of years.

Thus, although a glass is energetically unstable with respect to a crystal of the same composition and at the same temperature, it would appear that this metastability can be maintained indefinitely under the appropriate conditions of ambient temperature.

According to the formalism of classical thermodynamics the problem of precipitating a new phase may be approached in the following manner [2]:-

Consider the free energy of a system at constant temperature composed of a liquid phase of a substance plus a crystal of that substance. It is well known that, under conditions of supercooling, a plot of the free energy of the total system against crystal size will show a maximum at some value

of the crystal size (the critical nucleus). From a thermodynamic standpoint, crystals smaller than this are unstable with respect to dissolution, whilst for crystals larger than this critical size, the fluid phase surrounding them is unstable with respect to freezing. An analogous situation arises for the condensation of gaseous fluids.

However, it was recognised [3] that the metastability of a supersaturated phase is also a question of kinetics. This idea was pursued by Szilard [4] and Farkas [5] who arrived at a detailed Kinetic mechanism of homogeneous nucleation in vapours which has served as a basis of all subsequent developments.

The mechanism involves a series of reversible additions of single molecules m, to m_i embryos which contain i molecules. This may be represented by:-

$$\left.\begin{array}{l} m + m \rightleftharpoons m_2 \\ m_2 + m \rightleftharpoons m_3 \\ \cdots\cdots \\ m_i + m \rightleftharpoons m_{i+1} \end{array}\right\} \quad [1]$$

Other processes, such as the formation of a large embryo by the collision and union of two smaller embryos, or the fission of a large embryo, or the simultaneous aggregation of single molecules, are excluded as being too infrequent.

According to the conditions for the mechanical equilibrium of a surface, there is a critical droplet size, m_k, which is in unstable equilibrium with the medium. This is the critical nucleus, the formation of which constitutes the bottleneck to the phase change.

By imagining some mechanism which removes droplets above a certain size and returns them as single molecules, Volmer [6,7], Becker and Döring [8] and other workers [9,10,11,12] were able to apply standard thermodynamic techniques to the resulting steady state, and derive the classical nucleation theory.

These results were extended to single component condensed phases by Turnbull and Fisher [13] who derived for the steady-state nucleation rate, I,

$$I = n^* \left(\frac{4}{9} \frac{r^{*2} \sigma}{kT}\right) n \nu_o \exp - \left(\frac{\Delta G_a + W^*}{kT}\right) \quad [2]$$

ΔG_a is the activation energy for transport across the nucleus-liquid interface

W^* is the minimum work required to form a critical nucleus

r^* is the radius of a critical nucleus

n is the number of atoms or molecules per unit volume of the precipitating phase

n^* is the number of surface atoms of a critical nucleus

σ is the interfacial energy between the particle and the homogeneous medium

ν_o is the fundamental jump frequency

T is the temperature in degrees Kelvin

k is the Boltzmann's constant.

3.2. Criticism of the Classical Theory and its Application to Some Glass

Fundamental objections to the classical theories have been raised by several authors, notably Reiss [14], and Lothe and Pound [15]. These question the validity of extrapolating macroscopic thermodynamic properties such as surface tension and volume free energy to small clusters. These criticisms have been justified by modern calculations of the properties of small clusters, involving the determination of all the vibrational modes of the atoms in the clusters. These calculations, which can only be accomplished by the use of a digital computer, have shown that small assemblages of atoms are qualitatively unlike bulk crystals [16].

The classical theory is relatively insensitive to the structure of the liquid phase in question, in that it takes no account of the probable existence of more or less stable clusters in the liquid, which may persist over wide ranges of temperature. Instead it assumes that such clusters are formed by chance association. The probability of this is said to increase markedly with increased supercooling, but in general, the fluid phase is assumed to consist overwhelmingly of non-associated molecules. However, it has been shown [17] that, even very simple liquids, (such as liquid argon), may contain fairly large numbers of close-packed quasi-crystalline structures outside their homogeneous nucleation ranges.

In Fig.1. (after Bernal [17]) a-c are solid-like structures which could act as nucleation precursors, and d-h are pseudo-nuclei which, because they contain elements of five or seven-fold symmetry are unable to lead to long range order. Structures such as a-c could serve as templates for the imposition of regularity and, because they contain internal lattice modes for vibration, they will provide efficient energy absorbers for the dissipation of the thermal energy of any molecules which may condense on them. There is some evidence to support such a relationship between liquid structure and homogeneous nucleation for water [18]. For the purposes of comparison some silicate anion structures are shown in Fig 2. Hummel [19] has calculated that the radius of a critical nucleus in a soda-lime-silica glass is between 20 and 30 Å. It is perfectly easy to envisage more or less regular silicate anions of this size, particularly in a glass containing aluminium. If such structures should aquire further small anions and stabilising cations they would eventually become small crystals.

Furthermore, Turnbull and Fisher [13] derived their theory for pure single component liquids, using parameters which may be estimated in this case. In many glass systems such parameters are difficult to obtain with any degree of certainty.

Even so, quantitative data supporting homogeneous nucleation in glass have been obtained recently [19], and it has been found that in many cases the temperature dependence of nucleation rate follows that predicted by homogeneous nucleation theory [20,21,22], although it would appear that the truly homogeneous nucleation of crystallisation in glasses and polymers is probably rare [23,24].

Classical homogeneous nucleation requires the continuous initiation of embryo (pre-growth) nuclei. However, Lungu and Popescu-Has [25] have shown that, for several fluorine containing silicate glasses, the number of crystallisation centres formed during heat treatment fails to increase after a sufficient length of heat treatment. A similar phenomenon is observed for liquid-liquid phase separation in the soda-lime-silica system [26].

Mukherjee [27] and Mukherjee and Rogers [28] studied the nucleation of crystallisation in soda-lime-silica-alumina glasses containing calcium fluoride and discovered that the rate of nucleation as a function of temperature followed that predicted by the classical theory. However, unlike Lungu and Popescu-Has [25], they did not investigate the temporal development of crystallisation centres in its totality. Instead, they measured the number of nuclei formed in a standard time at a particular temperature. Such measurements do not permit a comparison with the work described in [25] above and do not establish the homogeneous nature of the nucleation with any certainty.

In all these cases, however, the observation of a temperature dependence of nucleation rate which follows that of classical nucleation theory is not sufficient to establish a homogeneous mechanism. In this context it should be noted that, in the heterogeneous nucleation of crystallisation in polydecamethyleneterephthalate [29], the heterogeneous nuclei have a spectrum of activities resulting in a temperature dependence of nucleation rate, and an eventual temperature dependence of nucleation density.

The high viscosity of glasses adds a further complication to the application of the classical nucleation theory. Pauling [30] has stated that, in second order continuous transformations, the entropy changes have been related, in many systems, to the potential barrier to rotation. These barriers are related to the energy barriers governing viscosity. A correlation between viscosity and crystal growth in glass has been known for some time [31,32]. Referring now to Equation 2, it can be seen that ΔG_a, being related to viscosity, is usually high, so that W* must become an

extremely small quantity before detectable nucleation will occur. One way in which this may be facilitated would be the existence of large regular anions of the kind represented in Fig.2.

However, the number of these would tend to be established under conditions of high fluidity, that is, in the melt. Such a situation would tend to destroy the basis of the classical theory. In other words, the high viscosity of glass makes the formation of nuclei by random fluctuations unlikely, and, in consequence, homogeneous nucleation (as described by the classical theories) an improbable process.

3.3. A Simplified Approach to Nucleation Kinetics.

In the cases referred to above the experimentally observed temperature dependence of nucleation rate can most easily be appreciated as a consequence of the Szilard and Farkas mechanism of Equation 1. Consider then the set of reactions described by the equations.

$$\left.\begin{aligned} a_o + m &\rightleftharpoons a_1 \\ a_1 + m &\rightleftharpoons a_2 \\ a_i + m &\rightleftharpoons a_{i+1} \end{aligned}\right\} \quad [3]$$

Here the a_i represent nuclei of various sizes and m represents one molecule of the condensing phase. As inferred earlier, these nuclei may be large anions or other ordered regions within the glass, persisting from above the glass transition.

If rate constants, α_k, are ascribed to the reactions from left to right and rate constants, β_k, to the reactions from right to left, a series of differential equations may be obtained whose solutions describe the rate of appearance of nuclei of any size.

If these equations could be solved, and the functional dependence of the α's and β's on the nucleus size and the temperature were understood, a clear picture of the kinetics of nucleation and growth would arise.

Solutions to this problem have been obtained or at least shown to exist [33,34] but, unfortunately, the explicit solutions are difficult to use because of their mathematical form.

A simplification of the problem may be introduced by considering the production of a nucleus and its subsequent growth as separate stages. This is often observed experimentally, but probably represents an inadequate experimental time scale rather than two distinct processes.

Even so, the observation that a two-stage heat treatment is necessary to obtain volume as opposed to surface crystallisation, requires that the embryo or germ nuclei require activation before they become stable growth nuclei. This indicates that there are peculiar conditions associated with the formation of growth nuclei and leads to the conclusion that the pre-growth

nuclei must attain a certain size before they become stable growth nuclei. This corresponds to the 'critical size' of classical homogeneous nucleation theory.

The classical thermodynamic explanation of critical nucleus size has been outlined above. A possible statistical mechanical interpretation is contained in the work of Adam and Gibbs[35] . These authors show theoretically that there is a limit to the size of the smallest region in a glass that can undergo a transition to a new configuration without a requisite simultaneous configurational change on and outside its boundary. They calculate that below this size no rearrangement can make any contribution to the configurational entropy of the glass. These calculations were made for substances which show a sharp glass transition. It is to be expected that, in glasses with a transformation range, there will be a distribution of sizes of such regions. Such a model would correspond conceptually to J.W. Gibbs' limit of stability.[12]

The kinetic problem may be further simplified by adopting the suggestion due to Goodrich [33] that the flux of nuclei through the critical size may be considered as the rate determining step. If this is so there is no need to consider the rate at which embryo nuclei arrive at a sub-critical size.

Some justification for considering the sub-critical to critical transformation as rate determining may be extracted from somewhat disparate sources. Macedo [36] analyses data from various measurements of relaxation phenomena in glasses in terms of flow units trapped in potential wells. He calculates the radii of these wells to be about 44Å, surprisingly close to the values for the radius of a critical nucleus of 20-30Å obtained by Hammel[19] .

Stevels [37] analyses the data from measurements of dielectric loss in glasses in terms of a potential-well model of glass structure, small potential barriers governing local motion and very-much larger ones governing long range transport. This picture is confirmed by the work of Bishop and Bray [38] on the diffusion of ^{7}Li ions in a lithium borate glass. By observing the motional narrowing of the ^{7}Li nuclear-magnetic resonance absorption they showed that two potential barriers govern the diffusional motion of the ions, a small one governing movement within a limited range, whilst a very much larger one governs long range diffusion.

By combining the ideas contained in[33—38] above the following model arises:-

It may be considered that within the body of the glass there may exist groups of molecules or, large molecules of regular structure, or remnants of some original crystalline structure, trapped within potential wells. In the first case the groups of molecules may undergo rearrangements to crystalline or quasi-crystalline configurations, the rates of these reactions

being governed by small local energy barriers. In all these cases the by now crystalline regions are too small to contribute to the overall entropy of the system and to do so must extend outside the potential well, which extension, because of the large energy barrier governing it, may be considered as the rate determining step.

Avrami [39] made the assumption that nucleation precursors were present in the melt, the number and size of them being determined by melt conditions. It seems likely, that for the precursors envisaged here, this assumption would be correct or substantialy so. Furthermore, at low nucleation densities, the nucleation precursors will be spatially separatedsothat they will not interfere with one another. Let the number per unit volume of these be N.

These grow rapidly by the addition of monomer units until they reach such a size that one further monomer addition converts them to critical nuclei, which are then assumed to become, by whatsoever means imagined, observable growth nuclei.

At any time let the concentration of sub-critical nuclei be A_s. Let the concentration of critical nuclei (i.e. observable growth nuclei) be A_c. Let the concentration of monomer units be M.

The reaction can be written as

$$a_s + m \rightleftharpoons a_c \qquad [4]$$

Let the rate constant for the forward reation be K and for the reverse K_2

The rate of appearance of critical nuclei will be given by (at constant temperature).

$$\frac{dA_c}{dt} = KMA_s - K_2A_c \qquad [5]$$

where t is the time

If the reaction is stopped at some time and the critical nuclei present are grown to observable dimensions at some temperature outside the nucleation range, all the growth nuclei present at the time and temperature of the nucleation stage will become observable nuclei and, in this kind of experiment, there will be no need to consider the removal of critical nuclei from the expression above. In other words, no growth of critical nuclei may take place within the nucleation range. This approximation will be true if the rate of growth within the nucleation range is very small.

It was assumed above that the total number of nucleation precursors was determined solely by the melt conditions. If therefore, the nucleation temperature is substantially lower than the liquidus temperature or the temperature at which these singularities arise, no new nucleation precursors will be injected into the system.

Now the rate of appearance of critical nuclei must be equal to the rate of dissappearance of sub-critical nuclei. This is important for the boundary conditions of the problem.

$$\frac{dA_s}{dt} = \frac{-dA_c}{dt} \qquad [6]$$

Differentiating [5] with respect to time and assuming M to be constant.

$$\frac{d^2A_c}{dt^2} = KM \frac{dA_s}{dt} - K_2 \frac{dA_c}{dt} \qquad [7]$$

Substituting for $\frac{dA_s}{dt}$ from [6]

$$\frac{d^2A_c}{dt^2} = \frac{KMdA_c}{dt} - K_2 \frac{dA_c}{dt} \qquad [8]$$

The assumption of M = constant will be substantially correct if the concentration of monomers in the immediate vicinity of a nucleus is large. Therefore we may write

$$KM = K_1 \qquad [9]$$

$$\frac{d^2A_c}{dt^2} + (K_1 + K_2) \frac{dA_c}{dt} = 0 \qquad [10]$$

This is a second order linear differential equation with constant coefficients which has a solution of the form

$$A_c = \exp(mt) \qquad [11]$$

Then

$$m^2 \exp(mt) + m(K_1+K_2) \exp(mt) = 0 \qquad [12]$$

[12] is a solution of [11] when m is a root of :

$$m^2 + m(K_1 + K_2) = 0 \qquad [13]$$

(the auxiliary equation)

$$m = 0 \qquad [14]$$
$$m = -(K_1 + K_2)$$

Hence:-

$$A_c = P + Q \exp -(K_1 + K_2)t \qquad [15]$$

Where P and Q are arbitrary constants which arise in the same way as constants of integration, Let the boundary conditions be, for the sake of simplicity.

$$\left.\begin{aligned} t = 0,\ A_c &= 0 \\ t = \infty\ A_c &= N \end{aligned}\right\} \qquad [16]$$

This assumes that all the nucleation precursors are sub-critical and approximately monodisperse. Substitution in [16] gives

$$\left.\begin{aligned} P &= N \\ Q &= -N \end{aligned}\right\} \qquad [17]$$

to give $$A_c = N - N \exp -(K_1 + K_2)\, t \qquad [18]$$

The form of this relationship is of the kind shown in Fig.3. However, nucleation/time relationships of the kind shown in Fig.5. are often observed.

The region OB has been called the 'induction period' and attempts have been made to explain its existence as a consequence of the slow rate of establishment of the steady-state condition of classical nucleation theory. These attempts have generally involved considerations of the diffusion of incoming monomer units [40]. In the present context this would manifest itself in the concentration of monomers M not being a constant. This would result in a more complex form of Equation [8] which may well have solutions of the form of Fig.5. This situation could also be the result of a distribution of nucleation precursor sizes, resulting in more complex boundary conditions. Furthermore, the complete solution of the set of the differential equations arising from the reaction sequence [3] has this form (see for example Ree, Ree, Ree and Eyring [41]). If this had to be considered it would mean that the sub-critical to critical transformation could no longer be considered as rate determing, meaning that either the reations between the nucleation precursor and monomer units are intrinsically slow because of large energy barriers, or that the monomer units have to diffuse into the nucleation site at a very early stage in the nucleation process.

Rearranging [18] and taking logarithms,

$$\ln(N - A_c) = \ln N - (K_1 + K_2)t \quad [19]$$

This is the equation of a straight line as illustrated in Fig.4. A similar plot for Fig 5. becomes straight at long times (Fig.6).

The two rate constants may be extracted from [19] by measuring the initial rate, for, from [5]

$$\frac{dA_c}{dt} = K_1 N \quad [20]$$

at $t = 0$, $A_c = 0$, $A_s = N$

Now, if $K_1 = A \exp\left(\frac{E_1}{RT}\right)$ and $K_2 = B \exp\left(\frac{-E_2}{RT}\right)$

where R is the gas constant, T is the absolute temperature and A and B are constants, the activation energies E_1 and E_2 may be obtained. The pre-exponential terms A and B are composed of various quantities, in particular, the partition functions for the reagent molecules and the activated complex [42]. In the solid state these partition functions will be, almost entirely, the vibrational partition functions of the participating molecules. The problem of nucleation kinetics then devolves on the calculation of the rate constants K_1 and K_2 for the simple case and the rate constants for all the steps in the complete solution. Unfortunately, little progress has been made in the calculation of rate constants for the most simple reactions [42].

Comparison with the equation of Turnbull and Fisher (Equation 2) shows that the classical treatment also views the sub-critical to critical transition as rate determining through the use of the factors W^* and ΔG_a. However, the classical theory imposes the further restriction that this step is also an

equilibrium. In this treatment such a condition would require that:-

$$\frac{dA_c}{dt} = \text{constant} \qquad [21]$$

If this were so

$$\frac{d^2A_c}{dt^2} = 0 \qquad [22]$$

and

$$KM\,\frac{dA_s}{dt} = K_2\,\frac{dA_c}{dt} \qquad [23]$$

which is obviously less general than Equation [7].

Nucleation following the model developed above would be heterogeneous insofar that the primitive nucleation precursors do not represent the overall composition of the glass but, homogeneous in that they require activation in order that they may become stable growth nuclei. Without further information concerning the nature of these it would not appear fruitful to enquire into their genesis and energetics in a theoretical manner but rather experimentally to see if they exist and under what constraints.

Finally there remains the operational distinction between the nucleation and crystallisation temperature ranges. When this is observed in a pure system it probably represents the reduced stability of a small crystal compared with a large one at the same temperature. However, in a complex system containing persistent embryo nuclei, considerable rearrangement or fractionation may be required for crystallisation to proceed, processes which may require long range diffusion, breaking of chemical bonds, or both. In such a case crystallisation would obviously occur very slowly at low temperatures. The upper cut-off in detectable nucleation rate would again correspond to the decrease in stability of a micro-crystal due to the violence of surface vibrational modes [16].

Key to Figures 1 and 2.

Figure 1. Crystal nuclei and pseudo-nuclei built from equidistant or quasiequidistant molecules.

Crystal nuclei a, b & c, are precursors to long range order and may therefore act as nucleation embryos.

Figure 2. Some silicate anion structures.

a) $Si_3O_9^{6-}$ ion

b) $Si_4O_{12}^{8-}$ ion

c) $Si_6O_{15}^{6-}$ ion

d) $Si_8O_{20}^{8-}$ ion

e) $Si_9O_{21}^{6-}$ ion

f) an aluminosilicate ion of the type found in zeolites.

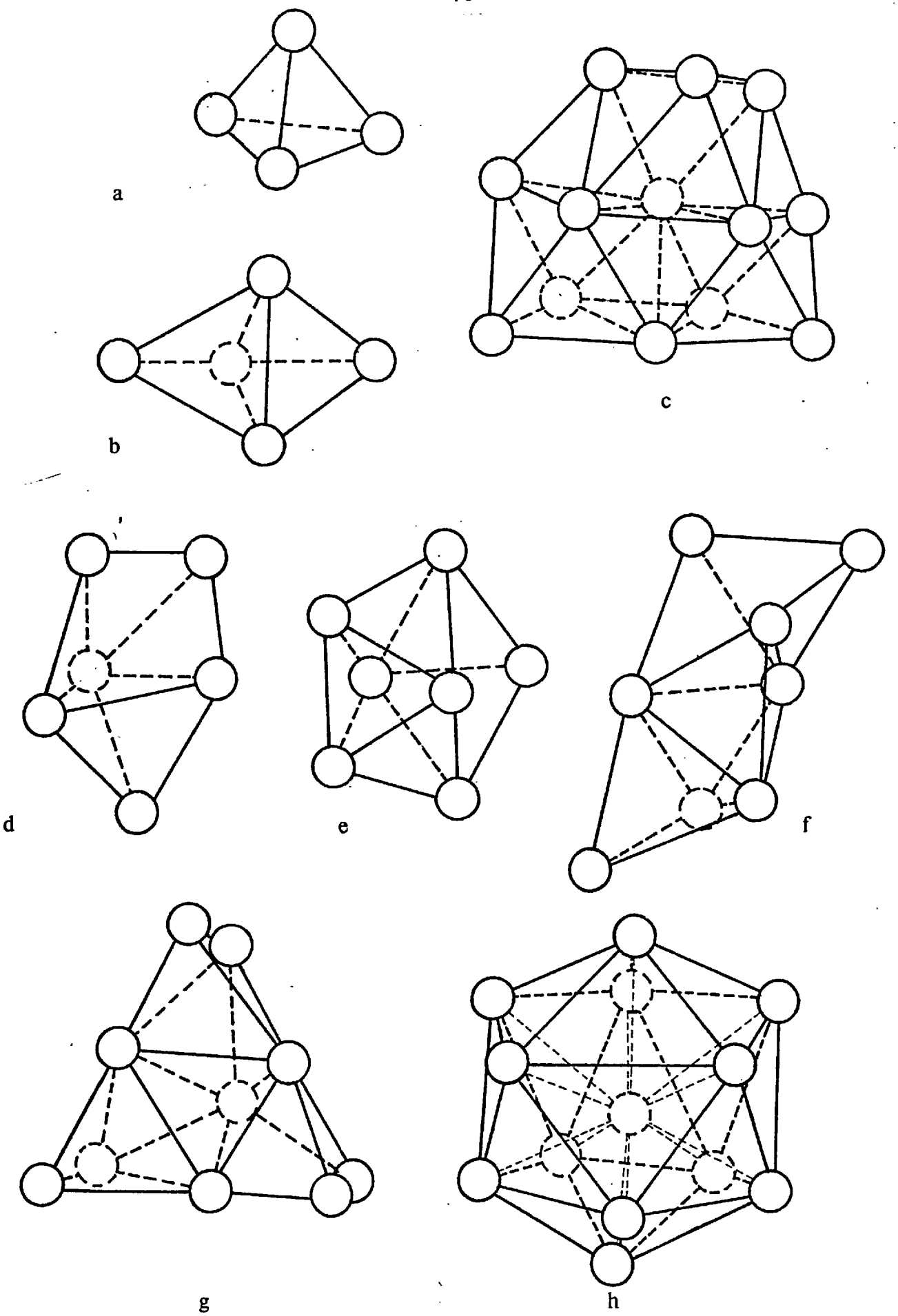
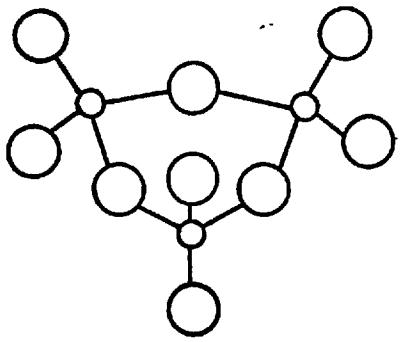
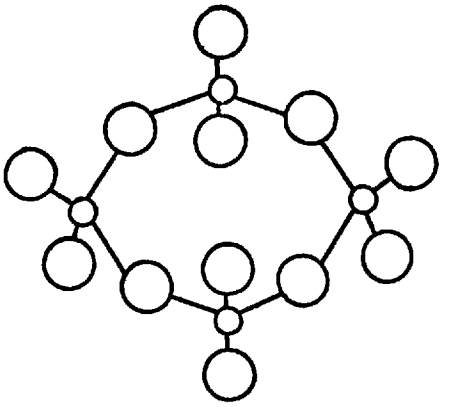


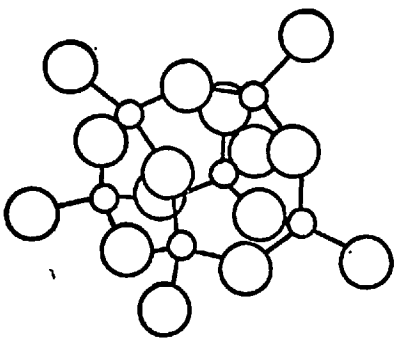
Fig. 1



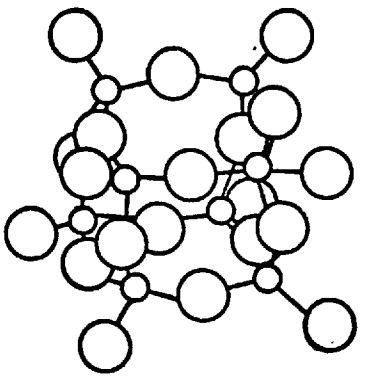
a



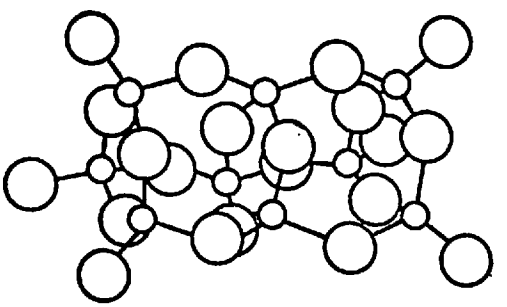
b



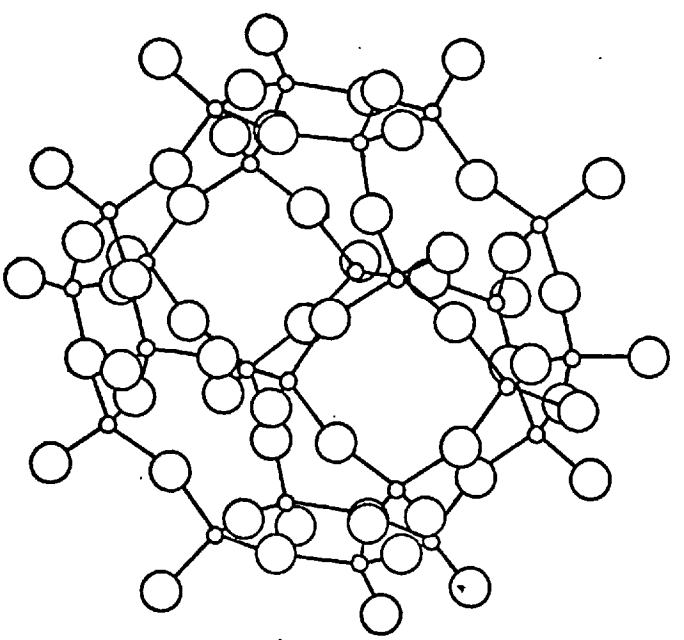
c



d



e



f

Fig. 2

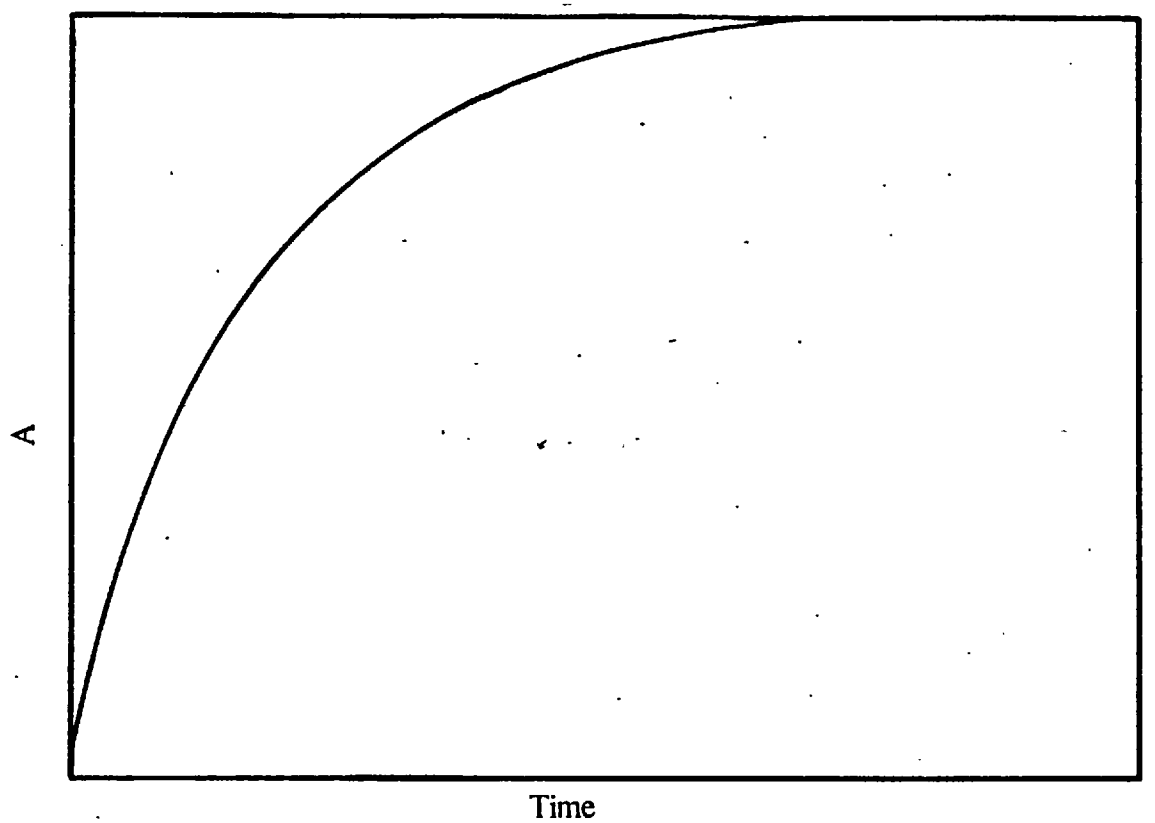


Fig. 3

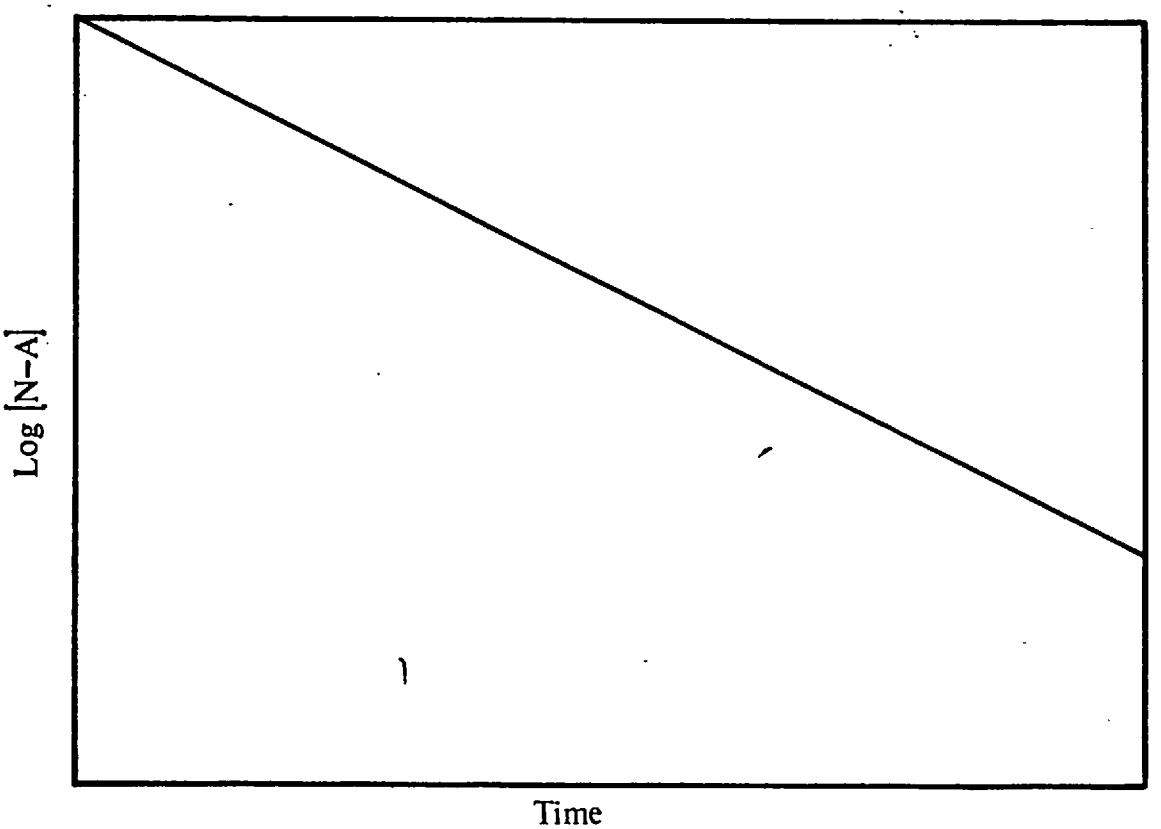


Fig. 4

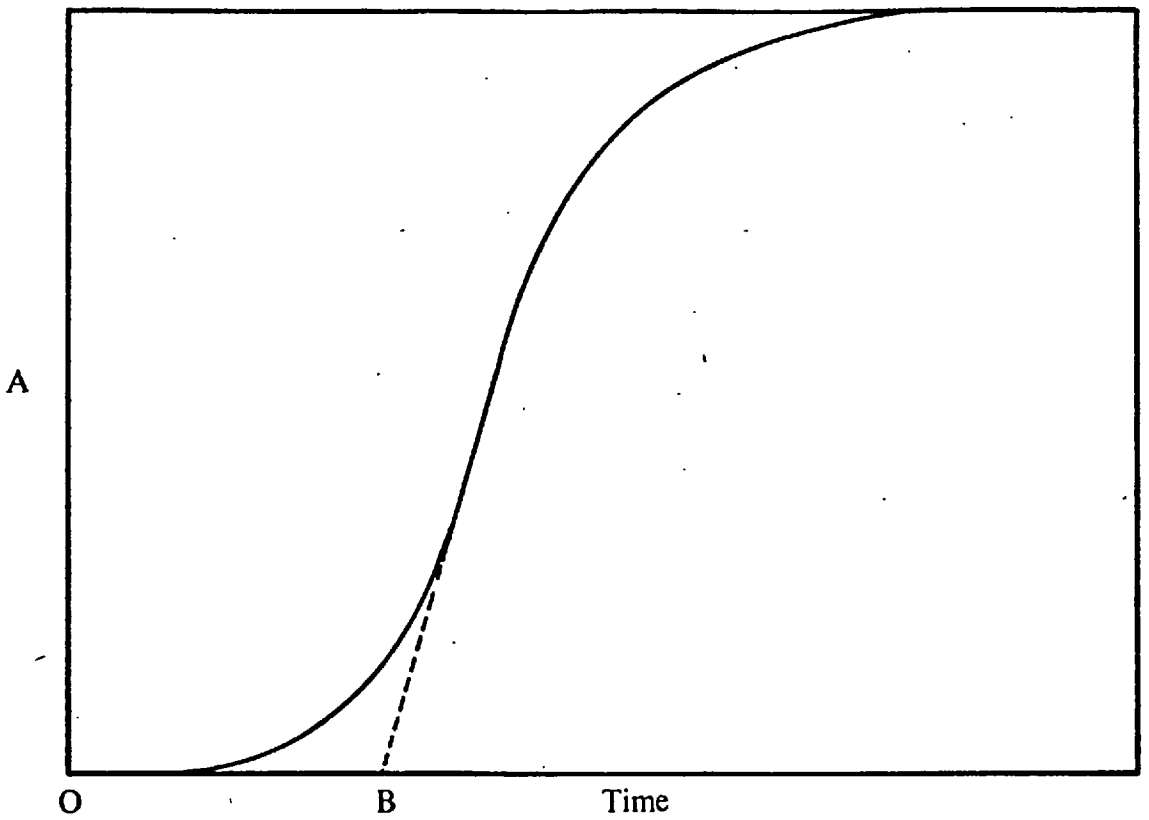


Fig.5

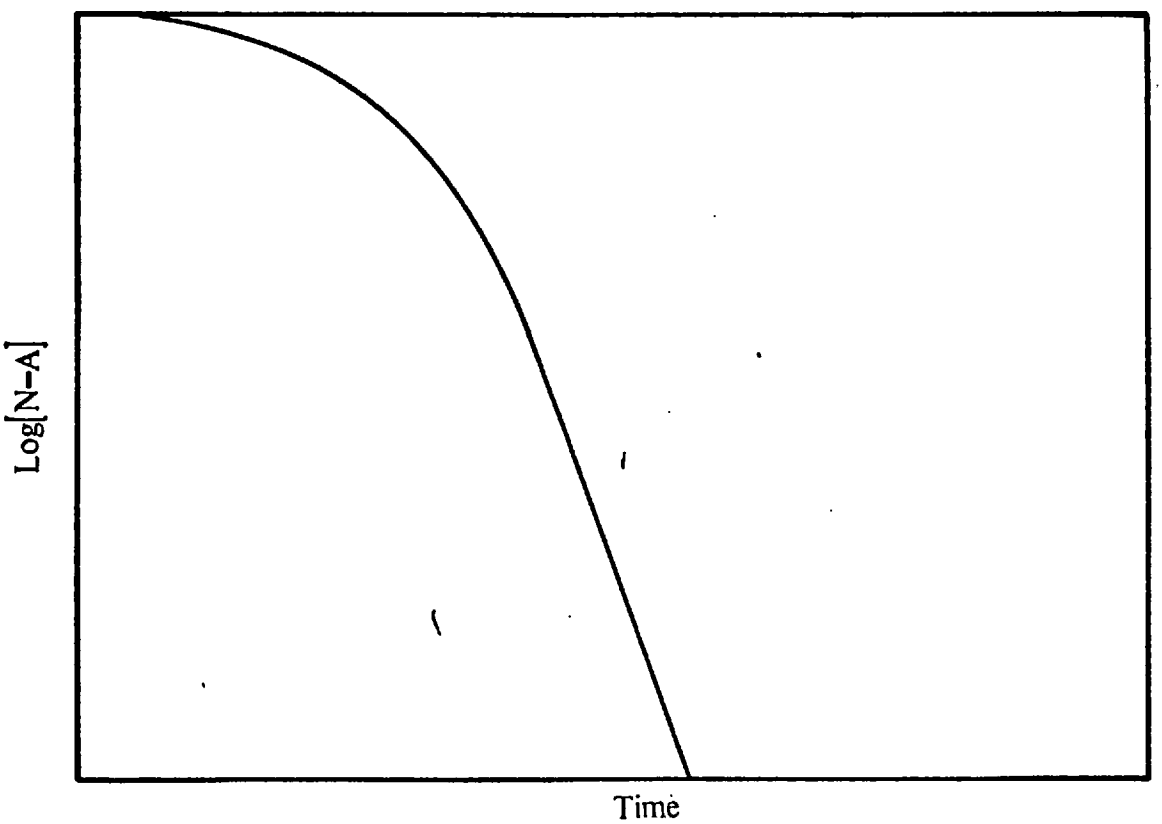


Fig. 6

References to Chapter 3

1) M.F. Williams, R.F. Landel and J.D. Ferry, J.Am.Chem.Soc., 77, 3701,(1955).

2) E.A. Guggenheim, 'Thermodynamics'. Amsterdam (1949).

3) M. Volmer, A. Weber, Z. Phys. Chem.(Leipzig), 119, 277, (1926).

4) L. Szilard see ref.(5).

5) L. Farkas, Z. Phys.Chem.(Leipzig), A125, 236, (1927).

6) M. Volmer, Z. Phys.Chem.(Leipzig), 25, 555, (1929).

7) M. Volmer, "Kinetik der Phassenbildung," Dresden, (1939).

8) R. Becker, W. Doring, Ann.Physik, 24, 719, (1935).

9) J.B. Zeldovich, Acta.physico chimica, U.R.S.S. 18, 1, (1943).

10) J. Frenkel. Kinetic Theory of Liquids, Oxford, (1946).

11) J. Frenkel, J.Chem.Phys., 7, 200, (1939).

12) W.G. Courtney, J.Chem. Phys., 36, 2009, (1962).

13) D. Turnbull and J.C. Fisher, J.Chem. Phys., 17, 71, (1949).

14) H. Reiss, J.Chem.Phys., 20, 8, 1216-1227, (1952).

15) J. Lothe, G.M. Pound, J. Chem.Phys., 48, 4, 1849-1852, (1968).

16) J.J. Burton, J. Chem.Phys., 52, 1, 345,(1970).

17) J.D. Bernal, Nature 181, 68, (1960).

18) W. Drost-Hansen, Intl.Sci.Technology, 86, (1966).

19) J.J. Hammel, J.Chem.Phys., 46, 6, 2234,(1967).

20) G. Tammann, Constitution of Glasses, Society of Glass Technology Sheffield, (1927).

21) S.D. Stookey, Glastech.Ber. Sonderband 32KI (1959).

22) I.I. Kitaigorodskii and R.Ya.Khodak ovskaya, 'The Structure of Glass' Vol.3, Consultants Bureau, New York (1964).

23) J.J. Hammel. 'Nucleation' A.C. Zettlemoyer ed, New York (1970).

24) F.P. Price, 'Nucleation' A.C. Zettlemoyer ed., New York (1970).

25) St. N. Lungu and D. Popescu-Has, Industria Usoara, 5, 11, 63-65,(1968).

26) D.G. Burnett and R.W. Douglas, Phys.Chem.Glasses, 11, (5), 125-135,(1970).

27) S.P. Mukherjee, M.Sc. Thesis. London (1967).

28) S.P. Mukherjee, and P.S. Rogers, Phys.Chem.Glasses, 8, (3), 81-87,(1967).

29) A. Sharples, Polymer, 3, 250,(1962).

30) L. Pauling Phys.Rev. 36, 430, (1930).

31) G. Tammann, Aggregat Zustand. Leipzig, (1922).

32) M. Volmer, Kinetik der Phasenbildung, Leipzig (1939).

33) F.C. Goodrich, Proc.Roy.Soc. A277, 155-66,(1964).

34) W. Lodermann and G.E.H. Reuter, Phil.Trans. A246, 321,(1954).

35) G. Adam and J.H. Gibbs, J.Chem.Phys. 43, (1), 139-146,(1965).

36) P.B. Macedo, J.H. Simmons, W. Haller, Phys.Chem. Glasses, 9, (5), 156-164, (1968).

37) J.M. Stevels, Philips Technical Review, 13, (12), 360, (1952).

38) S.G. Bishop, P.J.Bray, J.Chem.Phys., 48, (4), 1707,(1968).

39) M. Avrami, J.Chem.Phys., 8, 212-223,(1940).

40) J.W. Christian, 'The Theory of Trans formations in Metals and Alloys'. Oxford (1965).

41) F.H. Ree, T.S. Ree, T. Ree, H. Eyring, Advances in Chemical Physics, Vol IV (1962).

42) S. Glasstone, K.J. Laidler, H. Eyring, 'The Theory of Rate Processes' New York (1941).

Chapter 4

Experimental Techniques and Results

4.1. Materials

Silica was supplied by Thermal Syndicate Ltd. in the form of pure quartz powder of 99.9% purity. Water was removed by heating in a platinum crucible at about 1000°C for several hours.

Alumina was Hopkin and Williams Analar Grade fired in a muffle furnace for several hours. Lime and soda were added to the batch in the form of Analar calcium and sodium carbonates. The calcium fluoride used was B.D.H. extra-pure grade of 99.9% purity. All these materials were dried for several days at about 150°C. The batch materials were stored over magnesium perchlorate in a desiccator. Care was taken to eliminate water as much as possible so as to avoid fluorine loss through reactions such as

$$2F^- + H_2O \rightarrow 2HF + O^{2-}$$

4.2. Glass preparation

Glasses were prepared by heating the constituents in 70cm^3 platinum crucibles in resistance heated muffle furnaces at 1400°C. The furnaces were equipped with "Crusilite" furnace rods and temperature control to $\pm$ 10°C was obtained by inertial control.

The glasses were crushed and remelted three times in order to ensure homogeneity, the calcium fluoride being added in the final remelting (which was of a standard 1 hr duration) in order to further minimise volatilisation losses. The crushing was effected in a tungsten carbide percussion mortar, fragments of iron being removed with a strong magnet. After the final remelting the glass was poured

onto a large brass plate and allowed to cool in the air. The glass block so obtained was sawn into small pieces of between .5 and 1 cc in volume.

4.3. Heat treatment procedure.

The specimens were heated in "Kanthal" wound horizontal tube furnaces having constant temperature zones of about 6 cms in length. The samples were held in alumina boats lined with ceramic wool, connected to alumina or mullite tubes of about 1 cm external diameter which served as handles and channels for the introduction of chromel-alumel thermocouples. These latter rested against the samples and were used to measure sample termperature in conjunction with either a Tinsley or Cambridge slide-wire potentiometer. Temperature control to within $\pm$ 5°C was achieved by the use of either "Eurotherm" solid state controllers, or a combination of the "Ether "Mini" controller in conjunction with a 15 amp Mullard OTH series thyristor bank. The sensing element in both cases was a Pt/Pt-13%Rh thermocouple located in the constant temperature zone of the furnace.

The heat treatment schedule was a two stage one as indicated in Chapter 1. Nuclei were grown for a series of times at a particular temperature and developed for a standard period at a higher, crystallisation temperature. For a particular series of glasses the duration and temperature of the crystallisation treatment were standard. The choice of crystallisation temperature was determined in an ad-hoc fashion to attempt a compromise resulting in the minimum of volume crystallisation and substantial surface crystallisation. The nucleation range was determined empirically and was always assumed, in the first instance, to lie at some [redacted] temperature below that used for crystallisation.

The furnaces were set at the required temperature and, with the boats inside, were allowed to equilibrate for at least a day. Glass samples were placed in a boat at the temperature chosen for nucleation and, at the end of a chosen period, transferred from the nucleation

furnace to a boat maintained at the crystallisation temperature and placed in that furnace for the requisite time.

4.4. Optical Microscopy and Sample Preparation

The heat treated samples were sawn in half using a diamond saw. The sawn side of one half was ground flat on a diamond weel and then polished on a rotating lap with grade 180C and 600 carbonundum paper, the sample being washed at each stage. The sample was dried and cemented to a clean glass slide with 'Lakeside' cement, the polished side being in contact with the slide. The sample was then ground and polished as described above until a section of thickness 20-60 microns was obtained. The samples were examined under the optical microscope arranged for phase-contrast in polarised light, with or without crossed Nicol prisms.

4.5. Counting Procedure

In those glasses where internal nucleation of crystallisation had occurred, birefringent structures were observed (indicating the presence of crystalline material) of spherulitic or near-spherulitic type. These structures were counted using a modification of a technique described by Hilliard (1) [illegible]. The expected number of particles with centres lying within a slice of thickness, t, is $N_V t$ per unit area. In addition, images will be observed due to particles with centres lying outside the slice. The number of such images will be the same as the number of intersections occurring on a two-dimensional plane through the structures; namely $N_V \bar{K}$ where $\bar{K}$ is the mean distance between parallel tangent planes to a particle averaged over all particles i.e. the mean particle diameter. For finite fields of view there will be an edge effect arising from the presence of elements from particles whose centres lie outside the lateral boundaries of the field. On average half the images extending beyond the edges of the field will have originated from centres within the field.

$$N_A = \{N'' + (N'/2)\}/A.$$

N_A is number of particles per unit area.

N'' is the number of images lying wholly within the field of area A and N' the number of images intersected by the edges of the field. The total number of particles per unit volume is given by

$$N_v = \frac{N_A}{(t+\bar{K})}$$

when the slice thickness is comparable to the particle diameter and the volume fraction of the particles is small, the number of images lost through overlap is small. This was the case in most of the glasses studied.

The slice thickness was determined by taking the average of several measurements of the slide thickness and subtracting this from the average of several measurements of the thickness of the slide and sample. The Lakeside cement formed a layer of about 2 microns depth which was neglected. The measurements were made using a direct reading, digital micrometer, calibrated to read in microns.

The areas of the fields of view of the microscope objectives were determined by measuring the diameter of the field of view with a stage micrometer. The particle diameters were determined using an eyepiece graticule calibrated against the stage micrometer and the magnification of the objective being used. Counts of particle number were made over the entire area of the sample, at least 10 separate counts being made.

The number of particles per cm^3 determined in this way was found to be subject to an error of between $\pm$5% and $\pm$15%.

4.6. Technique for Electron Microscopy

Samples were mounted in Bakelite embedding resin and the surface was prepared by:-

(1) Grinding on a rotating lap with grade 180C and 600 carborundum papers.

(2) The polishing was completed on a cloth covered lap

with successively finer grades of diamond paste, finishing with 1 micron paste.

(3) The sample was then cleaned in an ultrasonic bath and etched for 5 to 10 seconds in .5% HF.

(4) Carbon replicas of the surface were made and shadowed with platinum.

4.7. Technique for Scanning Electron Microscopy.

Samples were fractured and the fracture surfaces were etched with .5% HF for 5 to 10 seconds and cleaned ultrasonically. The dry specimens were mounted on aluminium stubs with 'Durofix' and coated with aluminium or gold.

4.8. Technique for Infra-Red Spectroscopy.

Samples were crushed in a 'Torrington' tungsten carbide percussion mortar until the powder passed through a 350 mesh sieve. Tungsten carbide was used in preference to agate as this latter has a strong infra-red spectrum and tungsten carbide has none. About 50 mgm of this powder was taken and ground to dryness under acetone following the technique of Tuddenham and Lyon [2]. This powder was slurried with acetone and passed through an E.M.I. "Micromesh" of 2 micron aperture. The acetone was evaporated and the powder mixed with about 200 mgms of B.D.H. spectroscopic grade KBr, and formed into a clear disc under vacuum and pressure. The spectra were recorded on a Grubb-Parson's "Spectromaster" Infra-red Spectrometer in the double beam mode through the interval 5-25 microns.

4.9. Results

The premelt compositions of the glasses are given in Table 1. These are divided in four groups according to the compositional influence being investigated. All the glasses are based on the Mukherjee and Rogers Base Glass 1 composition, [3].

The glasses of group one were designed to investigate the influence of alumina on crystallisation kinetics. All the glasses were clear and stable except for 1.0 and 1.1 which were opalescent. The glasses of group 2 and 3 were designed to investigate the influence of fluoride content at 5 and 10 weight percent of soda respectively. All glasses were stable and clear except for 2.5 and 3.7 which were opalescent and showed fluoride gall. Glasses of series 4 were designed to investigate the influence of the soda/lime ration on a glass with a constant fluoride content. All these glasses were stable and clear.

The glasses were heat treated as in section 4.3 and their nucleation kinetics characterised as described above. All the glasses which could be internally crystallised exhibited a time dependence of nucleation corresponding to either of the cases described in Chapter 3. Figures 7 and 8 are typical nucleation curves and should be compared with their archetypes in Figures 3 and 5. It was assumed that all the glasses obeyed Equation 18 Chap. 3 at sufficiently long times. As such, plots of log (N-A)vs t were made for all the crystallising glasses where N is the maximum number of spherulites developed, A is the number of spherulites developed at any time t. Figure 9 shows that this assumption is indeed true, especially at high temperatures. The curves should be compared to Figure 6 of Chapter 3. This shows that, in general, the glasses obey the more complicated kinetic law. These plots are shown in Figs. 9-15, 27-34, 43-46. It can be seen that some of these plots do not pass through N at $t = 0$. This is taken as indicating that some nucleation has taken place during the crystallisation treatment and not that the maximum number of nuclei is dependent on the nucleation temperature.

The slope, I, was obtained from the linear portions of these graphs and, from Equation 18 Chap 3, equated to $-(K_1 + K_2)$ if the induction period, OB, in Fig. 5 is ignored for the glasses obeying this type of law, it can be assumed that, from Equation 20 Chap 3,

$$\frac{dA}{dt} = NK_1 \text{ at } t = 0.$$

Consequently, the initial slopes, subject to the provisions above, were determined from graphs of A vs t thus giving values of K_1.

Since $I = -(K_1 + K_2)$ K_2 may be determined.

Now $K_1 = A \exp\left(-\frac{E_1}{RT}\right)$, $K_2 = B\exp\left(\frac{-E_2}{RT}\right)$

where E_1 and E_2 are the activation energies in calories

T is the absolute temperature

R is the universal gas constant.

This is true when K_1 and K_2 are in units of nuclei per cm^3 per second. Thus a plot of $\log K_1$ against $\frac{1}{RT}$ should give a straight line of slope E_1

Knowing K_1, E_1 and T, the pre-exponential A can be calculated

Plots of $\log K_1$ vs $\frac{1}{2.303\ RT}$ and $\log K_2$ vs $\frac{1}{2.303\ RT}$

are shown in figures 17-22, 35-38, 47-48.

Most of these are very good straight lines. From these lines values of the activation energies and preexponential factors were obtained and plotted as functions of composition.

These properties are displayed in Figs. 23-24, 41-42, 52-53.

Summaries of the main bands observed in the spectra are given in Figs. 60-63 as functions of composition.

Table 1

Series 1 Glasses. Starting Compositions Wt%

Glass Number	CaF_2	Na_2O	CaO	Al_2O_3	SiO_2	Al.
1.0	7	5	26	0	62	0
1.1	7	5	26	1	61	.79
1.2	7	5	26	2	60	1.06
1.3	7	5	26	3	59	1.59
1.4	7	5	26	4	58	2.12
1.5	7	5	26	5	57	2.65
1.7	7	5	26	7	55	3.71

Table 2

Series 2 Glasses. Starting Compositions Wt%

Glass Number	CaF_2	Na_2O	CaO	Al_2O_3	SiO_2	F
2.1	2	5	31	7	55	.96
2.2	4	5	29	7	55	1.30
2.3	6	5	27	7	55	2.88
2.4	8	5	25	7	55	3.84
2.5	10	5	23	7	55	4.80

Table 3

Series 3 Glasses. Starting Compositions Wt%

Glass Number	CaF_2	Na_2O	CaO	Al_2O_3	SiO_2	F
3.0	0	10	28	5	57	0
3.1	2	10	26	5	57	.96
3.2	5	10	23	5	57	1.30
3.3	6	10	22	5	57	2.88
3.4	8	10	20	5	57	3.84
3.5	10	10	18	5	57	4.80
3.6	12	10	16	5	57	5.76
3.7	14	10	14	5	57	6.72

Table 4

Series 4 Glasses. Starting Compositions wt%

Glass number	CaF_2	Na_2O	CaO	Al_2O_3	SiO_2	Na
4.0	7	0	31	7	55	0
4.1	7	2	29	7	55	1.48
4.2	7	4	27	7	55	2.86
4.4	7	8	23	7	55	5.71
4.6	7	12	19	7	55	8.55

Table 5 Example of counting technique and computation.
Showing typical microscopic observations.
Glass 2:3, 3 hrs at 706°C and .5 hrs at 879°C.

Thickness of slide + Section cm.	Thickness of slide cm.
.1595	.1556
.1595	.1559
.1595	.1567
.1596	.1565
.1595	.1555

Spherulite Diameter x 3.9×10^{-3} cm.		Area of the Field of View.
1.8	1.8	
1.9	1.6	
2.0	2.1	$1.288 \times 10^{-3} cm^2$
2.0	1.7	
1.0	1.5	

Number of Spherulites Lying Completely Within Field of View.			Number of Spherulites Intersected by Field Boundary.		
0	2	8	0	0	2
0	3	17	0	0	3
1	6	15	1	0	5
1	14	8	1	5	2
0	4	7	0	5	0

If t is the average slice thickness, $\bar{K}$ the average particle diameter, N' the average number of particles lying completely within the field of view and N'' the average number of particles intersected by the boundary of the field of view, with A the field area, the number of particles per unit volume, N_v, is given by

$$Nv = \frac{(N' + N''/2)}{A(t + \bar{K})}.$$

Key to figures.

Fig. 7. Plot of spherulite number A, against nucleation time t, in hours for glass 1.1. Nucleation temperature 642 ± 2°C.

Fig. 8. Plot of spherulite number A, against nucleation time t, in hours for glass 1.7. Nucleation temperature 662.0± 1°C.

Figs. 9-15, 27-34, 43-46. Plots of log (N-A) against nucleation time t, in hours for all glasses. A is the number of spherulites at any time and N is the eventual maximum number of spherulites.

Figs. 9-15 Series 1 glasses. Nucleation temperatures:-
A,642°C, B,663°C, C,684°C, D,707.8°C,
E,727.4°C. Crystallisation 1 hour at 863,8°C.

Fig. 9 Glass 1.0.
Fig. 10 Glass 1.1.
Fig. 11 Glass 1.2.
Fig. 12 Glass 1.3.
Fig. 13 Glass 1.4.
Fig. 14 Glass 1.5.
Fig. 15 Glass 1.7.
Figs. 27-34 Series 2 and 3 glasses.

Series 2 nucleation temperatures:-

A,593.9°C, B,530.9°C, C,706.9°C,
D,767.5°C. Crystallisation .5 hrs at 878.8°C,

Series 3 nucleation temps:—

A,504.1°C, B,551.2°C, C,607.0°C, D,663.1°C
E,706.3°C, F,745.8°C, G.815.0°C,
Crystallisation .5 hrs at 914.5°C.

Fig. 27 Glass 2.4 and 2.3
Fig. 28 Glass 2.5
Fig. 29 Glass 3.3
Fig. 30 Glass 3.2
Fig. 31-32 Glass 3.4
Fig. 33-34 Glass 3.5
Fig. 43-46 Series 4 glasses. Nucleation temperatures:-

A,603.8°C, B,659.5°C, C,665.3°C, D,703.6°C
E,740.5°C, F,809.9°C, Crystallisation .5 hrs.
at 917.2°C.

Fig. 43 Glass 4.1
Fig. 44 Glass 4.2
Fig. 45 Glass 4.4
Fig. 46 Glass 4.6

Figs. 16-22, 35-38 and 47 and 48 show the variation of $\log K_1$ and $\log K_2$ (see text) with nucleation temperature vs $\frac{1}{RT}$

Fig. 16. Glass 1.0.
Fig. 17. Glass 1.1.
Fig. 18. Glass 1.2.
Fig. 19. Glass 1.3.
Fig. 20. Glass 1.4.
Fig. 21. Glass 1.5.
Fig. 22. Glass 1.7.
Fig. 35. Glass 3.3.
Fig. 36. Glass 2.5.
Fig. 37. Glass 3.5.
Fig. 38. Glass 3.4.
Fig. 47. Glass 4.4 and Glass 4.6.
Fig. 48. Glass 4.2.

Fig. 23. The variation of the activation energy for nucleation as a function of the aluminium to total alkali ratio. Series 1 glasses.

Fig. 24. The variation of the pre-exponential factors as a function of aluminium content. Series 1 glasses.

Fig. 25. The variation of the maximum number of nuclei as a function of aluminium content. Series 1 glasses.

Fig. 26. The maximum degree of crystallisation after 1 hour at 863.8°C as a function of aluminium content. Series 1 glasses.

Fig. 39. The variation of the maximum number of nuclei as a function of fluoride content. Series 2 and 3 glasses.

Fig. 40. The maximum degree of crystallinity after .5 hrs at 900°C as a function of fluorine content. Series 2 and 3 glasses.

Fig. 41. The activation energy for nucleation as a function of fluorine content. Series 2 and 3 glasses.

Fig. 42. The pre-exponential factors as a function of fluorine content, Series 2 and 3 glasses.

Fig. 50. The maximum number of nuclei as a function of sodium content. Series 4 glasses.

Fig. 51. The maximum degree of crystallinity as a function of sodium content after .5 hrs at 917°C. Series 4 glasses.

Fig. 52. The activation energy for the nucleation process as a function of sodium content, Series 4 glasses.

Fig. 53. The pre-exponential factor as a function of sodium content. Series 4 glasses.

Fig. 54. The influence of melting time of the nucleation kinetics of glass 1.4.

Fig. 55. The influence of melting time on glass 1.1.

Fig. 56. The influence of melting time on glass 3.3.

Fig. 57. The influence of melting time on glass 3.4.

Fig. 58 A.B. The influence of melting time on glass 4.2.

Fig. 59. The influence of melting time on glass 4.6.

Fig. 60. A. The infra-red spectrum of glass 1.0.
B. Glass 1.0 after 6 hours at 715°C
C. Glass 1.0. after 4 hours at 707.8°C and 1 hour at 864°C.

D. Glass 1.0 after 10 days at 900°C.

Fig. 61 A. The infra-red spectrum of Glass 1.1.
B. Glass 1.1 after 5 hours at 684°C and 1 hour at 864°C.
C. Glass 1.7 after 6 hours at 708°C and 1 hr at 864°C.
D. Glass 1.7 after 10 days at 900°C
E. Glass 1.5 after 6 hrs at 715°C

Fig. 62 A. Infra-red spectrum of glass 2.1.
B. Glass 2.1. after 6 hrs at 715°C
C. Glass 2.4
D. Glass 2.4 after 6 hrs at 715°C
E. Glass 2.5.
F. Glass 2.5 after 6 hrs at 715°C

Fig. 63 A. Infra-red spectrum of Glass 3.3
B. Glass 3.3 after 10 days at 900°C
C. Glass 3.7
D. Glass 3.7 after 10 days at 900°C

Fig. 64 A. Infra red spectrum of Glass 4.1.
B. Glass 4.1 after 6 hours at 715°C
C. Glass 4.2.
D. Glass 4.2 after 6 hrs at 715°C
E. Glass 4.6
F. Glass 4.6 after 6 hrs at 715°C
G. Cryolite.

Fig. 65 The main infra-red bands as a function of aluminium content. Series 1 glasses.

Fig. 66 The main infra-red bands as a function of fluoride content at 5 wt% soda. Series 2 glasses.

Fig. 67 The main infra-red bands as a function of fluorine content at 10 wt% Soda. Series 3 glasses.

Fig. 68 The main infra-red bands as a function of soda-content. Series 4 glasses.

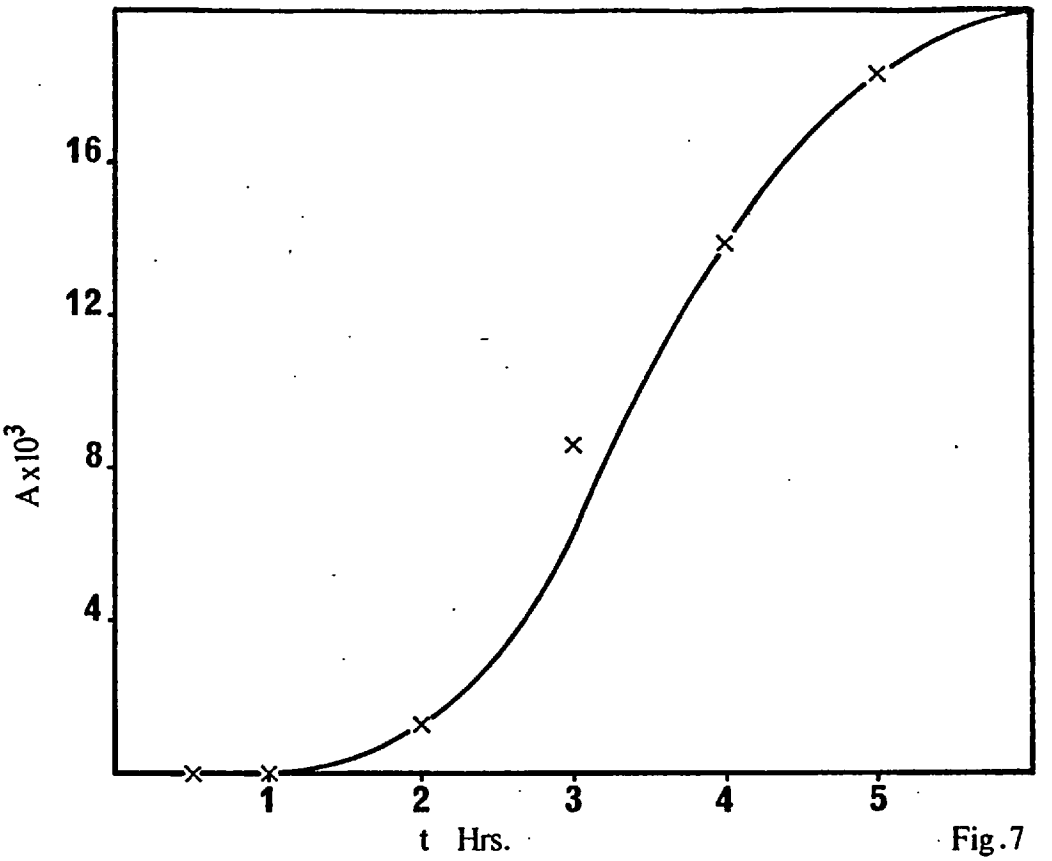


Fig.7

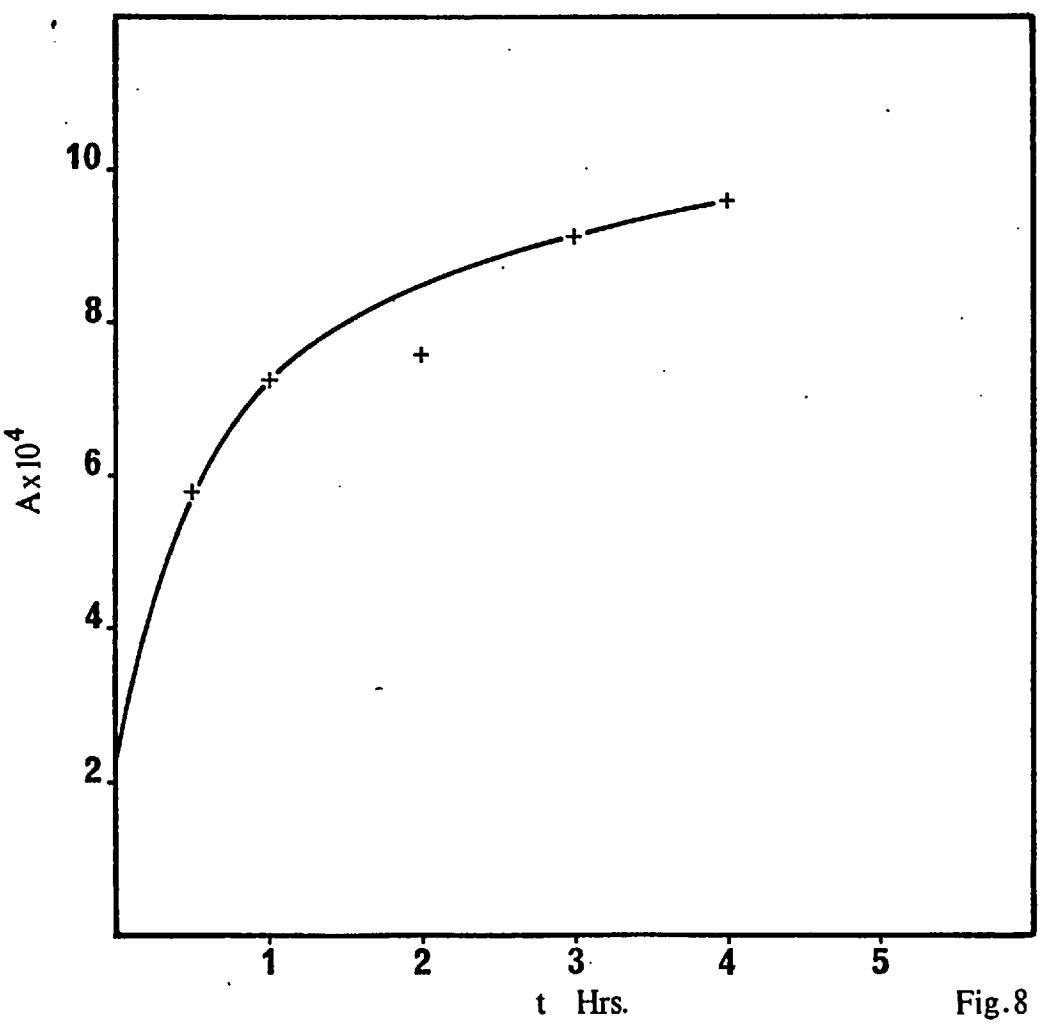


Fig.8

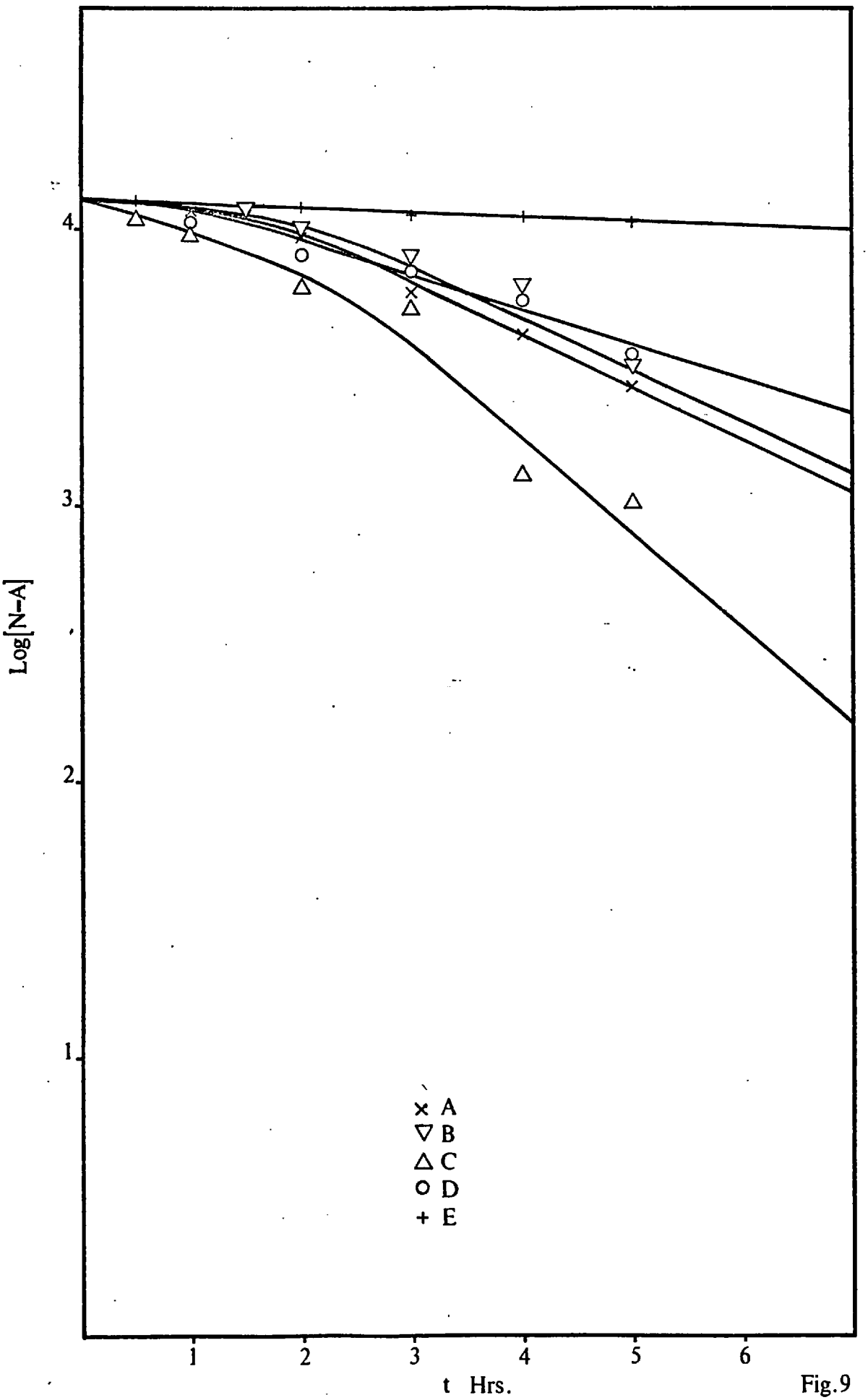


Fig.9

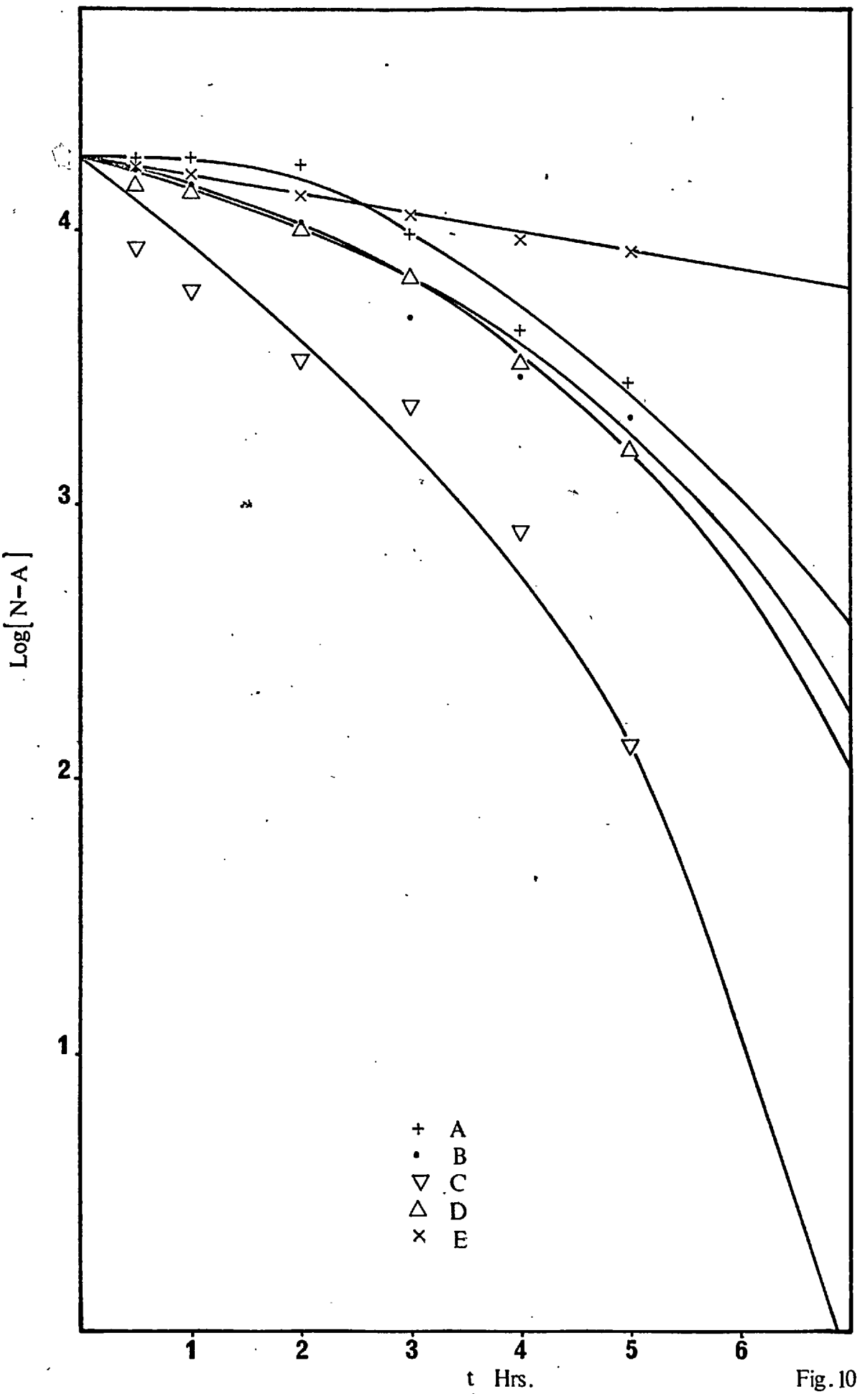


Fig. 10

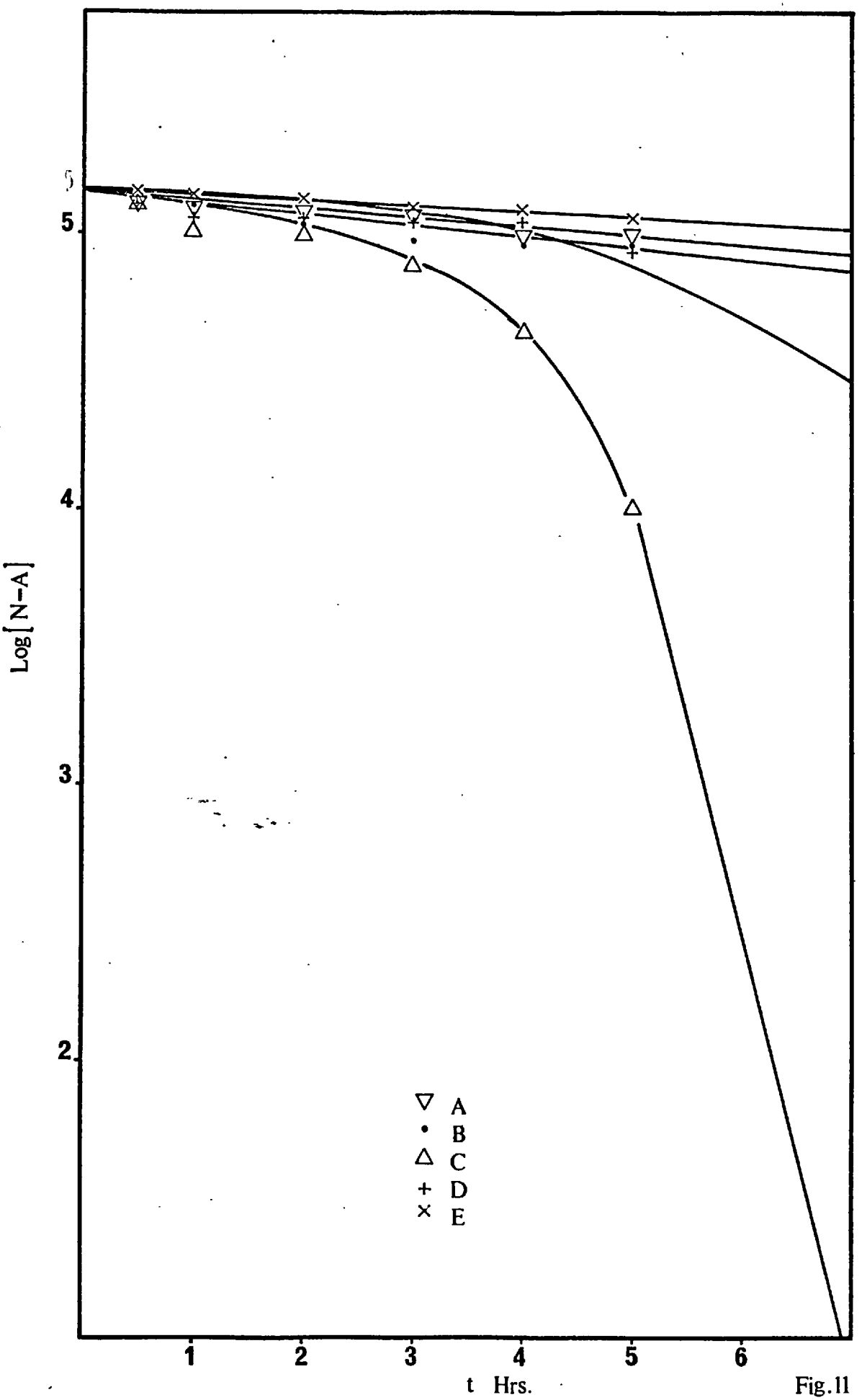


Fig.11

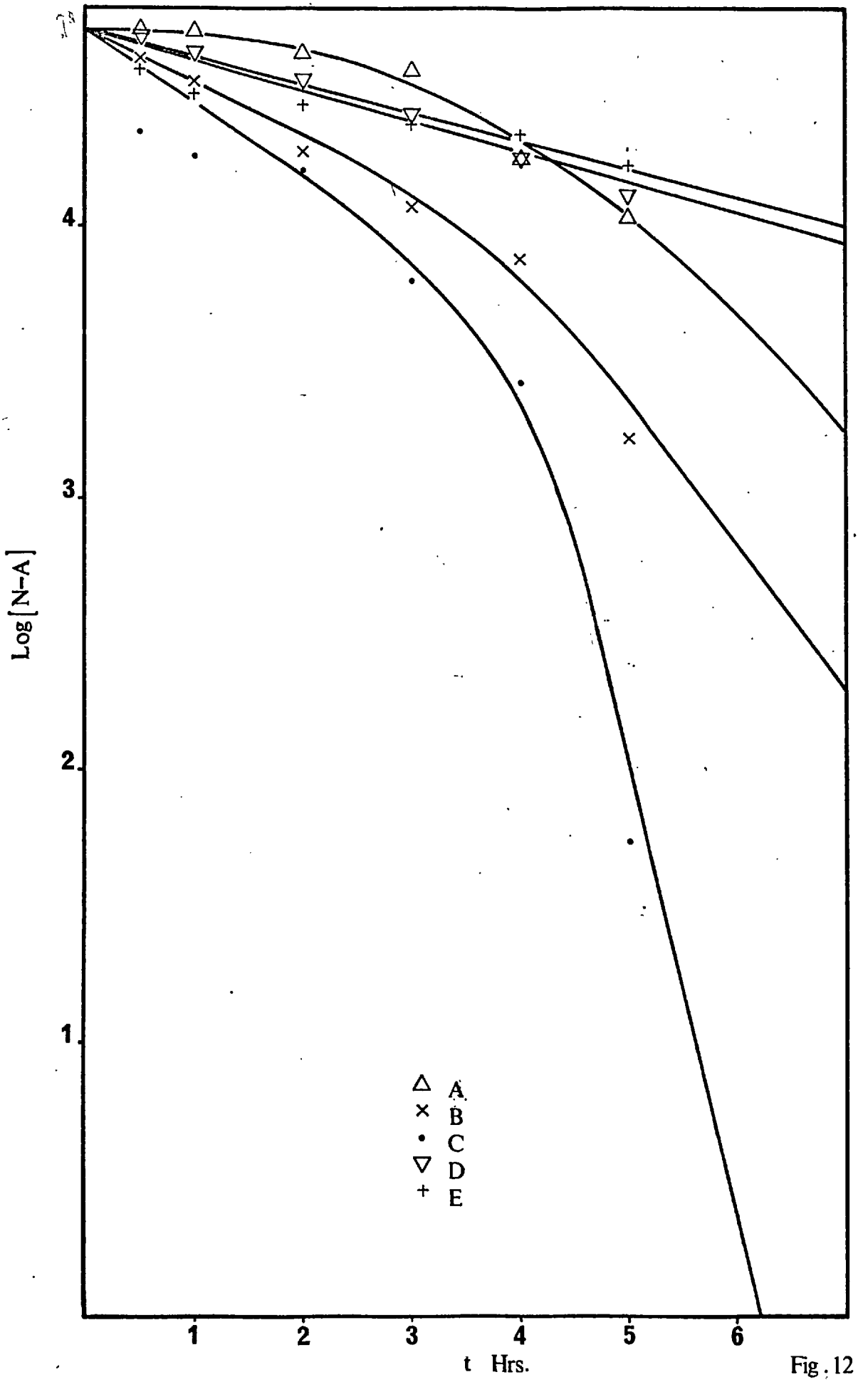


Fig. 12

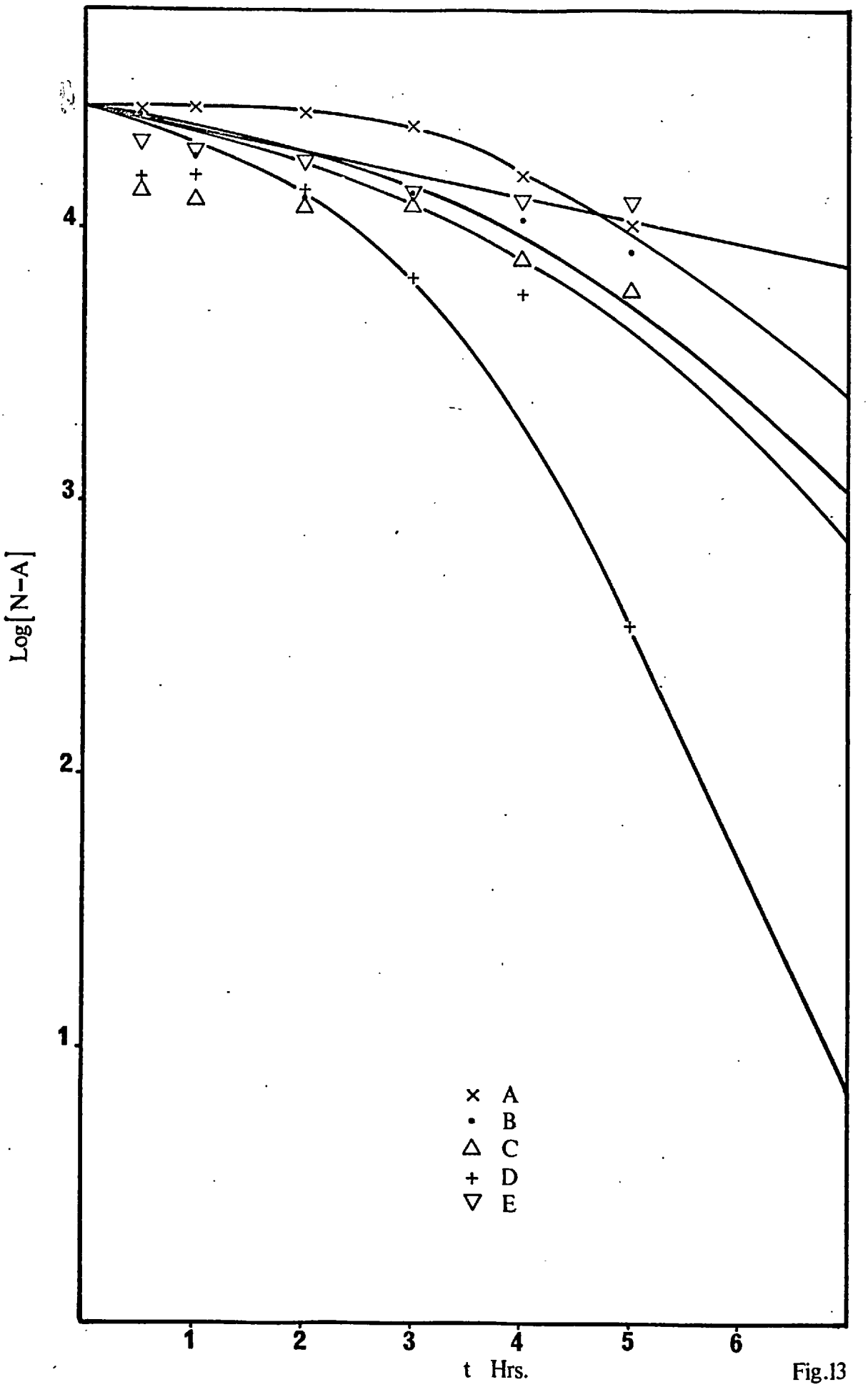


Fig.13

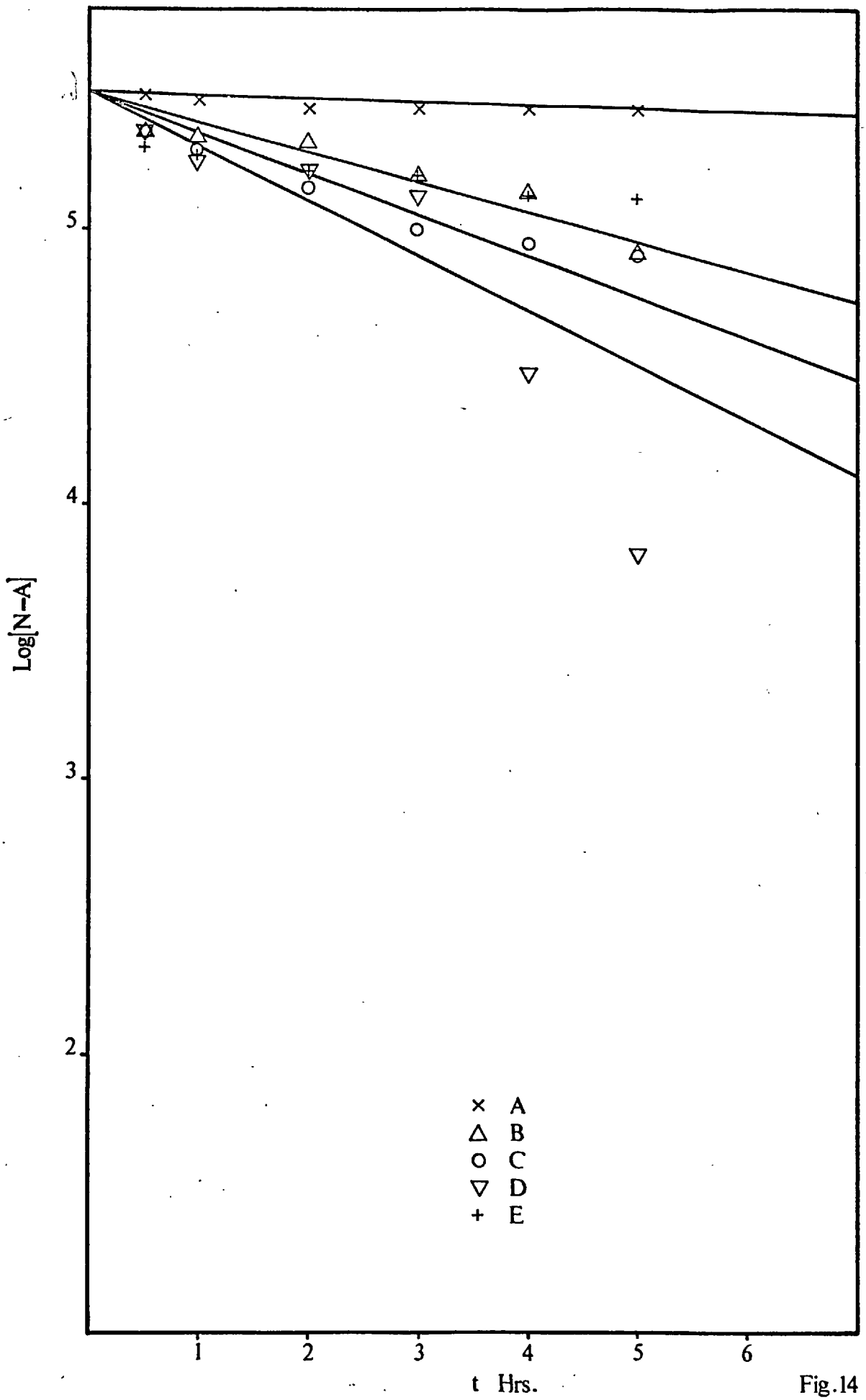


Fig.14

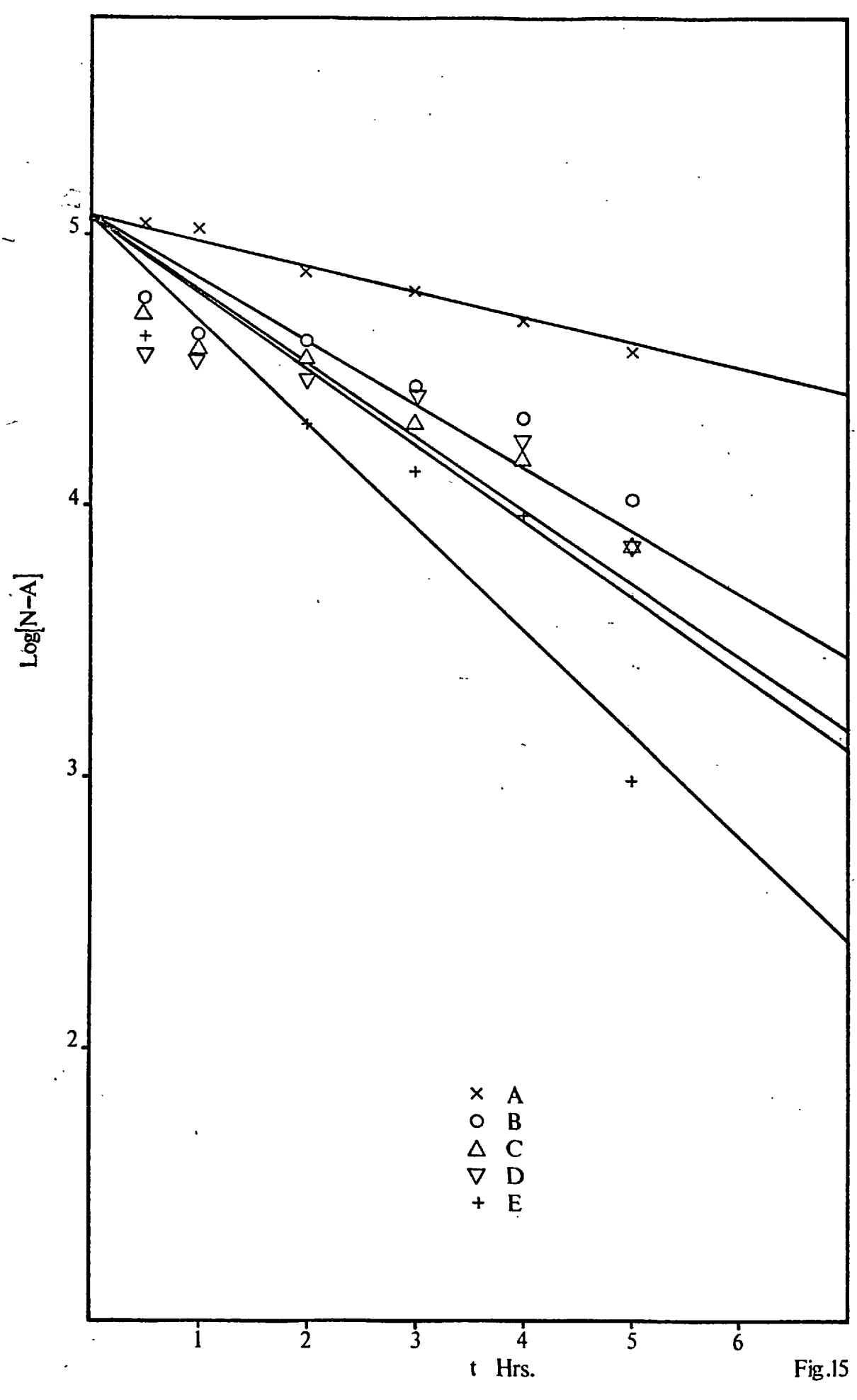


Fig.15

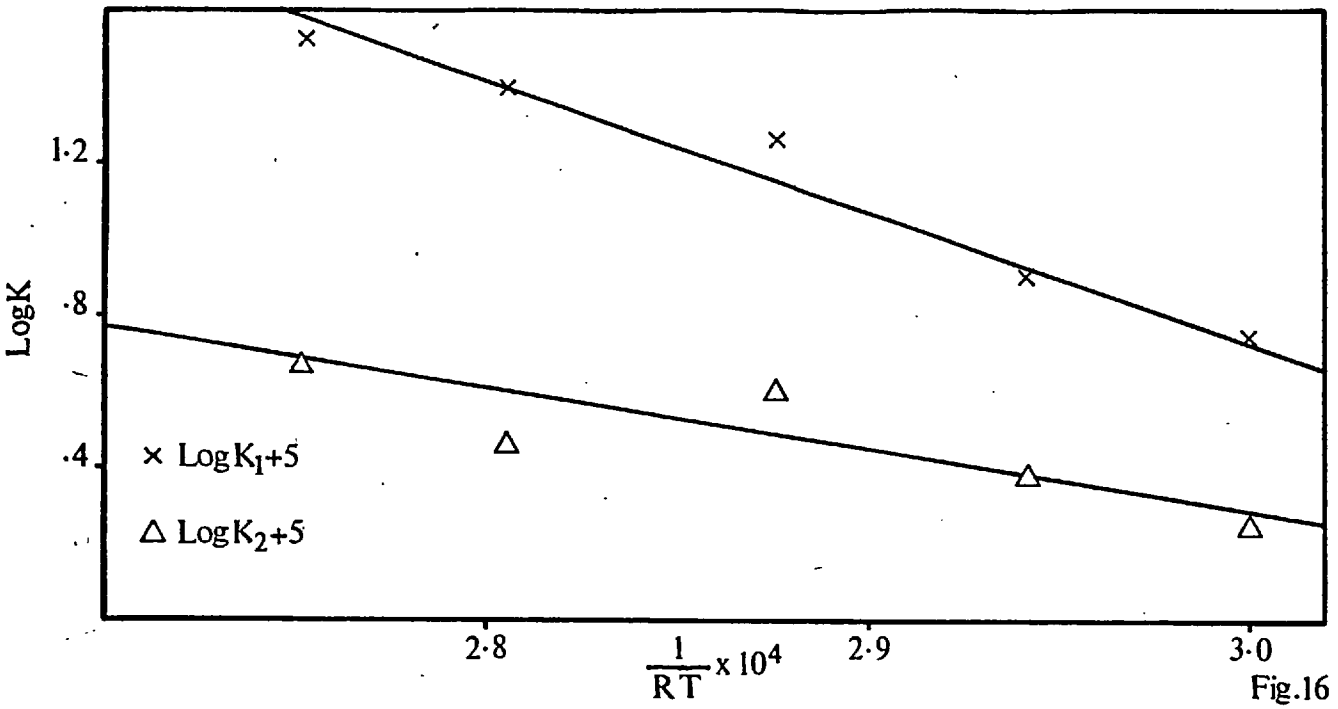

1·2
·8
·4
LogK
× Log K1+5
△ Log K2+5
2·8
2·9
3·0
1/RT x 10⁴

Fig.16

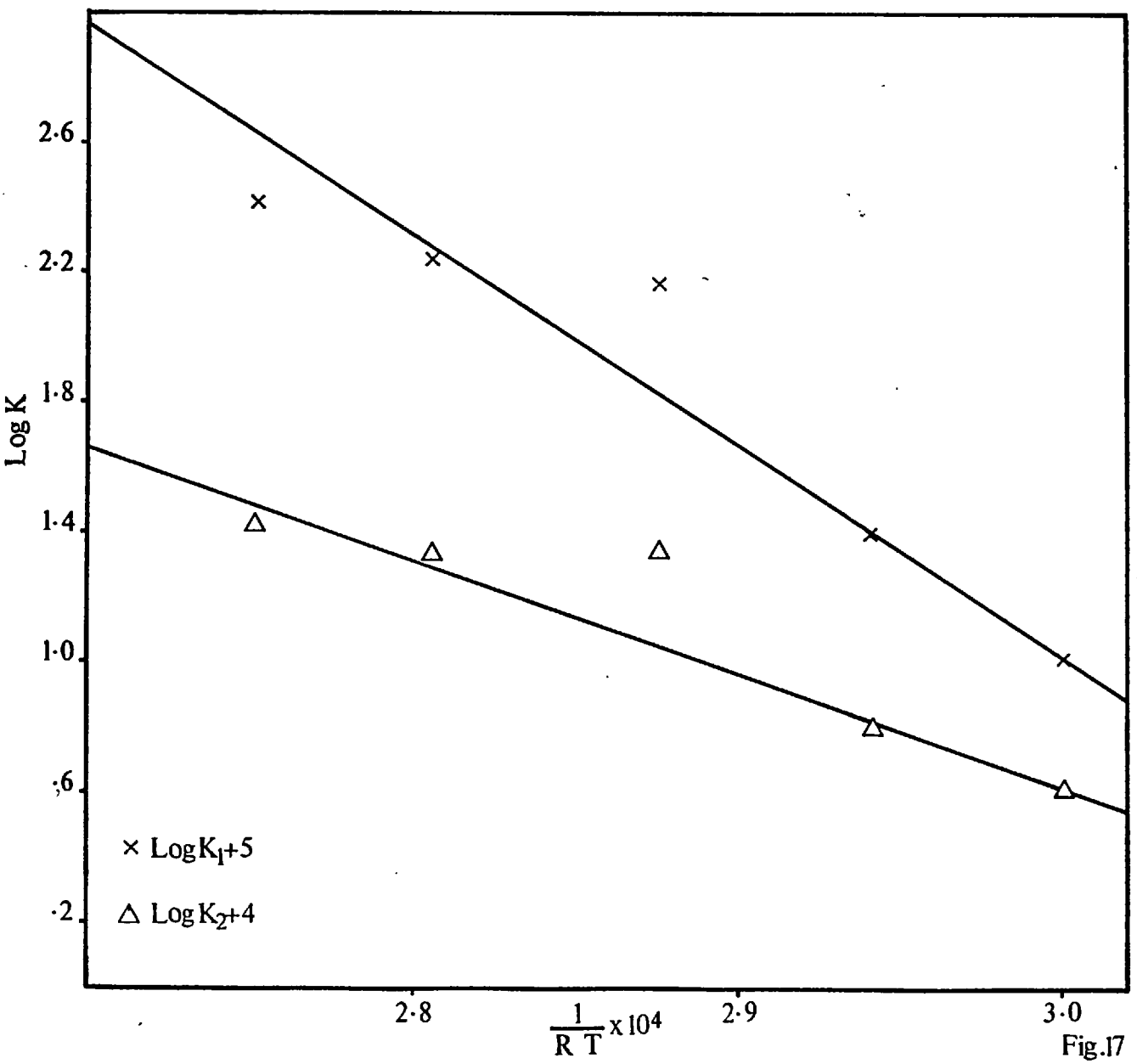

2·6
2·2
1·8
1·4
1·0
·6
·2
Log K
× Log K1+5
△ Log K2+4
2·8
2·9
3·0
1/RT x 10⁴

Fig.17

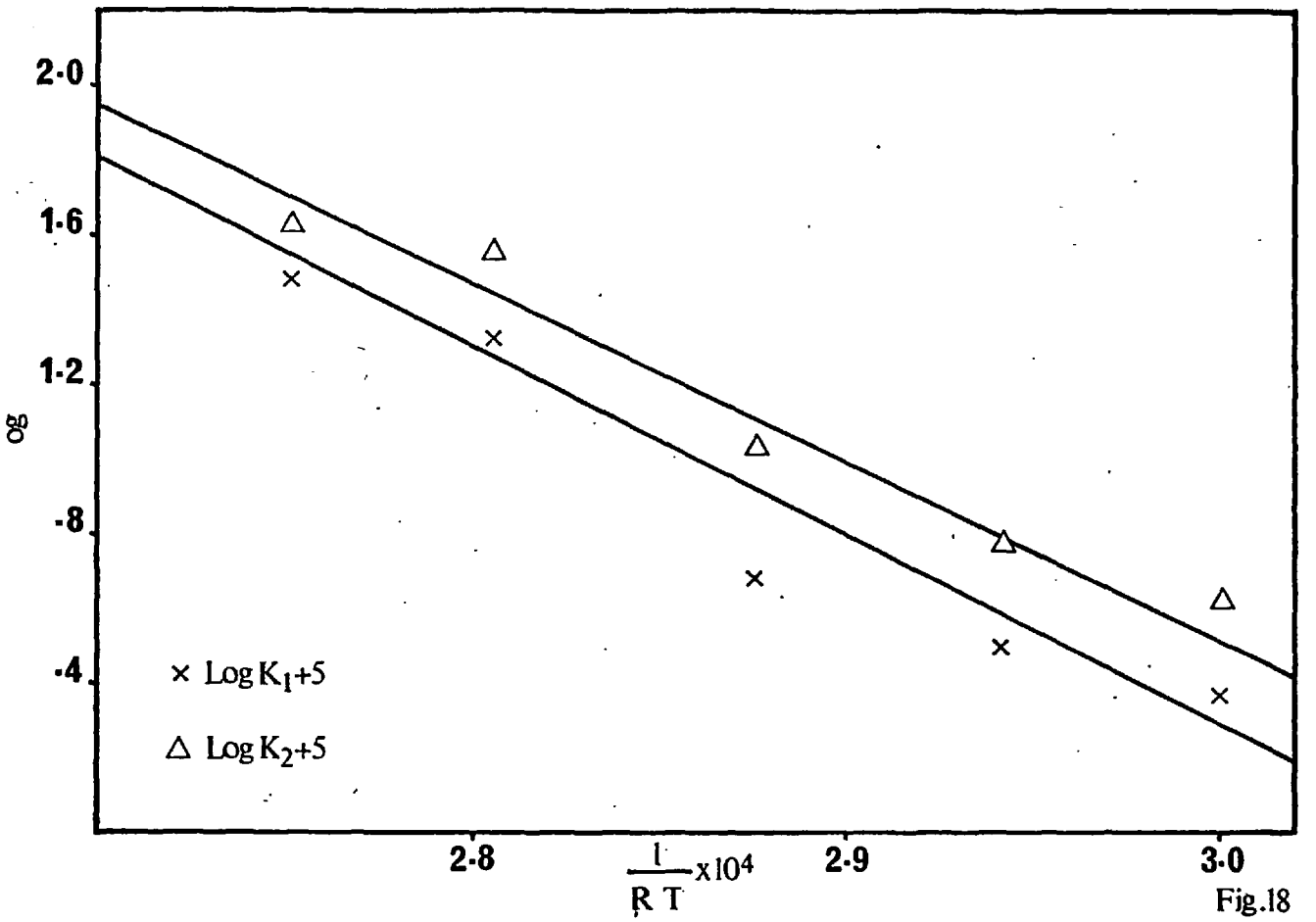

2·0
1·6
1·2
·8
·4
log
× Log K1+5
△ Log K2+5
2·8
2·9
3·0
1/RT x10⁴

Fig.18

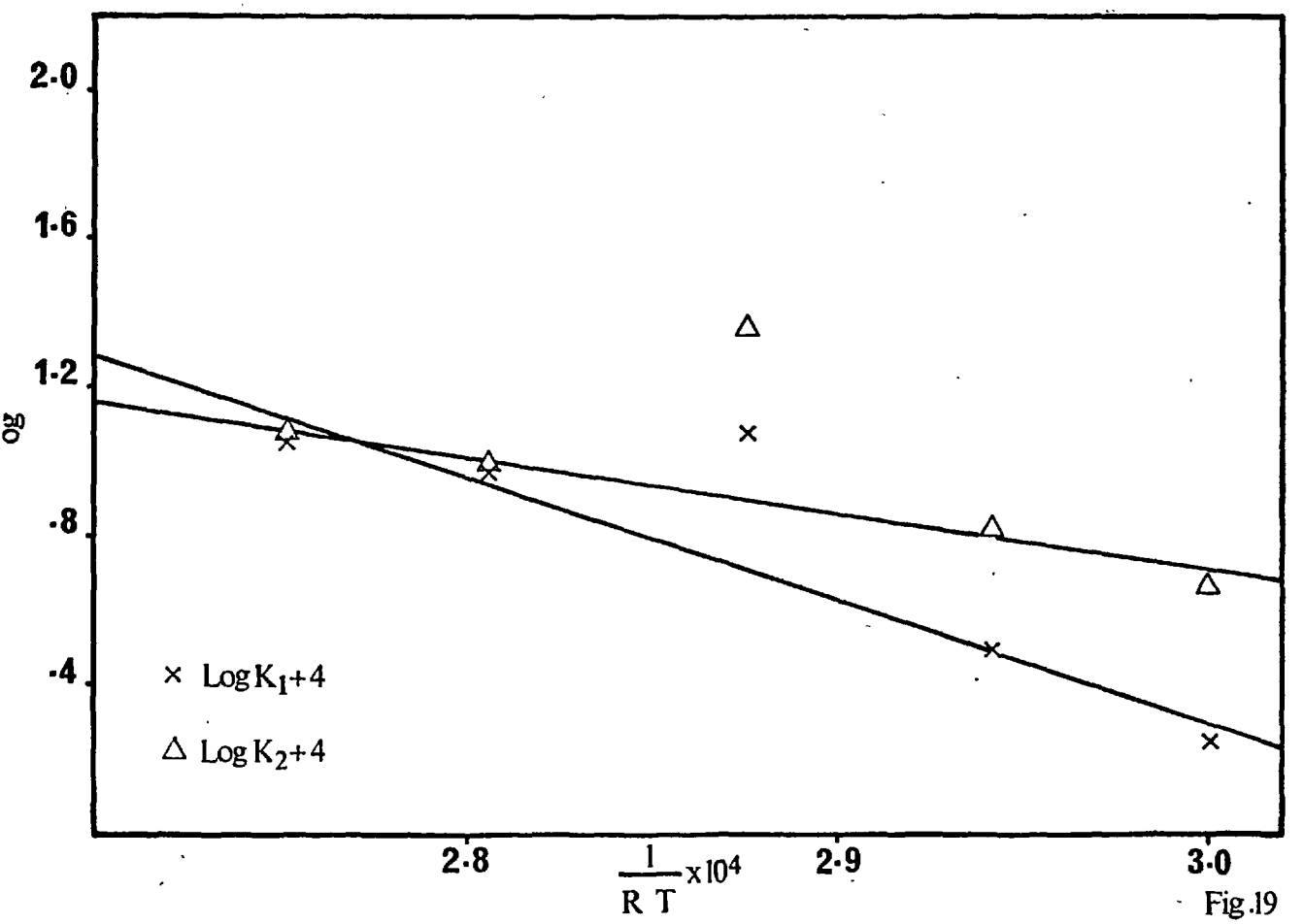

2·0
1·6
1·2
·8
·4
log
× Log K1+4
△ Log K2+4
2·8
2·9
3·0
1/RT x10⁴

Fig.19

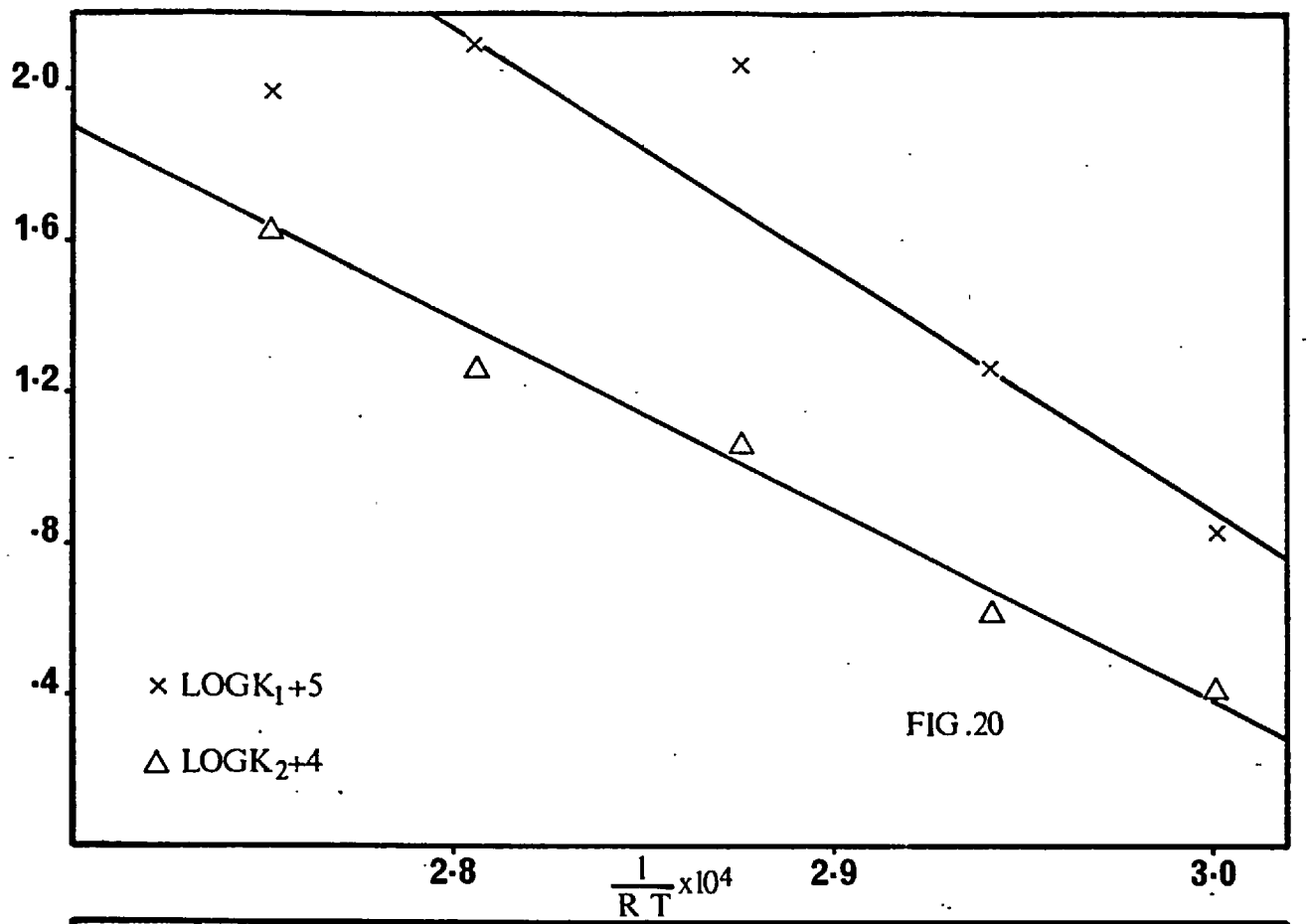

2·0
1·6
1·2
·8
·4
× LOGK1+5
△ LOGK2+4
2·8
1/RT x10⁴
2·9
3·0

FIG .20

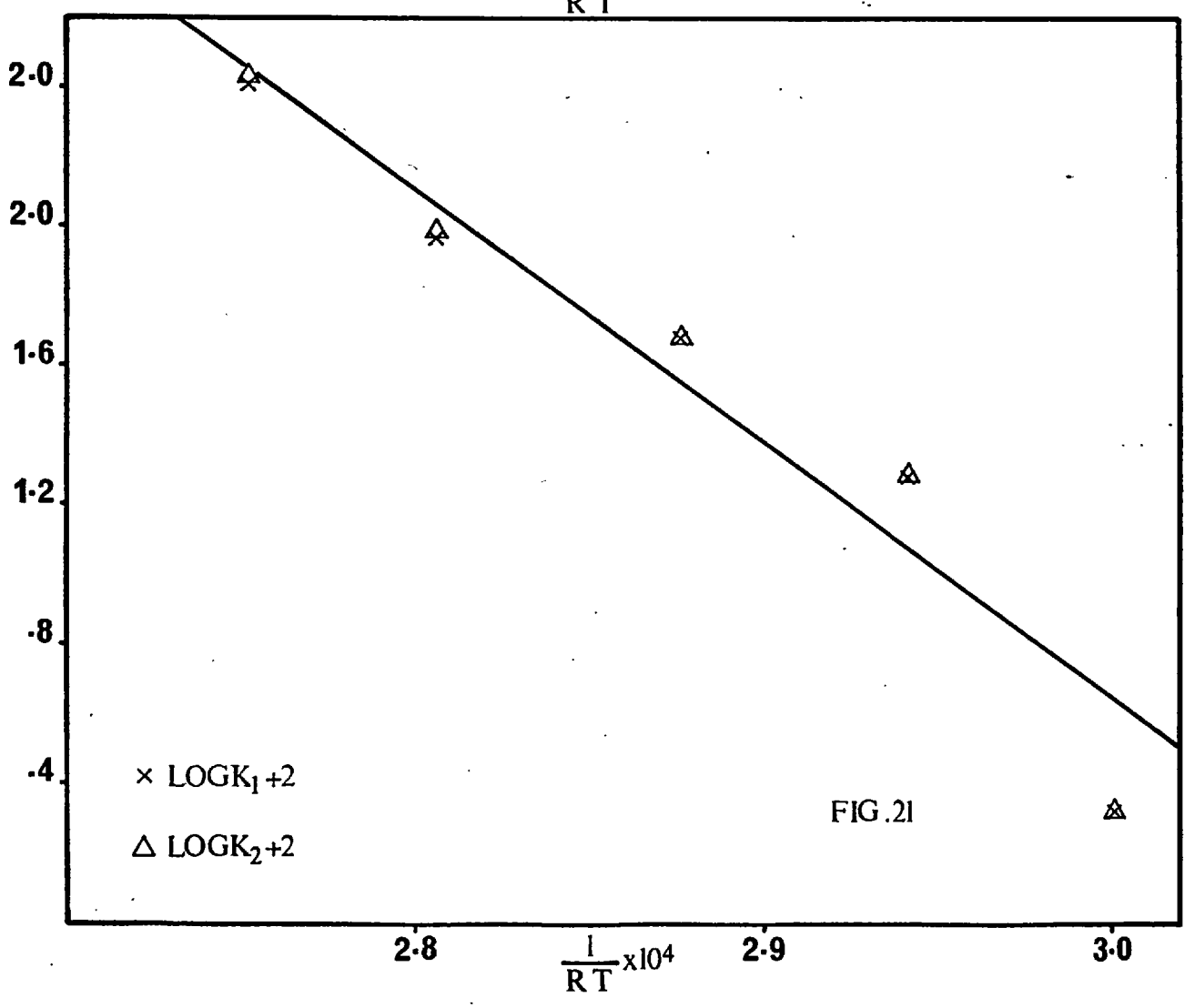

2·0
2·0
1·6
1·2
·8
·4
× LOGK1+2
△ LOGK2+2
2·8
1/RT x10⁴
2·9
3·0

FIG .21

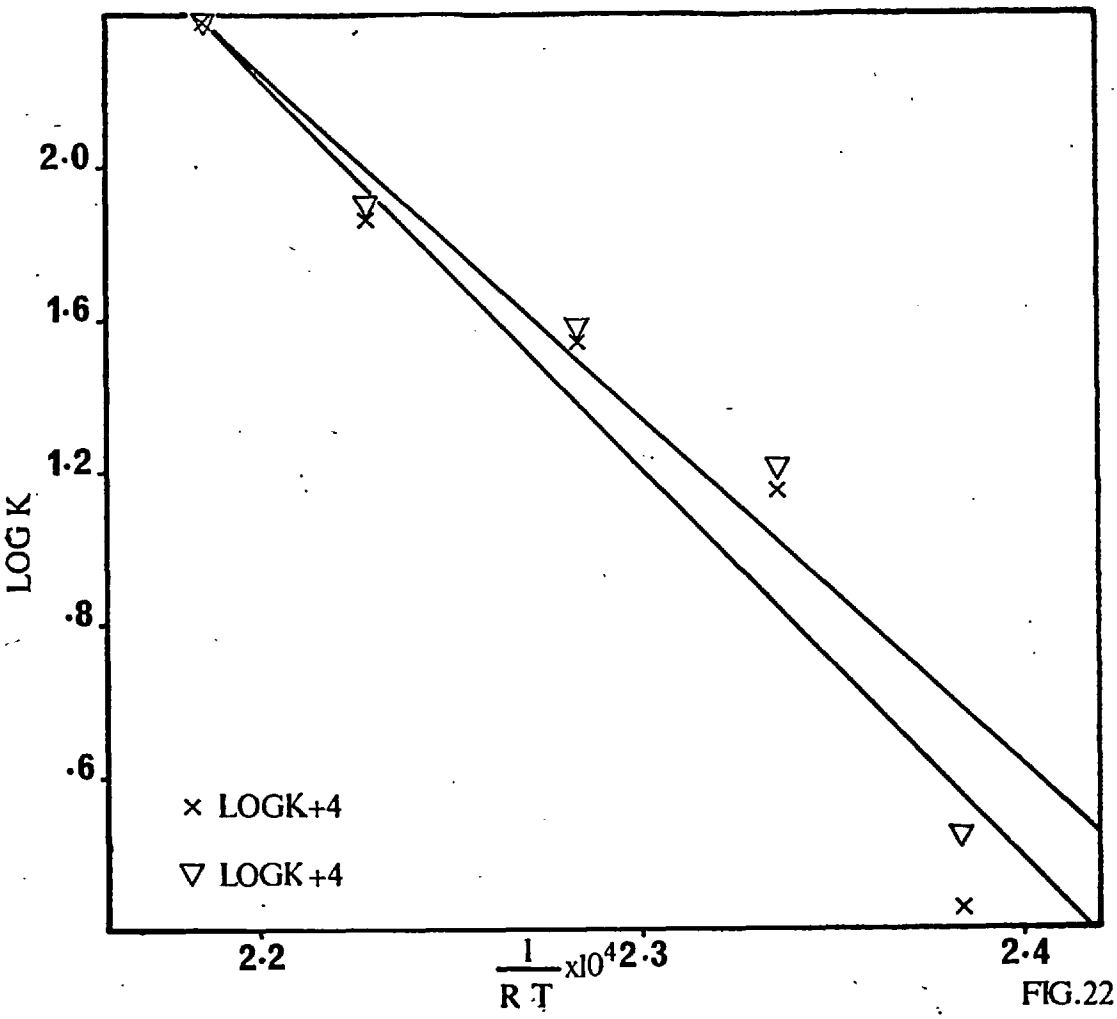

2·0
1·6
1·2
·8
·6
LOG K
× LOGK+4
▽ LOGK+4
2·2
2·3
2·4
$\frac{1}{RT}$ x10⁴

FIG.22

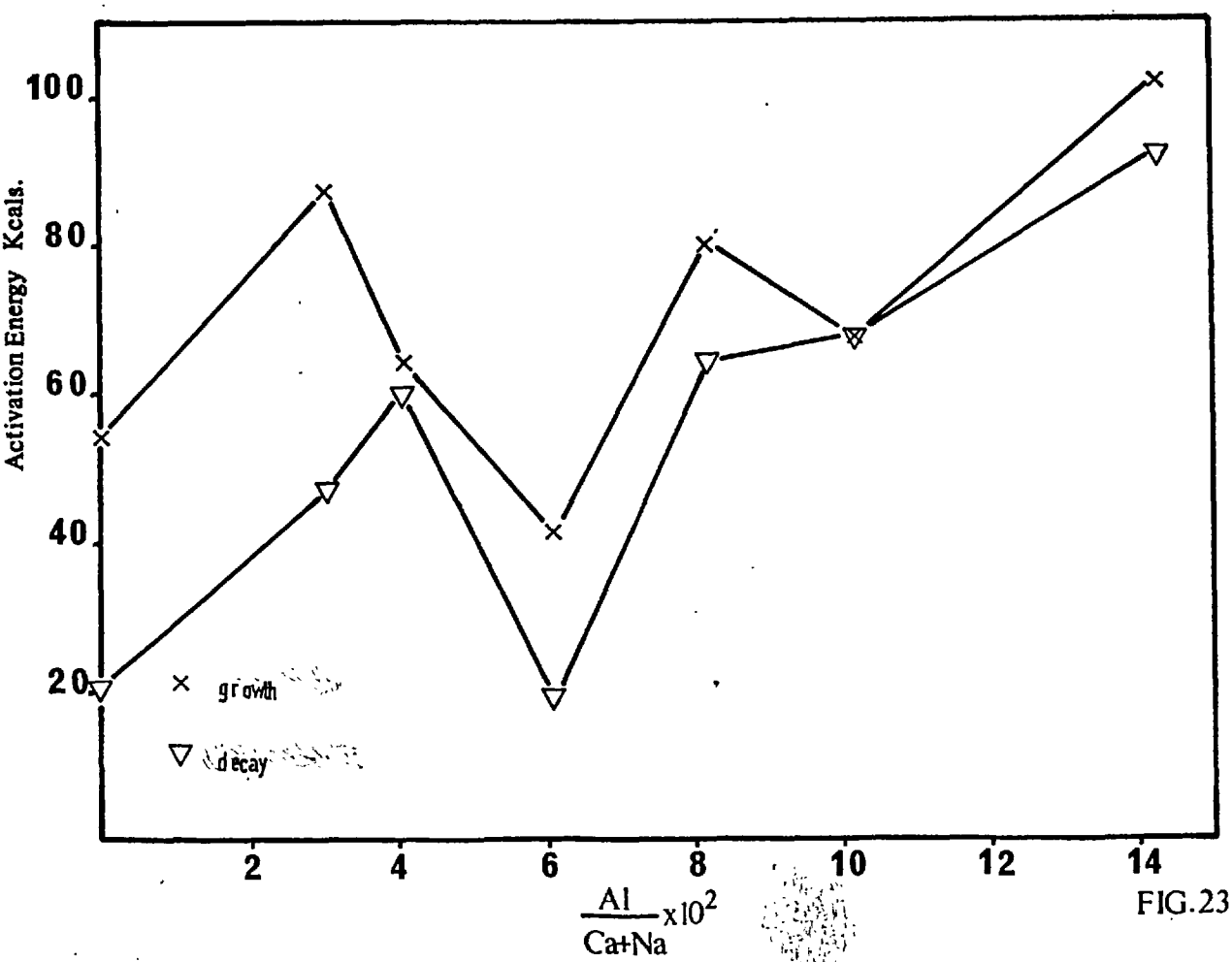

100
80
60
40
20
Activation Energy Kcals.
× growth
▽ decay
2
4
6
8
10
12
14
$\frac{Al}{Ca+Na}$ x10²

FIG.23

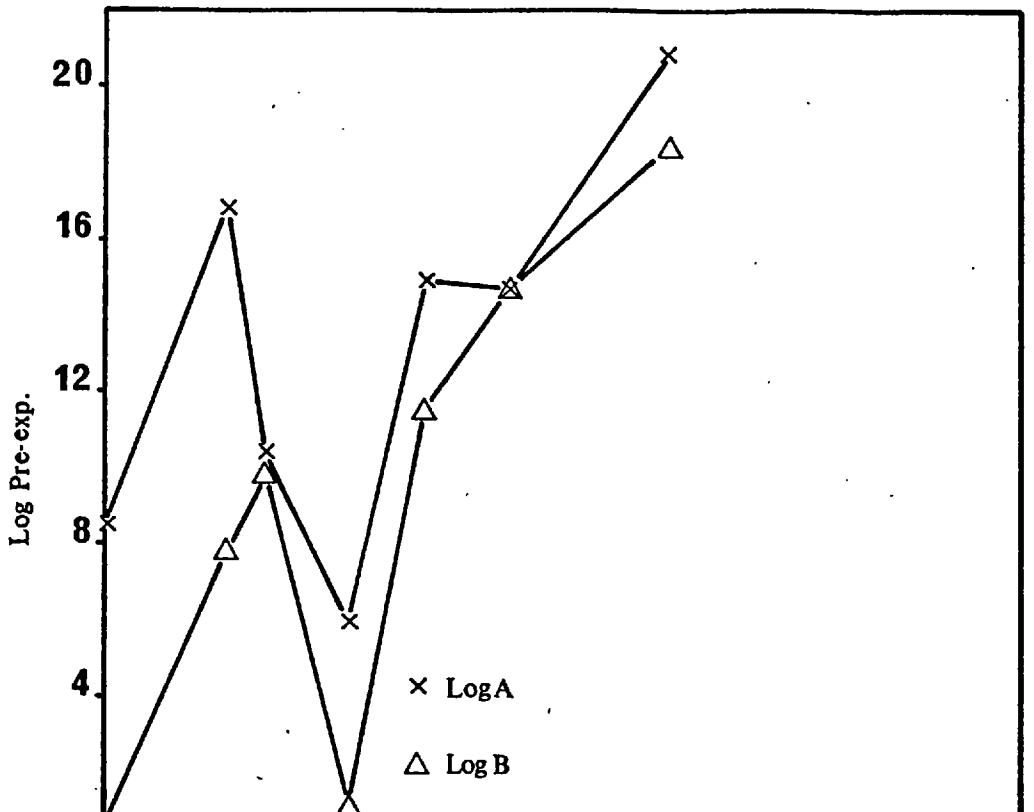

20
16
12
8
4
Log Pre-exp.
× Log A
△ Log B
1
2
3
4
5
Wt. % Al_2O_3

FIG.24

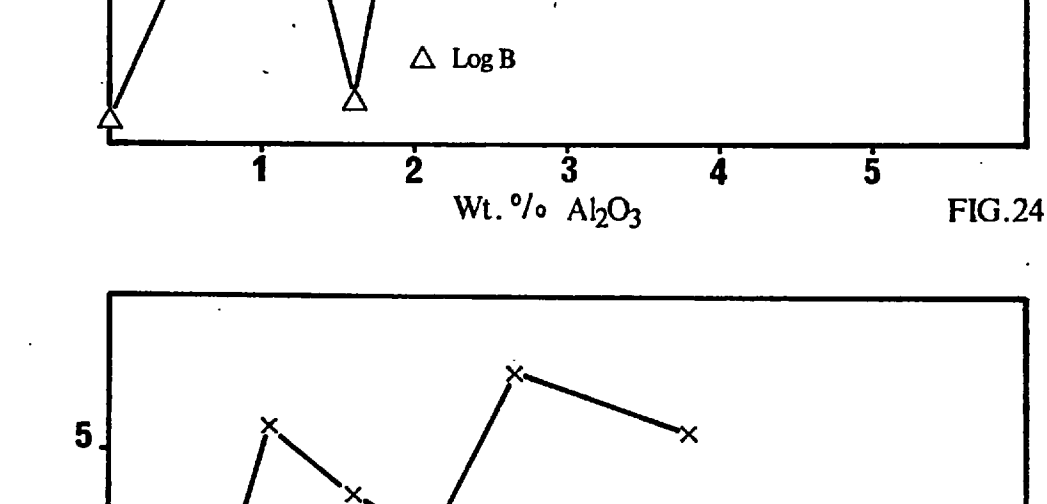

5
4
3
2
1
LOG N
1
2
3
4
5
Wt. % Al_2O_3

FIG.25

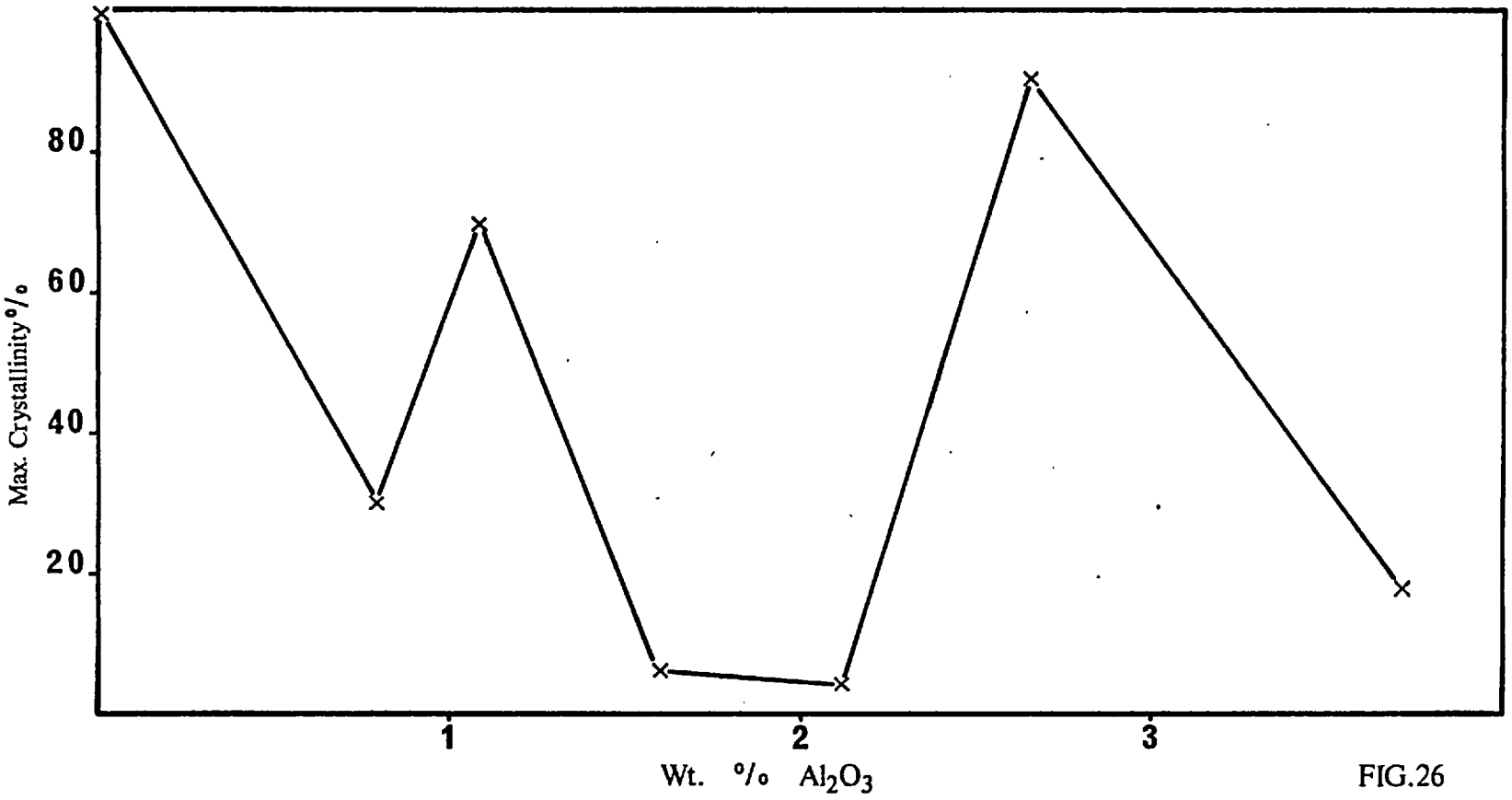


FIG.26

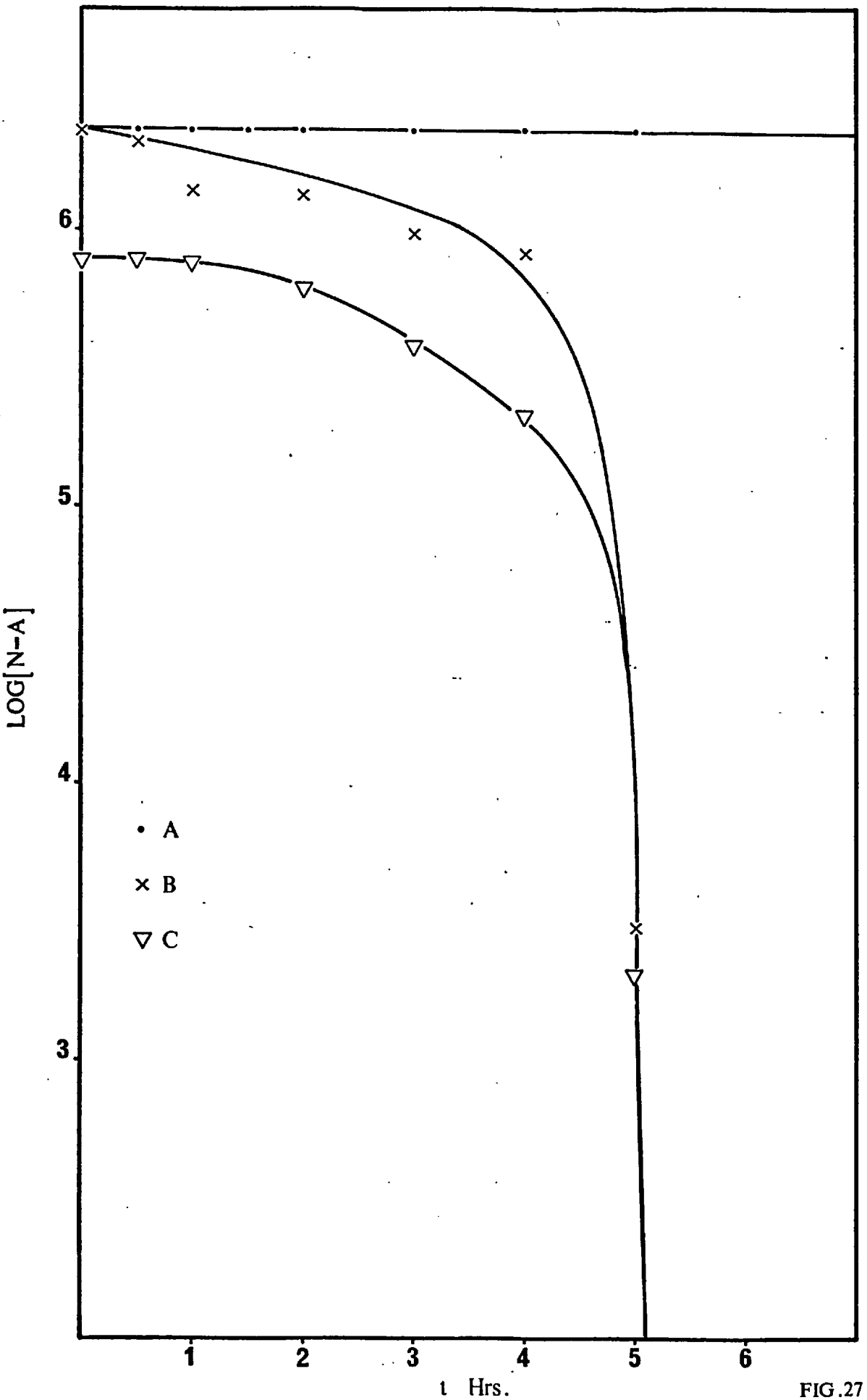


FIG.27

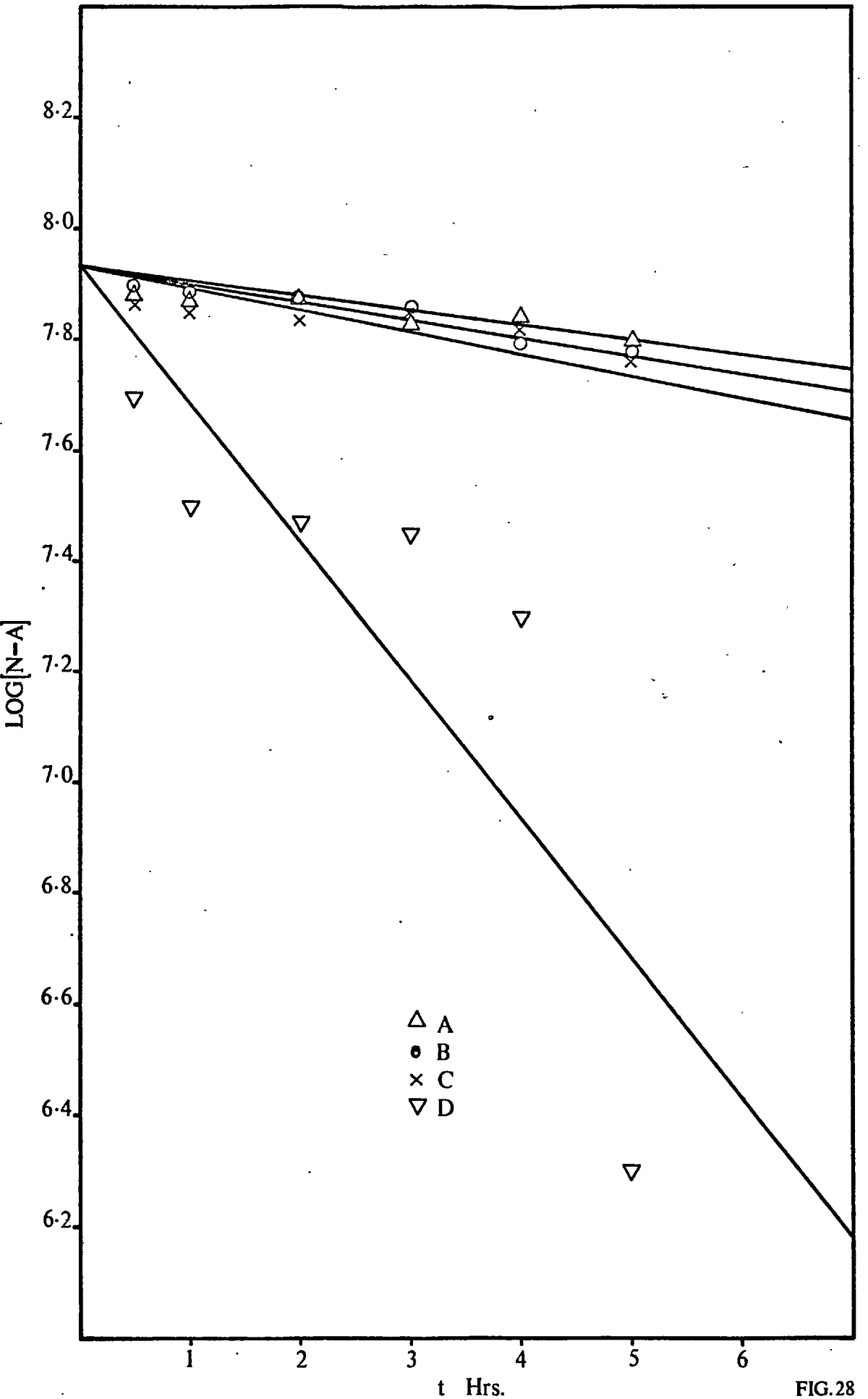


FIG.28

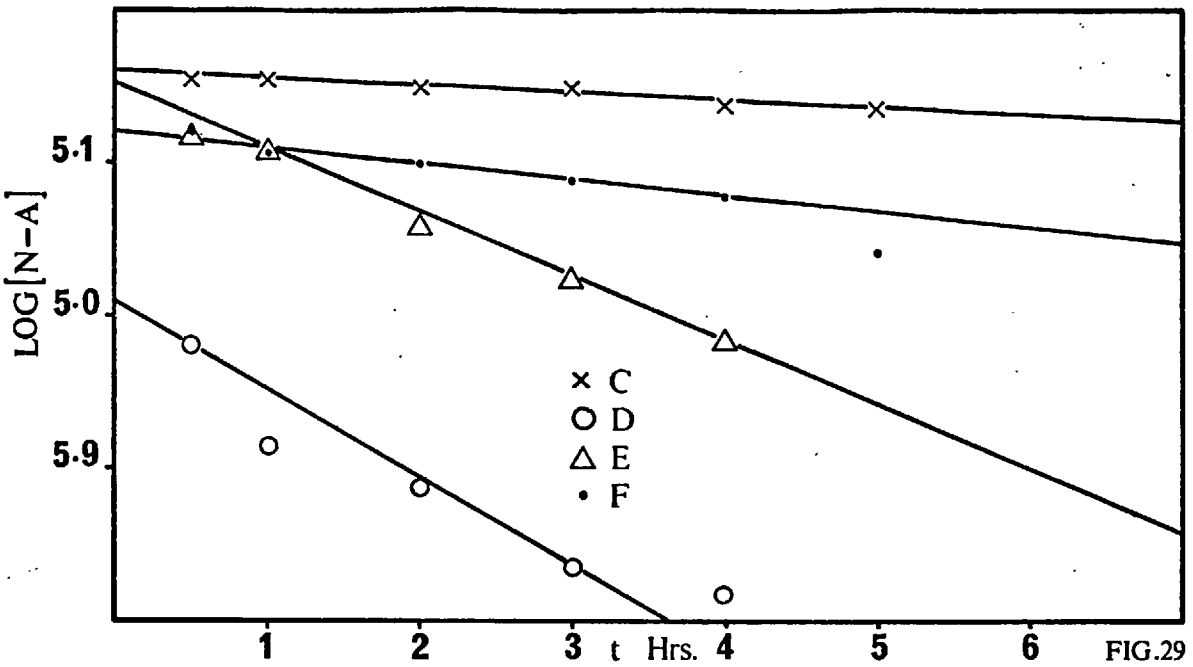

LOG[N-A]
5·1
5·0
5·9
× C
O D
△ E
• F
1
2
3
t Hrs.
4
5
6

FIG.29

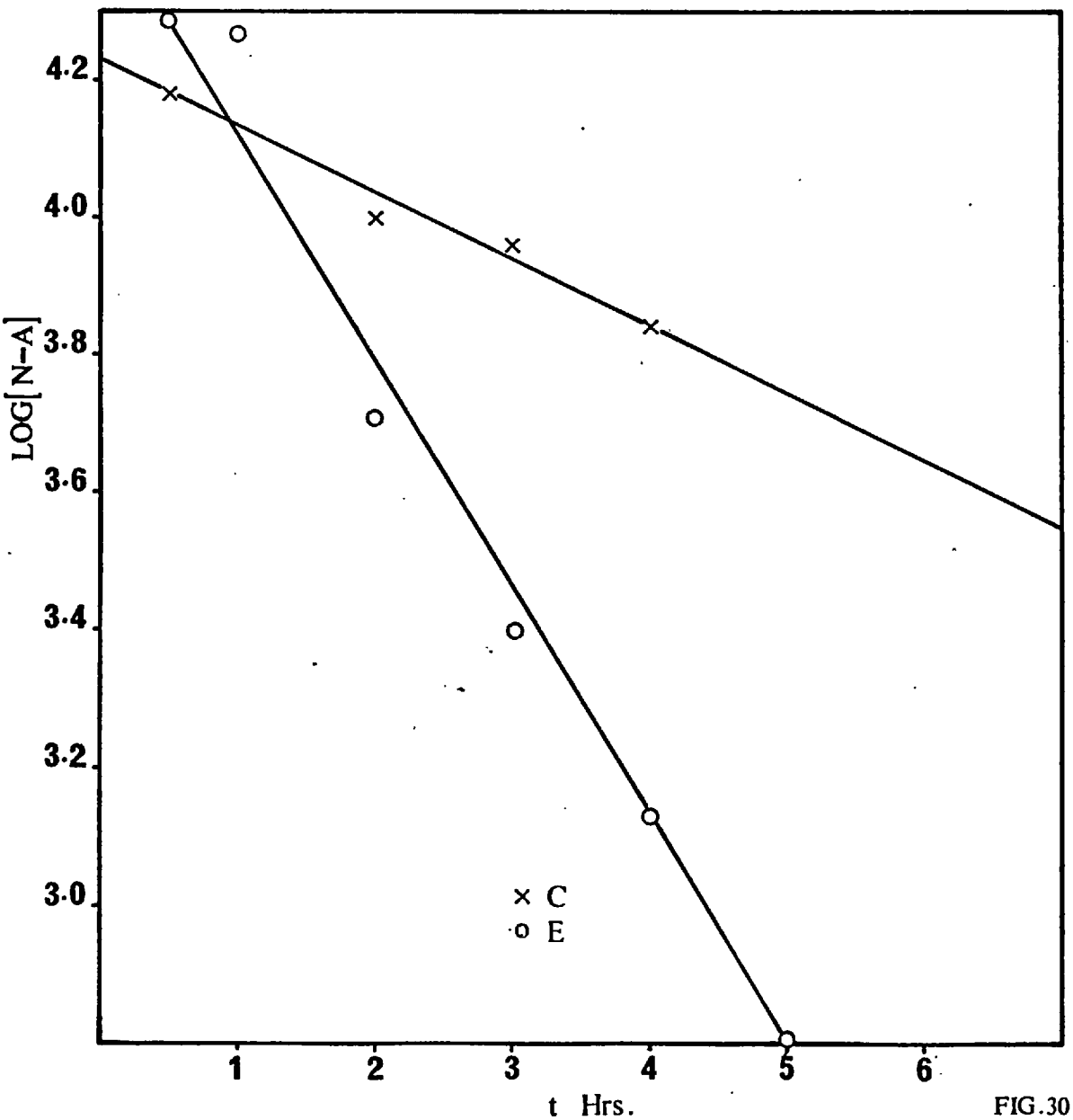

LOG[N-A]
4·2
4·0
3·8
3·6
3·4
3·2
3·0
× C
o E
1
2
3
4
5
6
t Hrs.

FIG.30

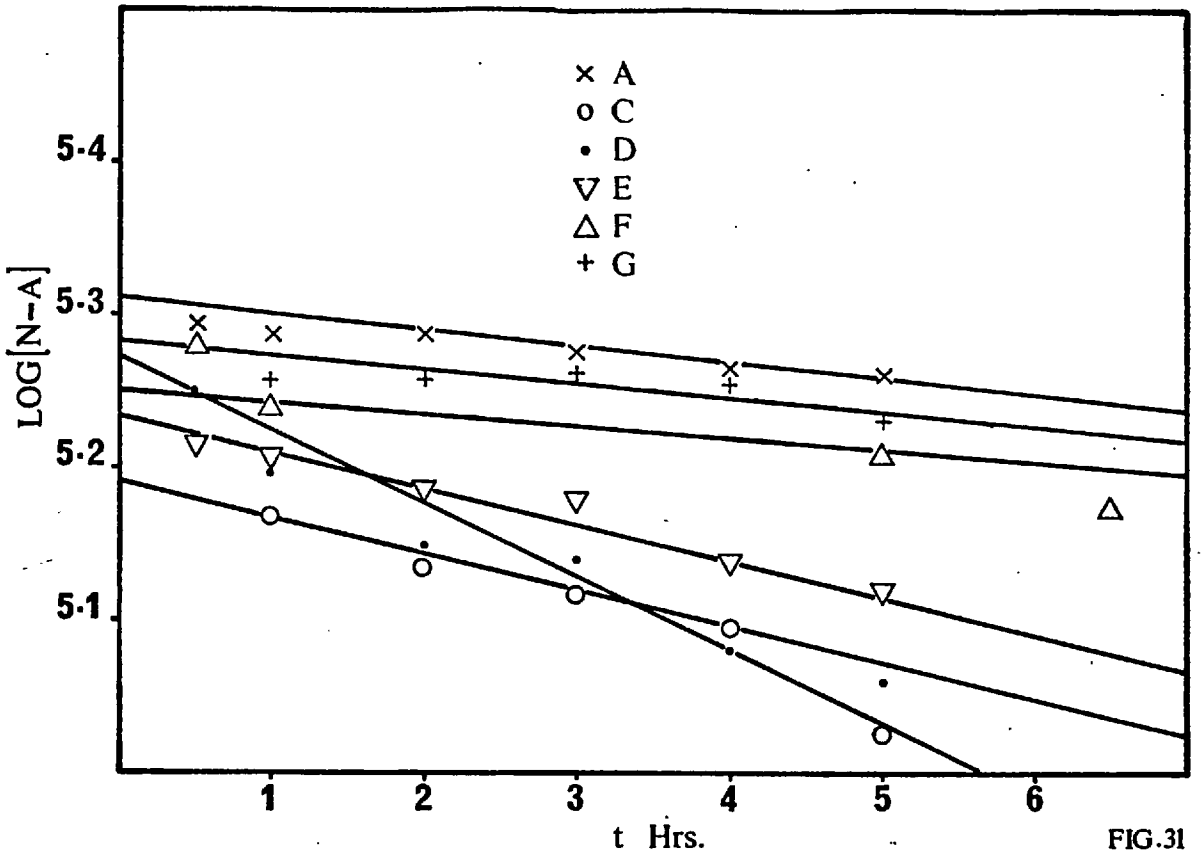

× A
o C
• D
▽ E
△ F
+ G
5·4
5·3
5·2
5·1
LOG[N-A]
1
2
3
4
5
6
t Hrs.

FIG.31

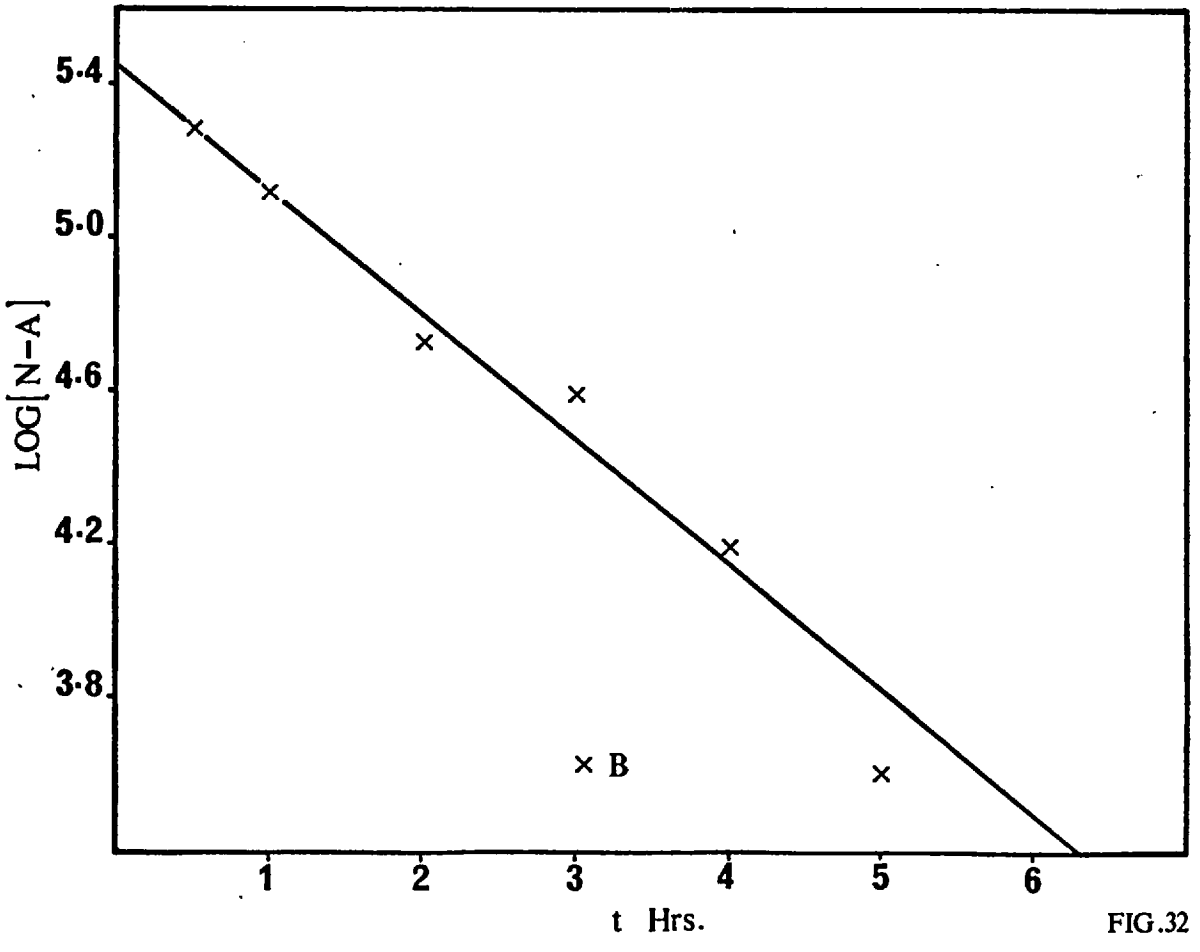

5·4
5·0
4·6
4·2
3·8
LOG[N-A]
× B
1
2
3
4
5
6
t Hrs.

FIG.32

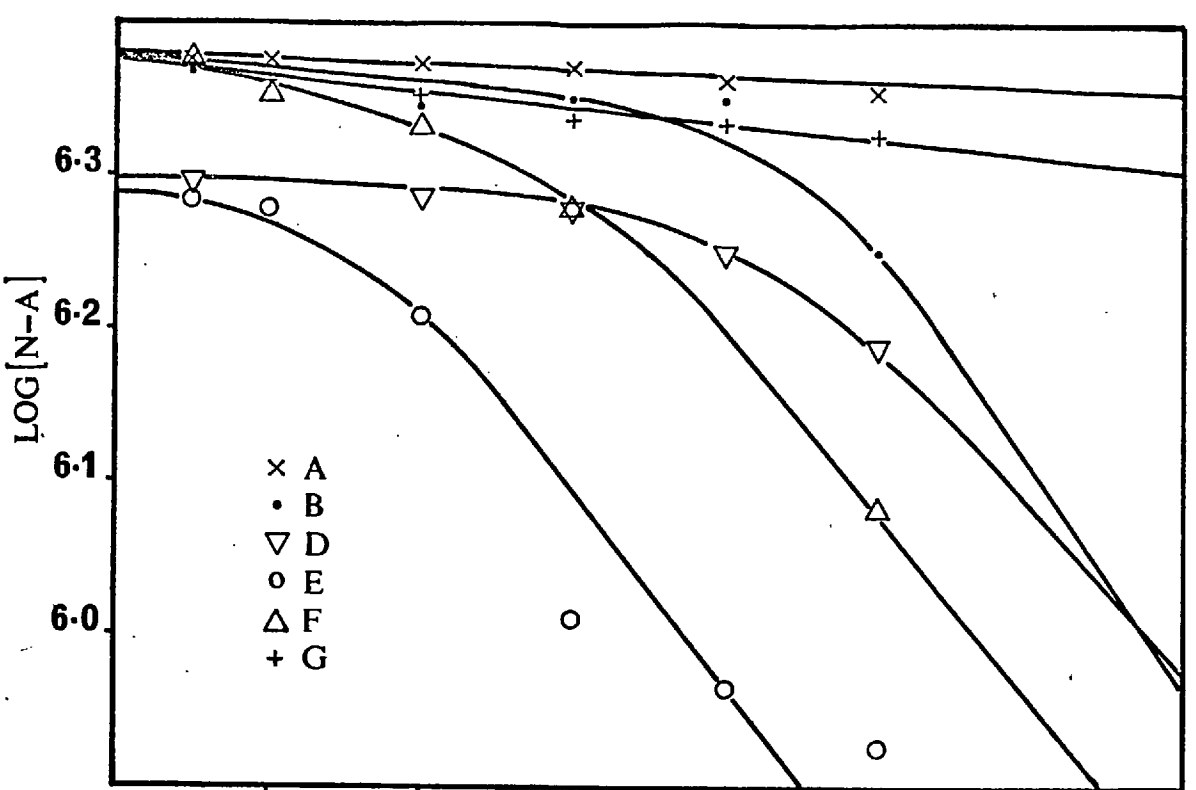

LOG[N-A]
6·3
6·2
6·1
6·0
× A
• B
▽ D
o E
△ F
+ G
1
2
3
4
5
6
t Hrs.

FIG.33

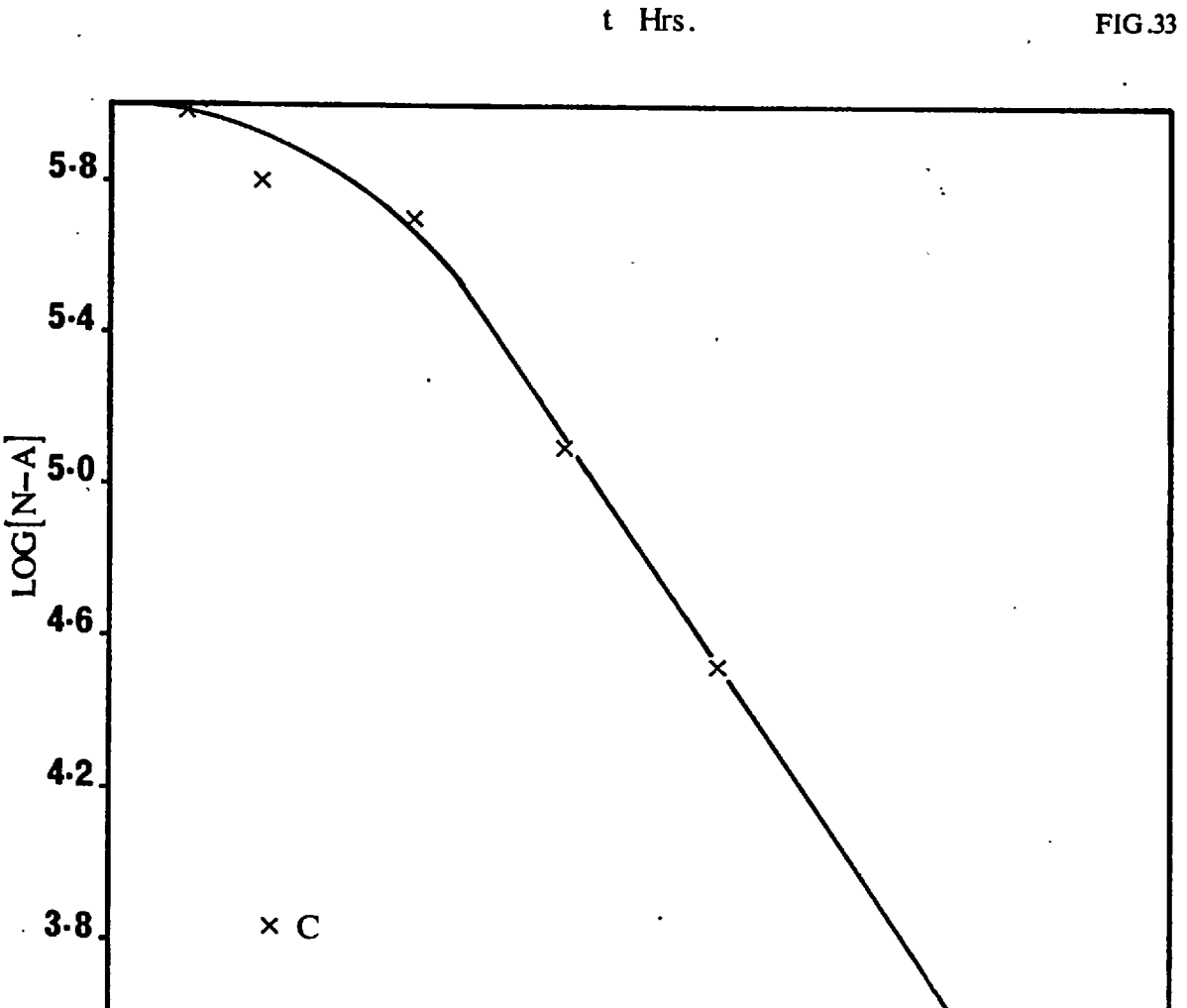

LOG[N-A]
5·8
5·4
5·0
4·6
4·2
3·8
× C
1
2
3
4
5
6
t Hrs.

FIG.34

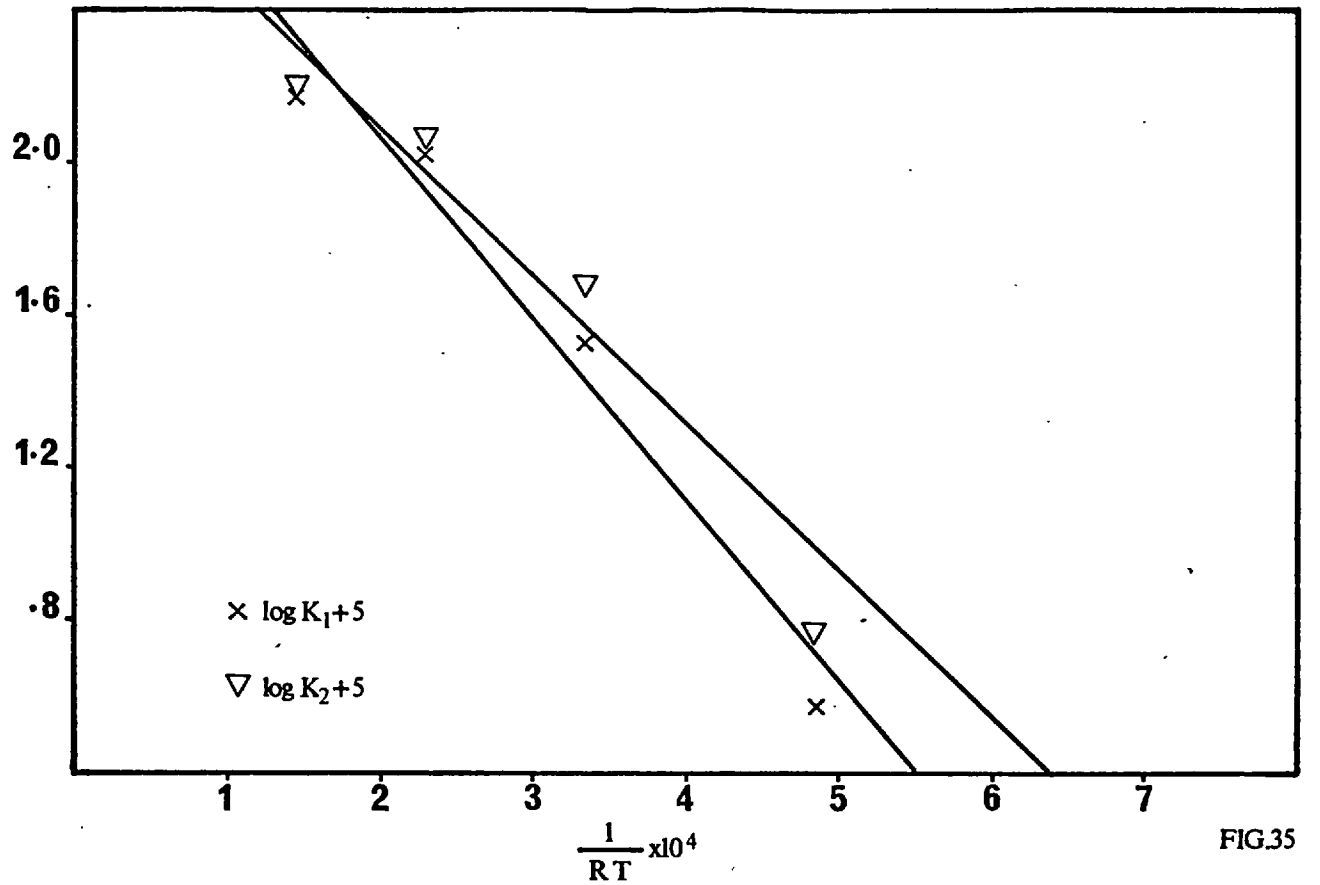

2·0
1·6
1·2
·8
× log K1+5
▽ log K2+5
1
2
3
4
5
6
7
1/RT x10⁴

FIG.35

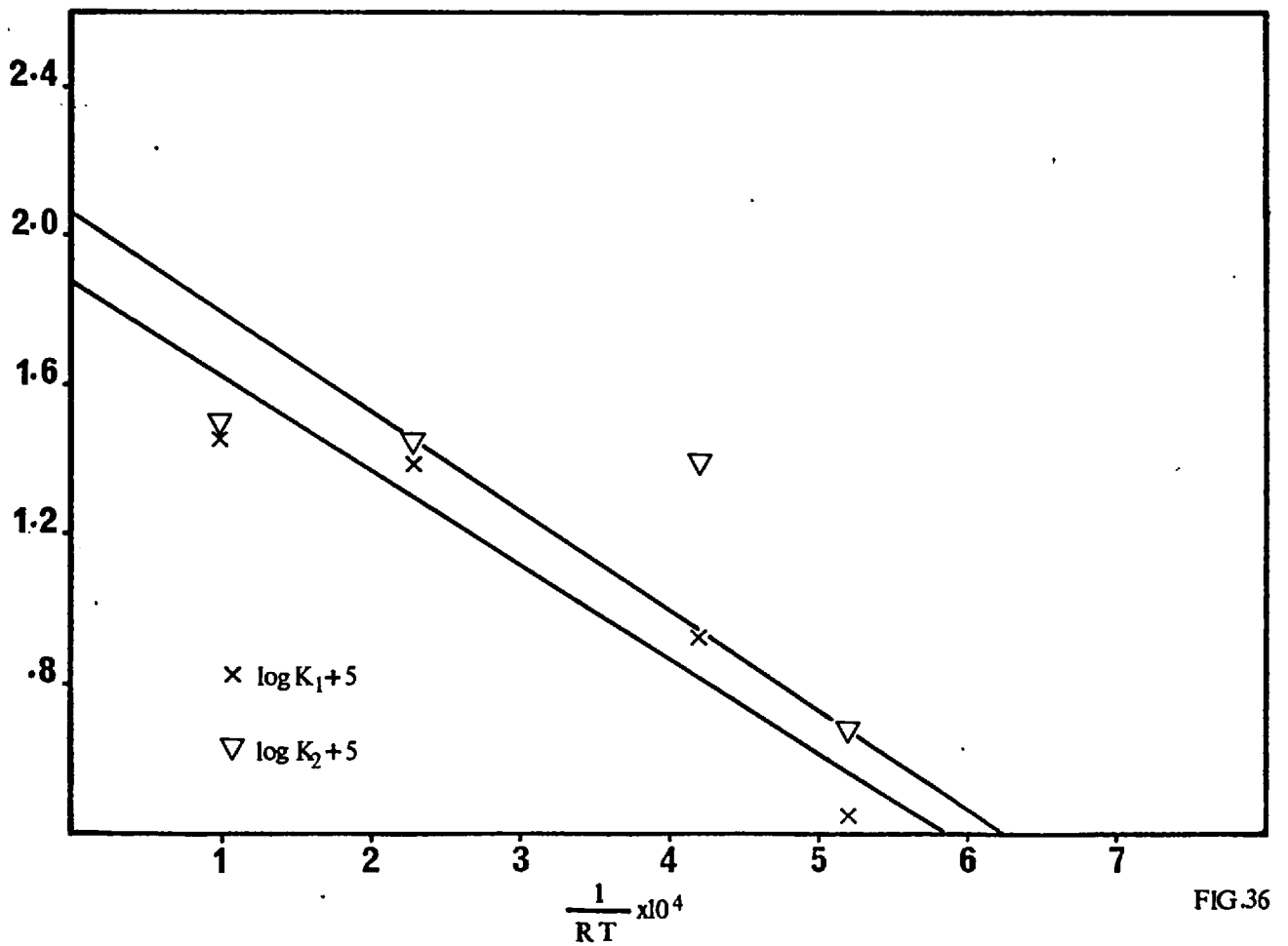

2·4
2·0
1·6
1·2
·8
× log K1+5
▽ log K2+5
1
2
3
4
5
6
7
1/RT x10⁴

FIG.36

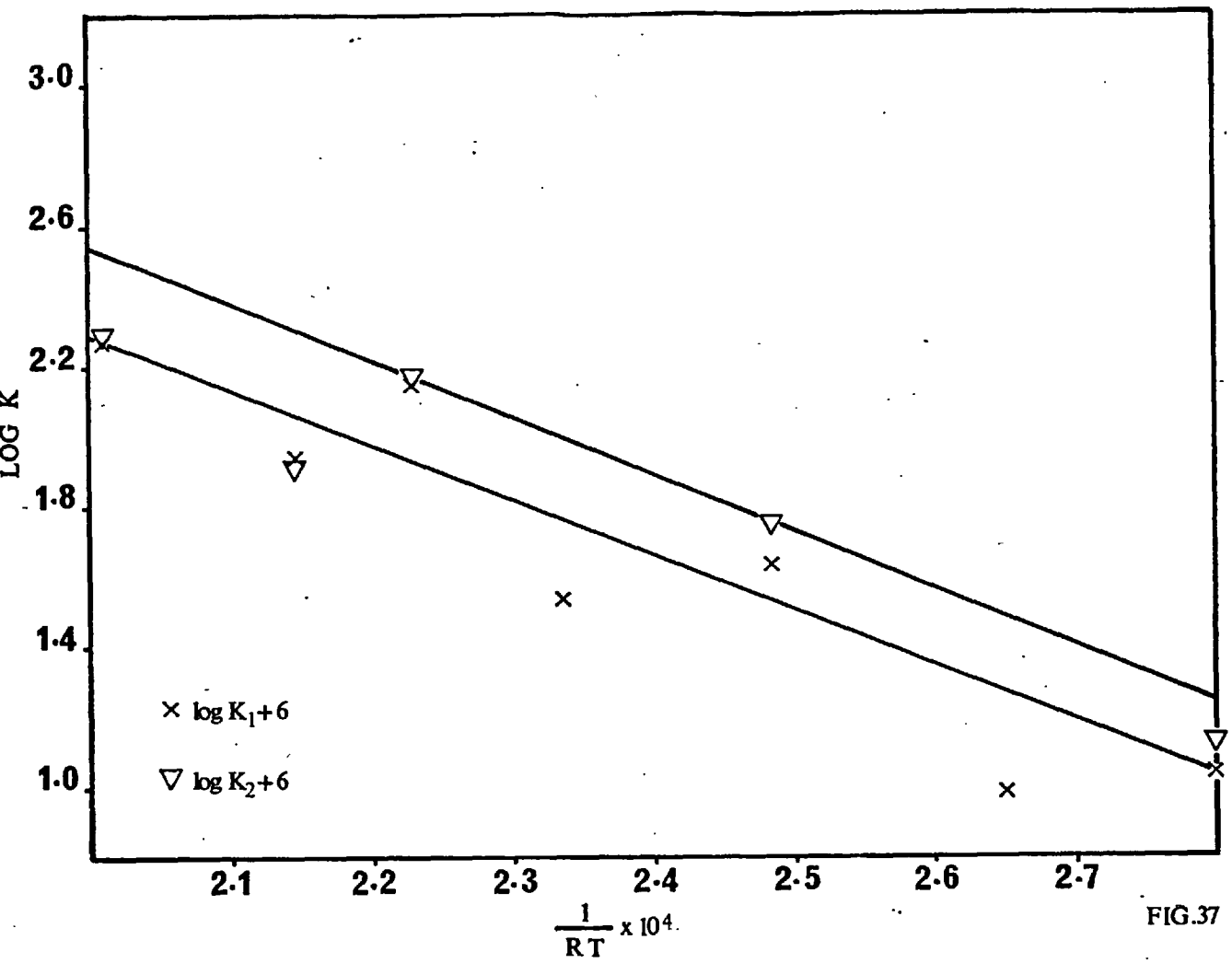

3·0
2·6
2·2
1·8
1·4
1·0
LOG K
× log K1+6
▽ log K2+6
2·1
2·2
2·3
2·4
2·5
2·6
2·7
1/RT x 10⁴

FIG.37

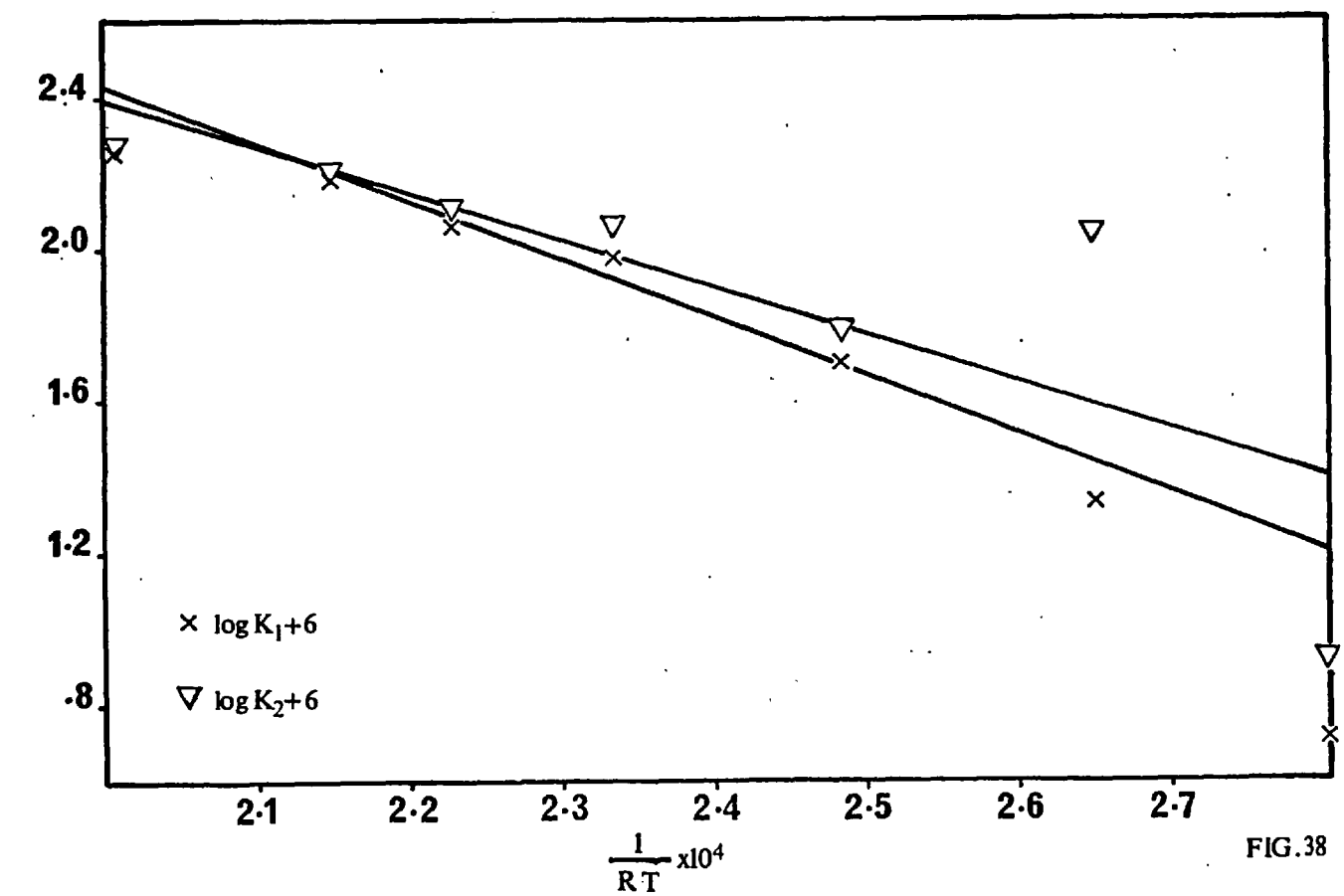

2·4
2·0
1·6
1·2
·8
× log K1+6
▽ log K2+6
2·1
2·2
2·3
2·4
2·5
2·6
2·7
1/RT x10⁴

FIG.38

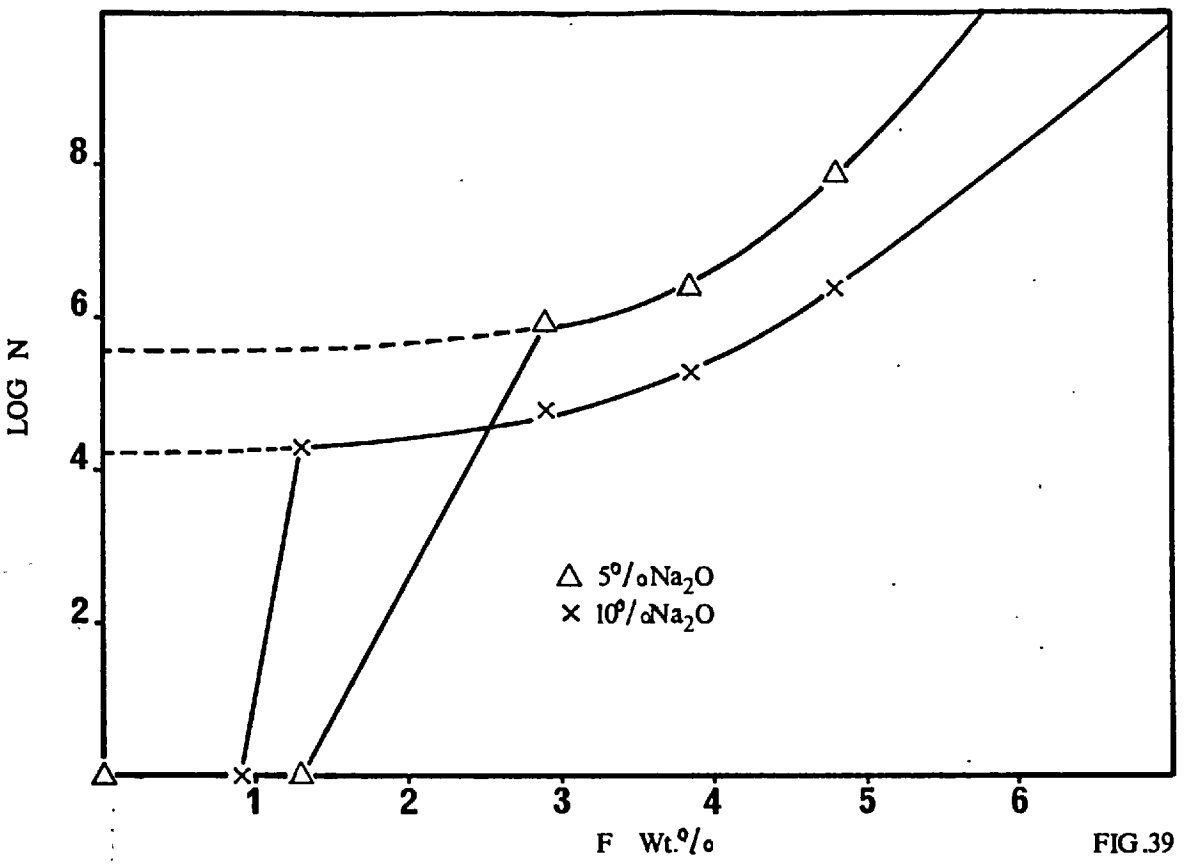

LOG N
8
6
4
2
1
2
3
4
5
6
F Wt.%
△ 5%Na2O
× 10%Na2O

FIG.39

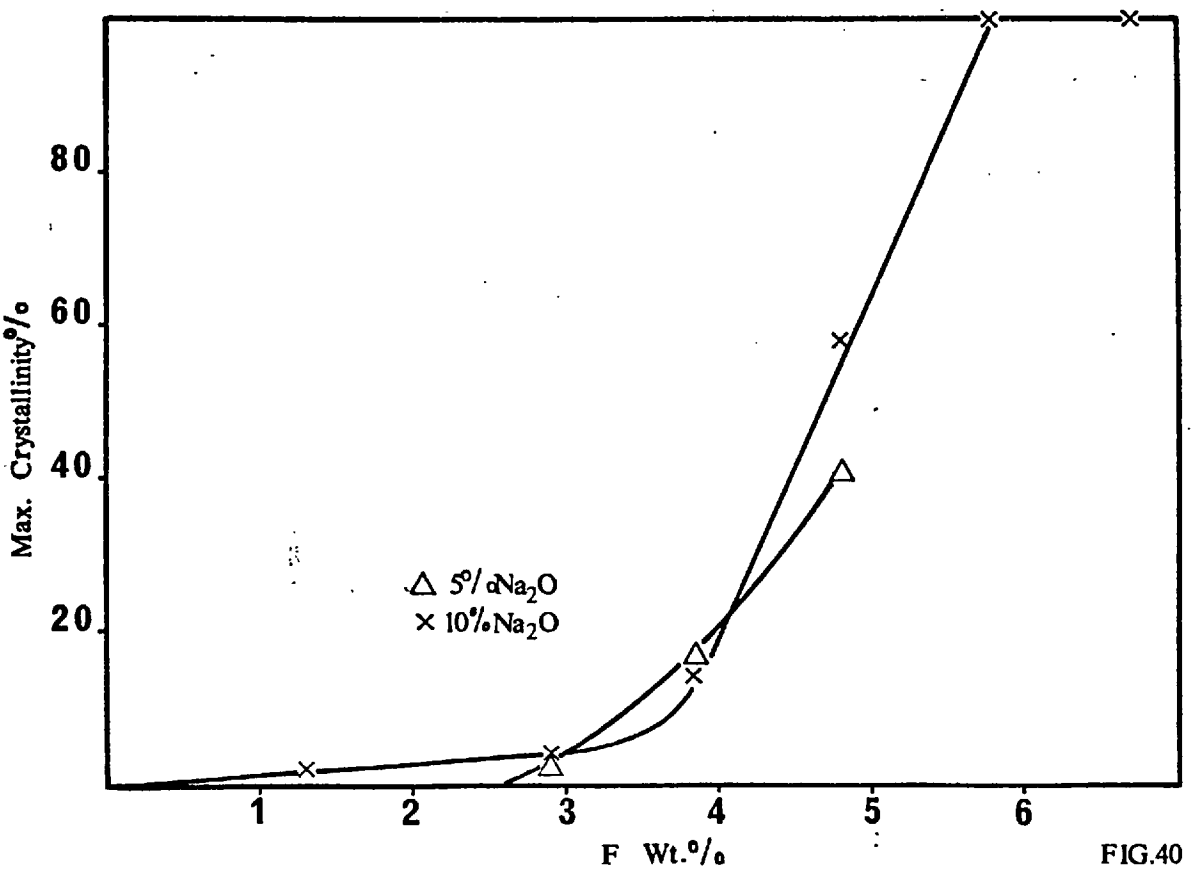

Max. Crystallinity%
80
60
40
20
1
2
3
4
5
6
F Wt.%
△ 5%Na2O
× 10%Na2O

FIG.40

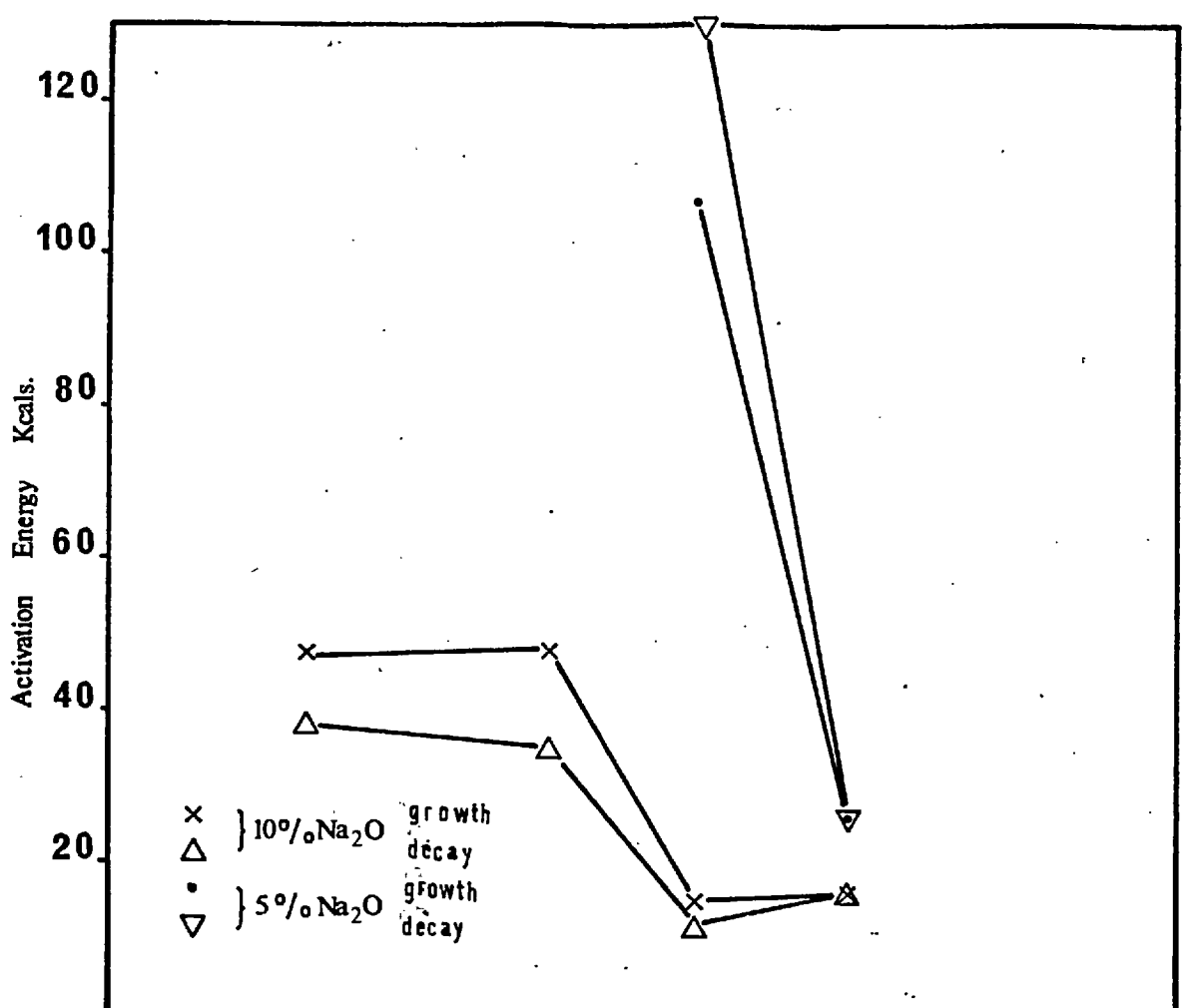

120
100
80
60
40
20
Activation Energy Kcals.
1
2
3
4
5
6
F Wt.%
10%Na2O growth
decay
5%Na2O growth
decay

FIG.41

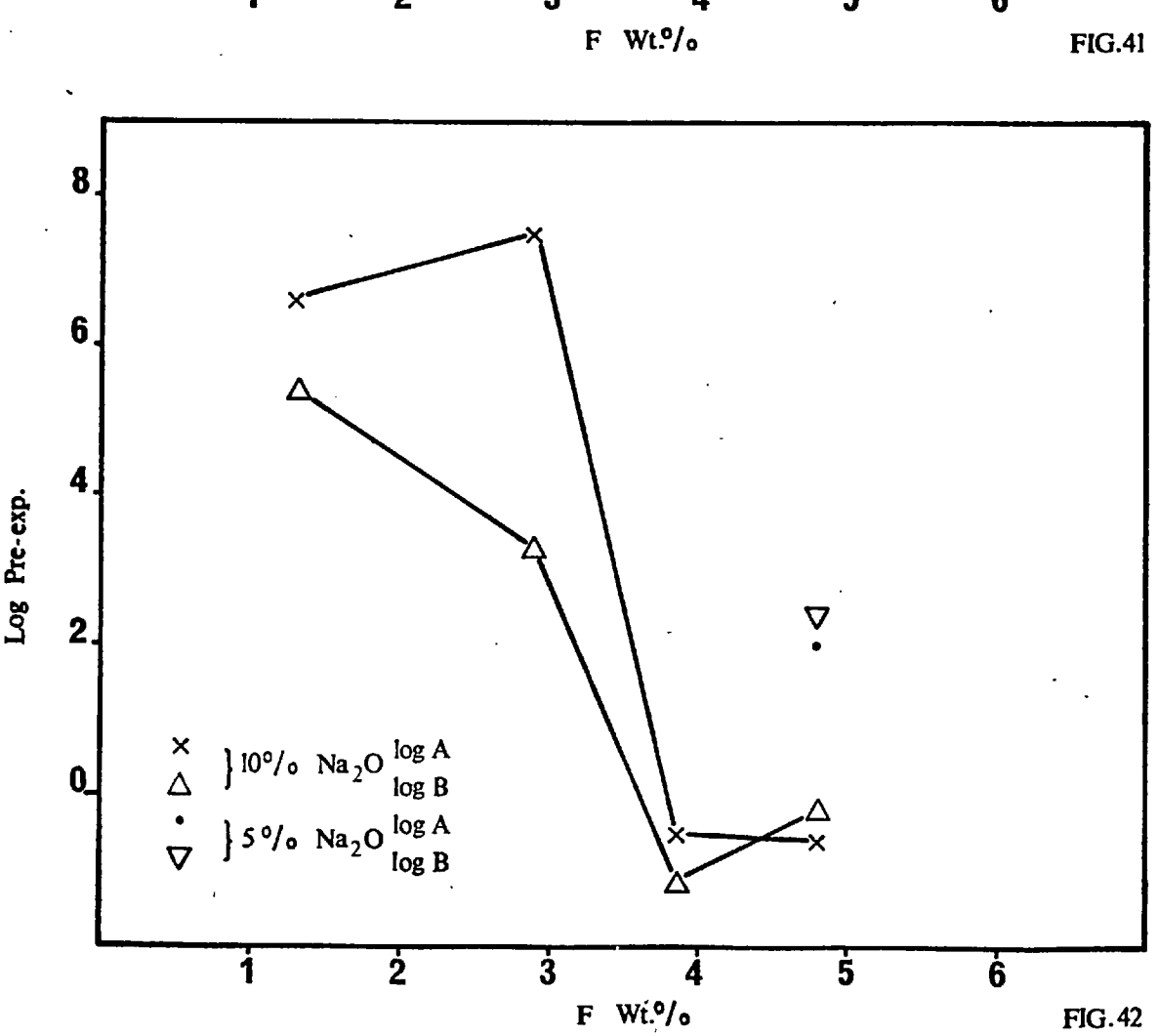

8
6
4
2
0
Log Pre-exp.
1
2
3
4
5
6
F Wt.%
10% Na2O log A
log B
5% Na2O log A
log B

FIG.42

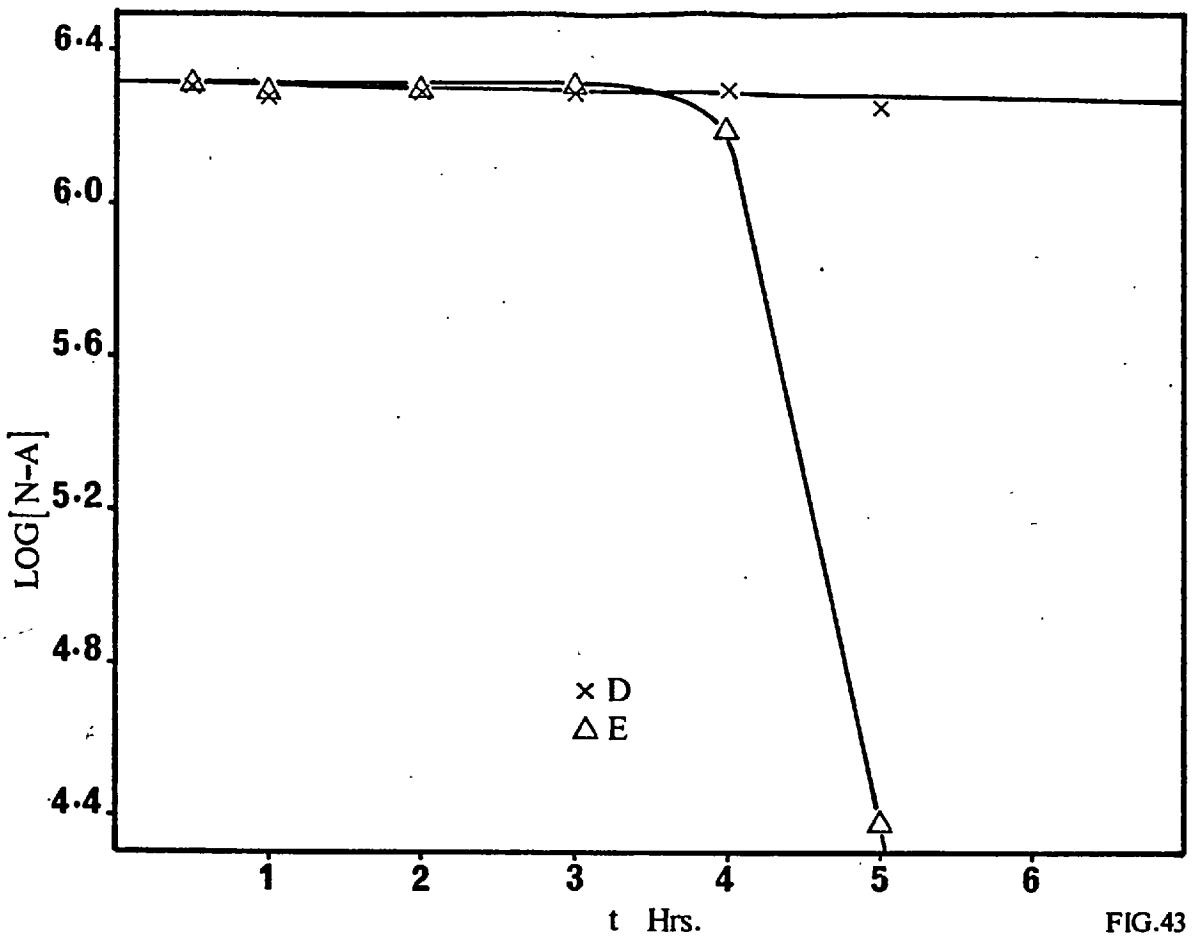

6·4
6·0
5·6
5·2
4·8
4·4
LOG[N-A]
× D
△ E
1
2
3
4
5
6
t Hrs.

FIG.43

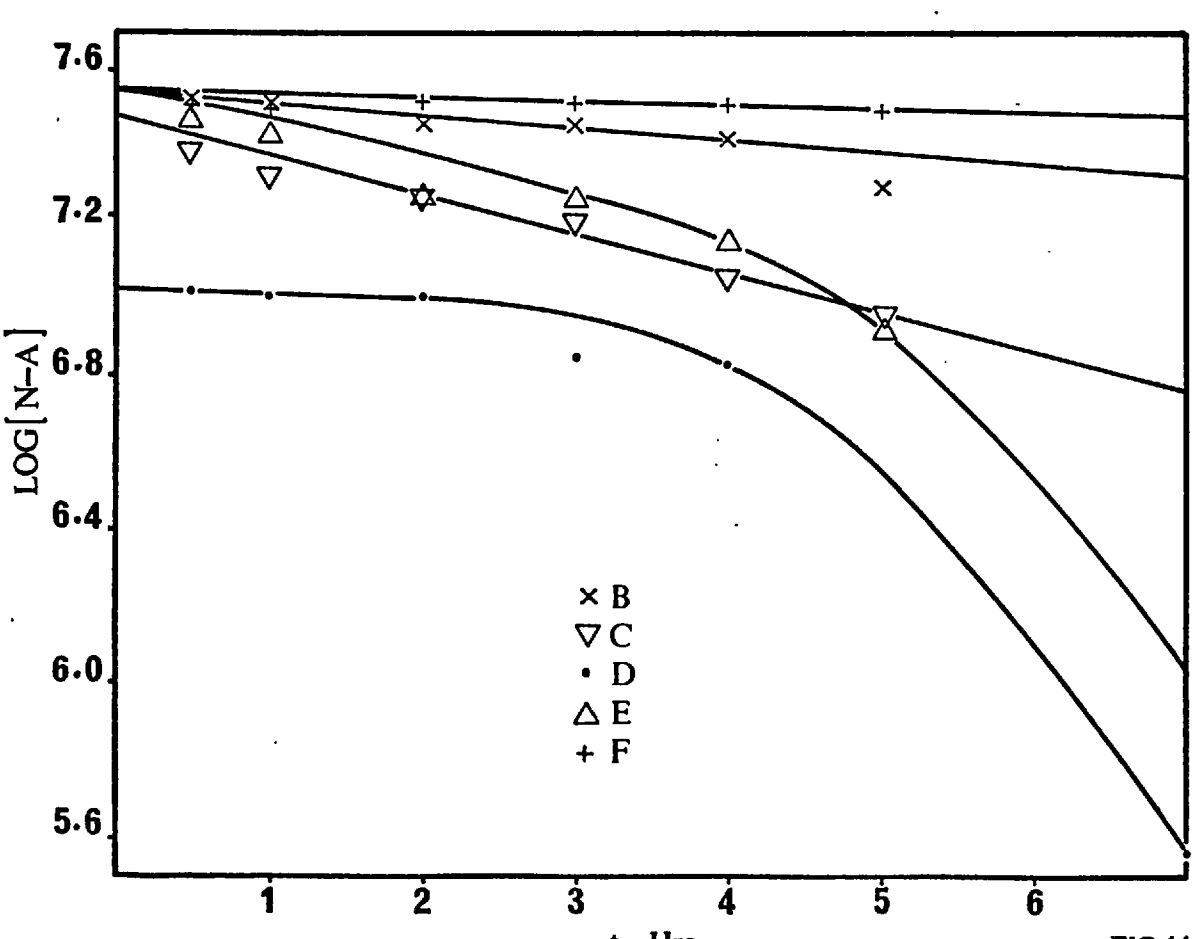

7·6
7·2
6·8
6·4
6·0
5·6
LOG[N-A]
× B
▽ C
• D
△ E
+ F
1
2
3
4
5
6
t Hrs.

FIG.44

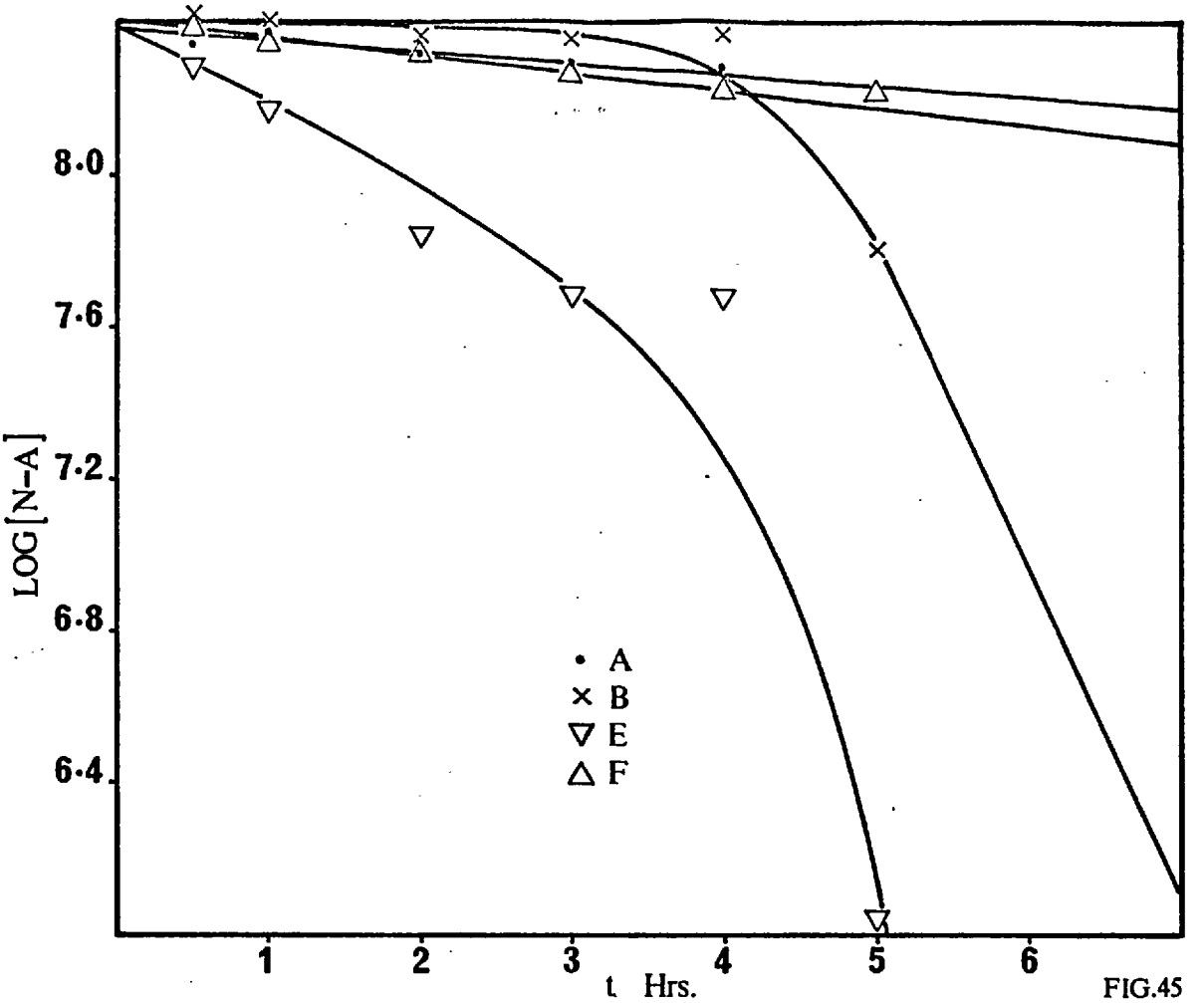

8·0
7·6
7·2
6·8
6·4
LOG[N-A]
• A
× B
▽ E
△ F
1
2
3
4
5
6
t Hrs.

FIG.45

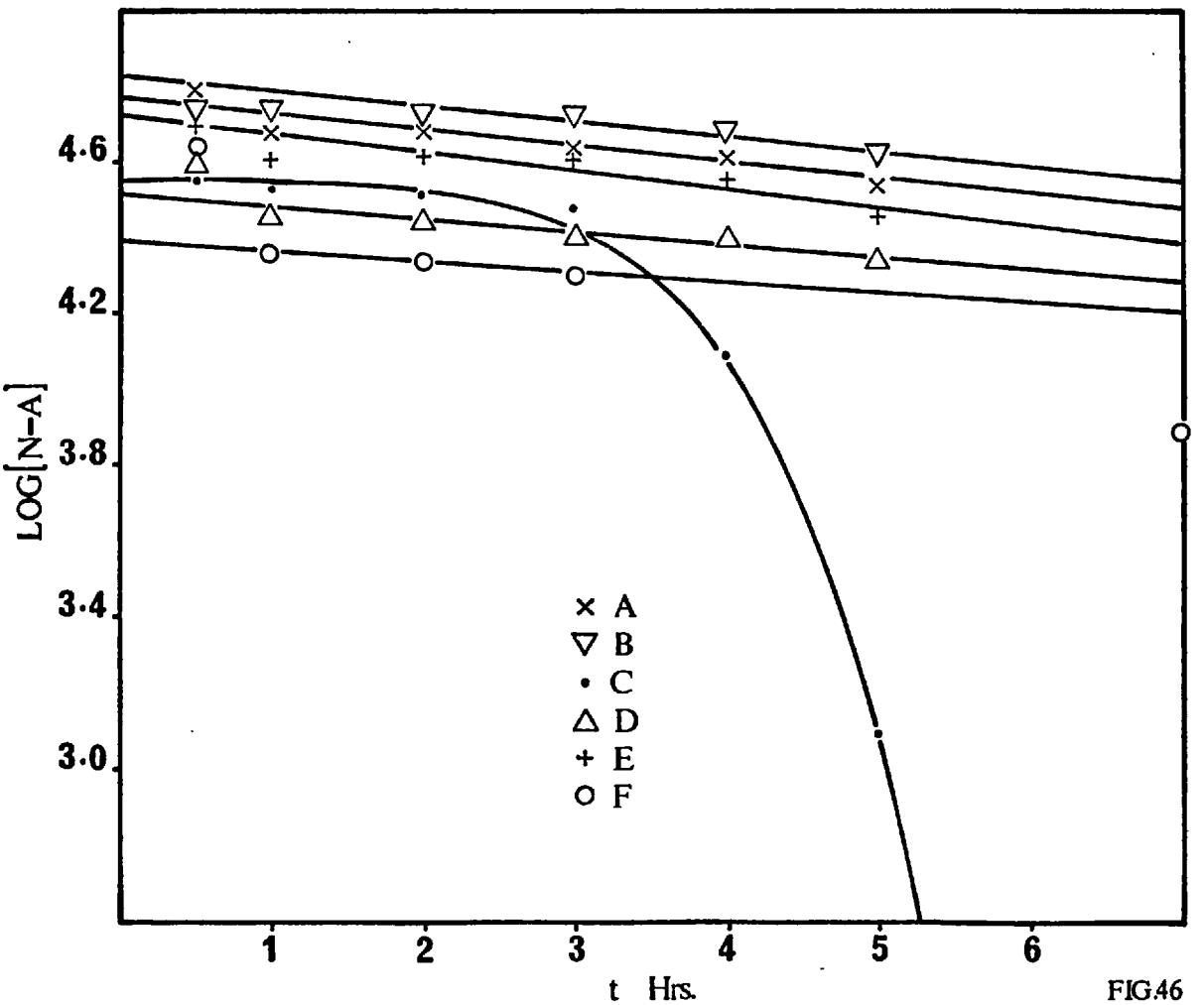

4·6
4·2
3·8
3·4
3·0
LOG[N-A]
× A
▽ B
• C
△ D
+ E
o F
1
2
3
4
5
6
t Hrs.

FIG.46

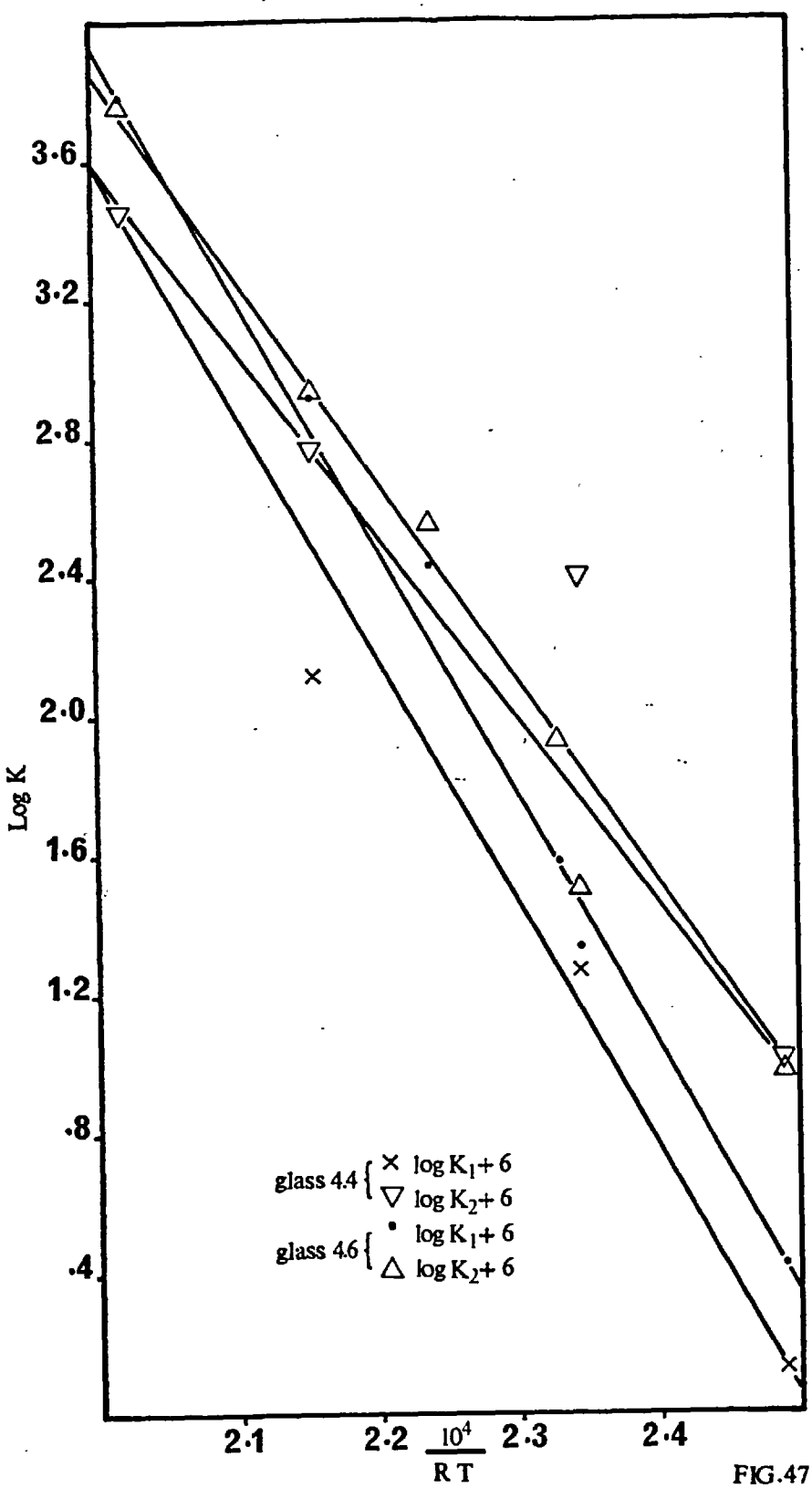

3·6
3·2
2·8
2·4
2·0
1·6
1·2
·8
·4
Log K
2·1
2·2
2·3
2·4
10⁴/RT
glass 4.4 { × log K1+6 ▽ log K2+6
glass 4.6 { • log K1+6 △ log K2+6

FIG.47

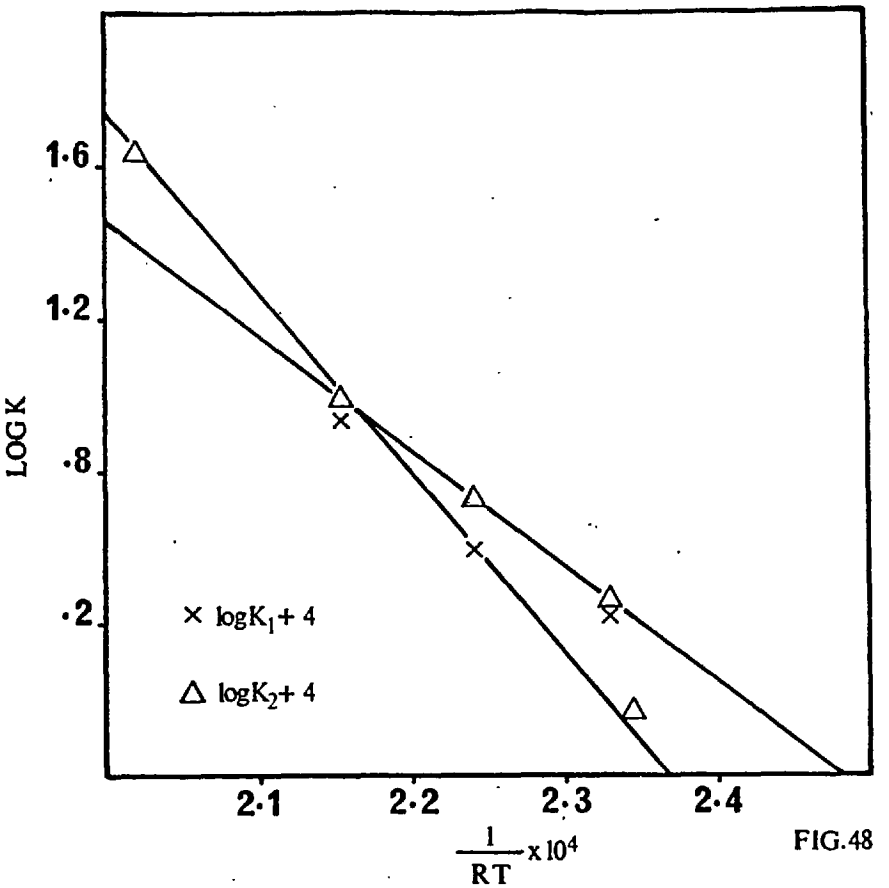

1·6
1·2
·8
·2
LOG K
× logK1+ 4
△ logK2+ 4
2·1
2·2
2·3
2·4
1/RT x 10⁴

FIG.48

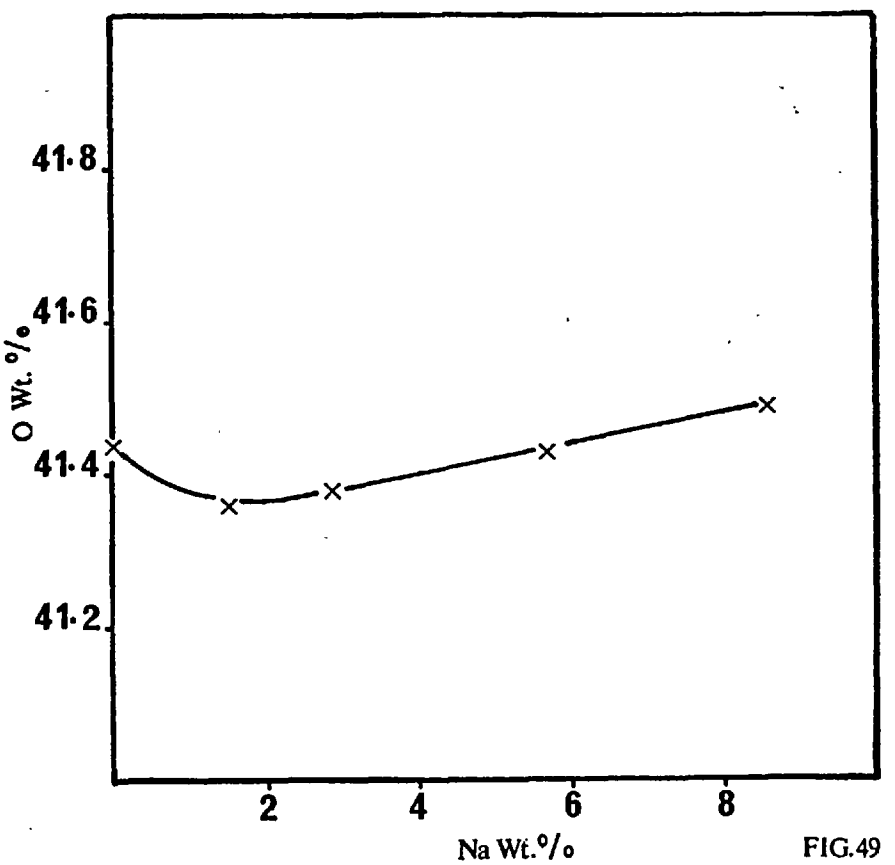

41·8
41·6
41·4
41·2
O Wt. %
2
4
6
8
Na Wt.%

FIG.49

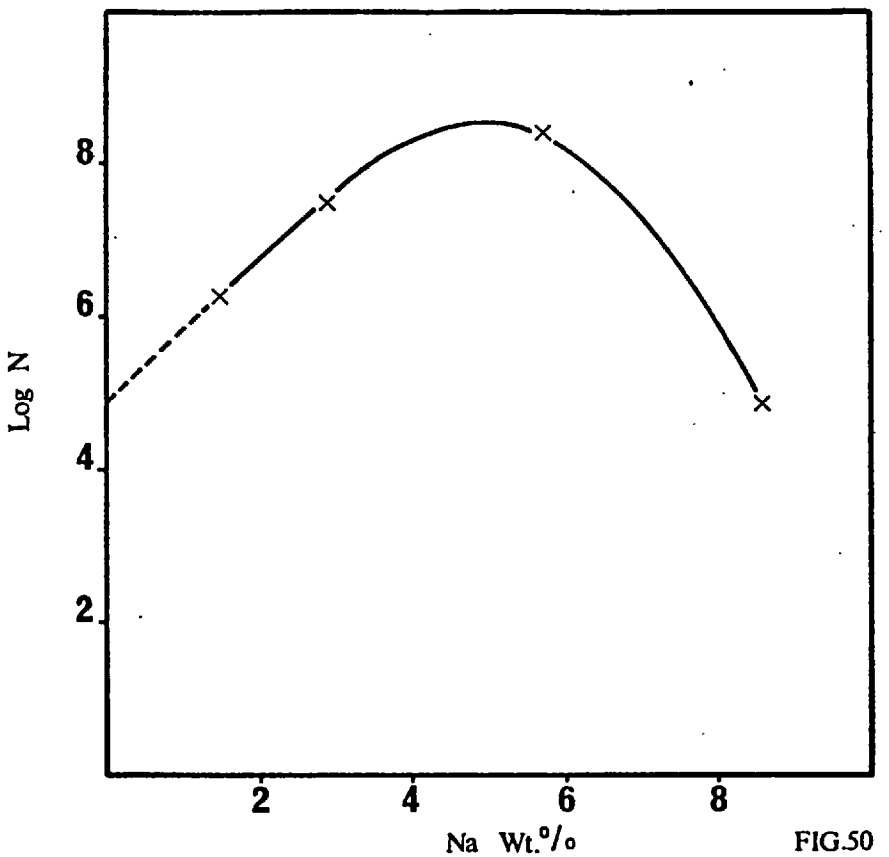

Log N
8
6
4
2
2
4
6
8
Na Wt.°/o

FIG.50

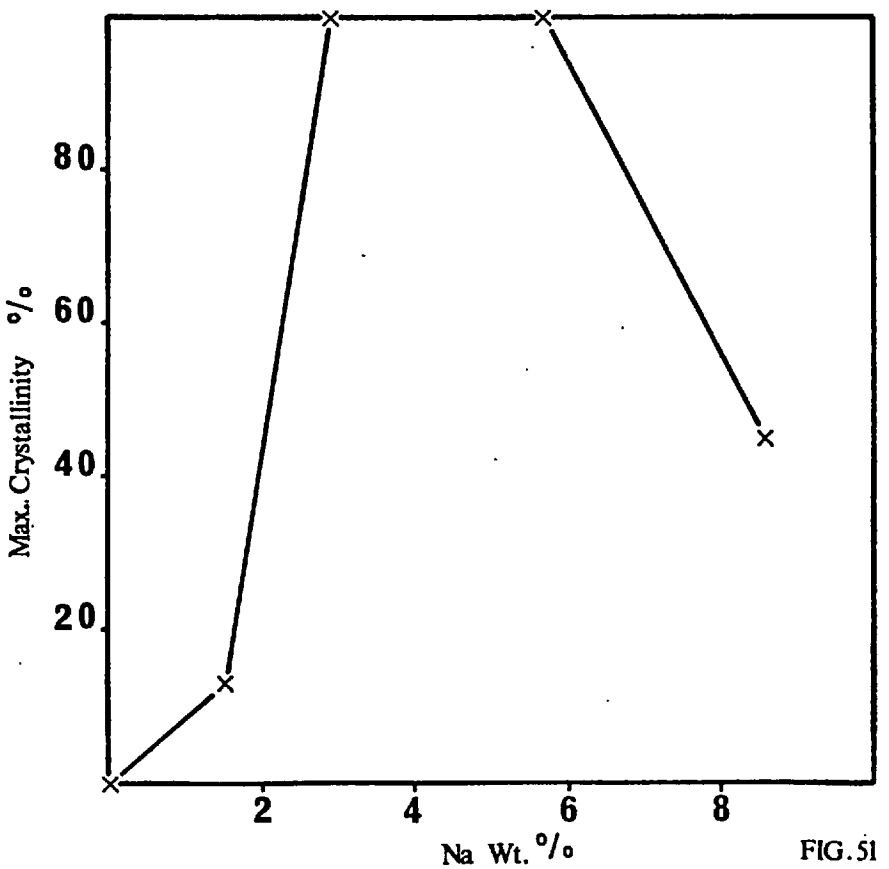

Max. Crystallinity °/o
80
60
40
20
2
4
6
8
Na Wt. °/o

FIG.51

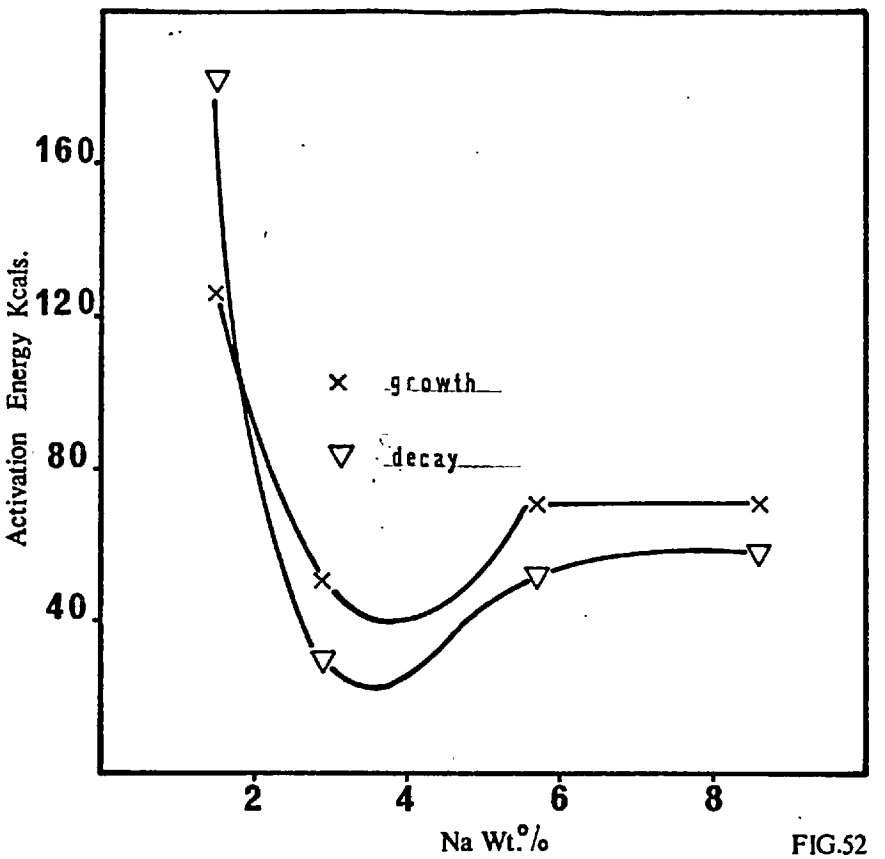

Activation Energy Kcals.
160
120
80
40
× growth
▽ decay
2
4
6
8
Na Wt.°/o

FIG.52

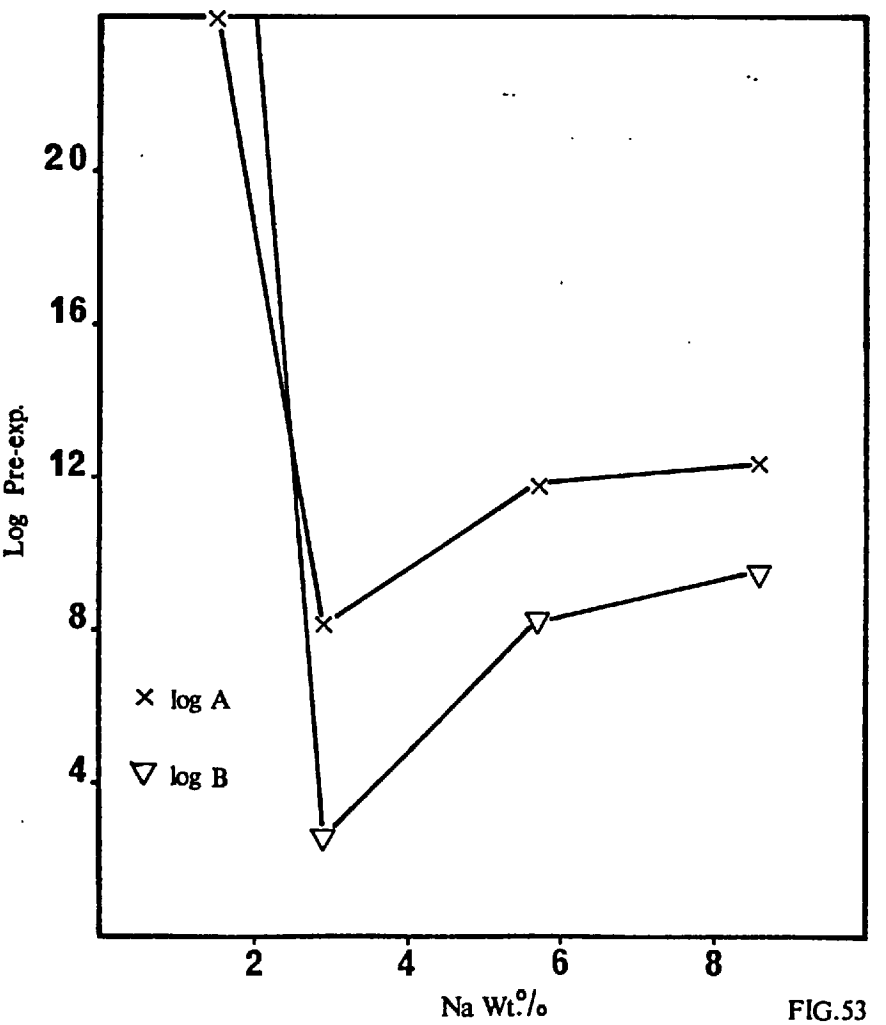

Log Pre-exp.
20
16
12
8
4
× log A
▽ log B
2
4
6
8
Na Wt.°/o

FIG.53

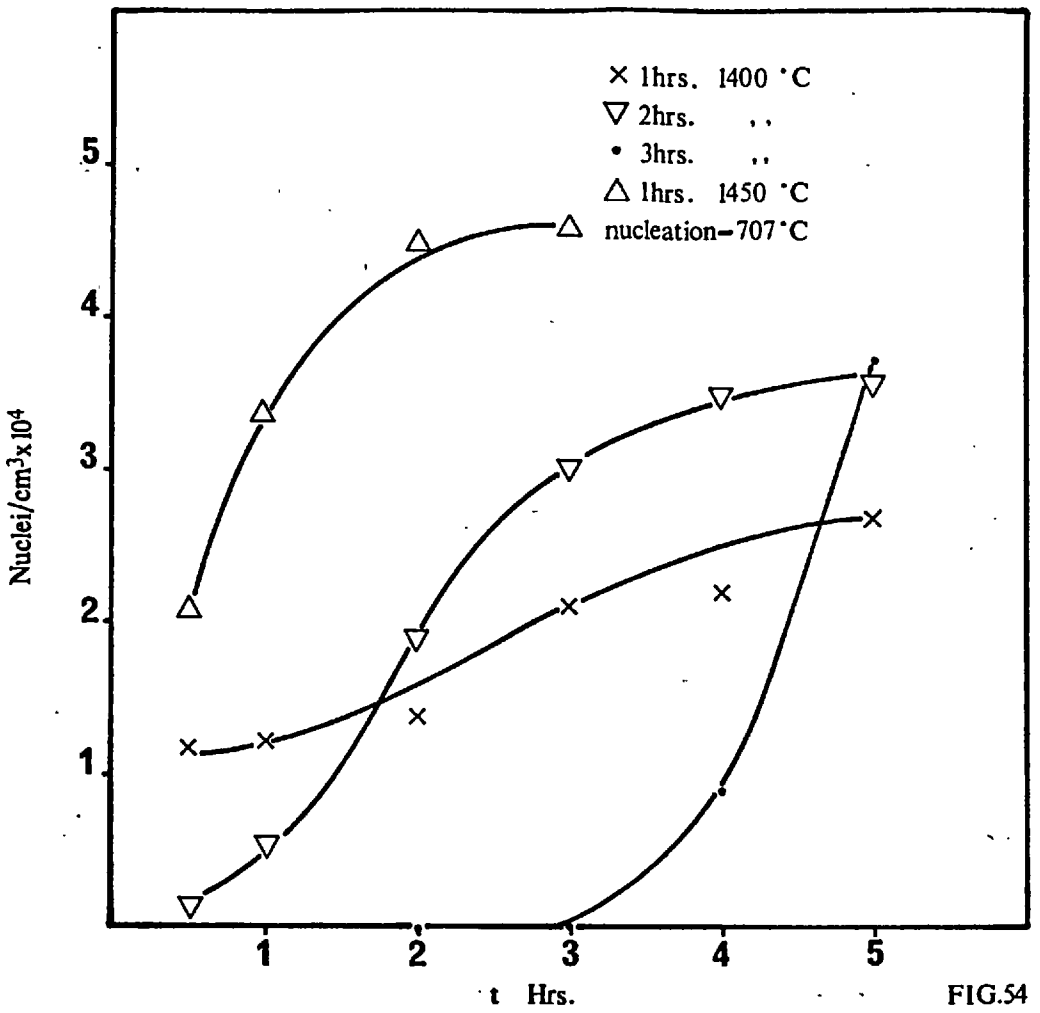

× 1hrs. 1400 °C
▽ 2hrs. ,,
• 3hrs. ,,
△ 1hrs. 1450 °C
nucleation–707°C
Nuclei/cm³x 10⁴
1
2
3
4
5
t Hrs.

FIG.54

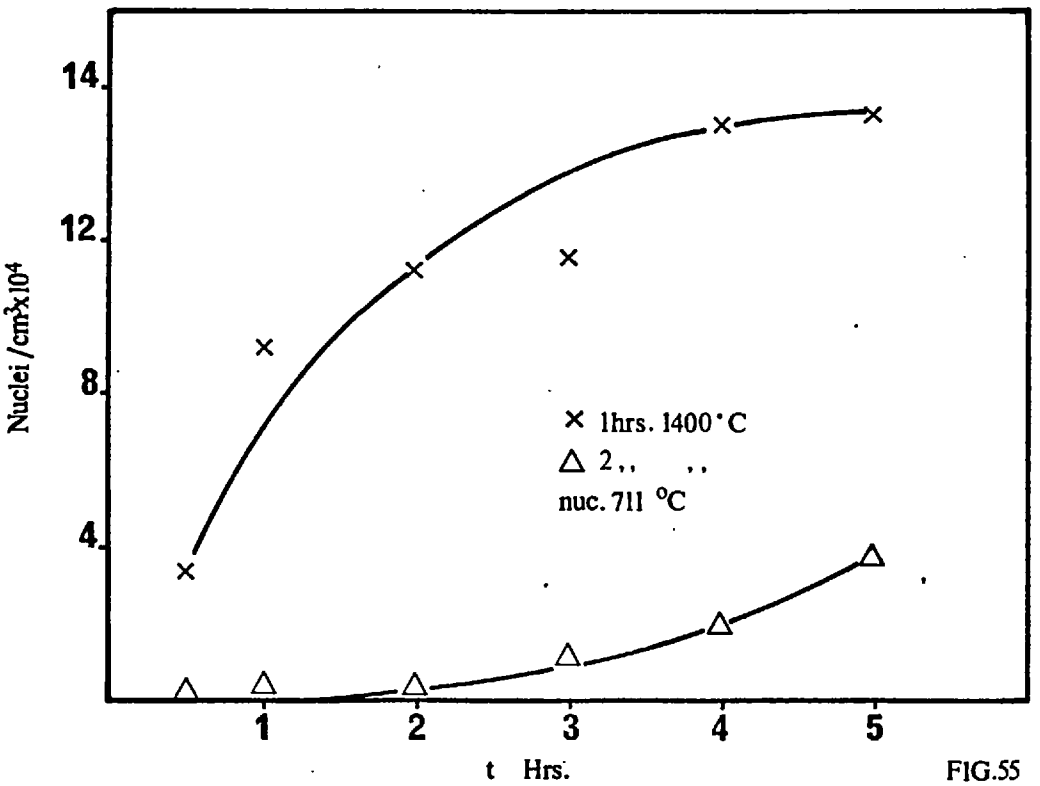

× 1hrs. 1400°C
△ 2,, ,,
nuc. 711 °C
Nuclei /cm³x10⁴
4
8
12
14
1
2
3
4
5
t Hrs.

FIG.55

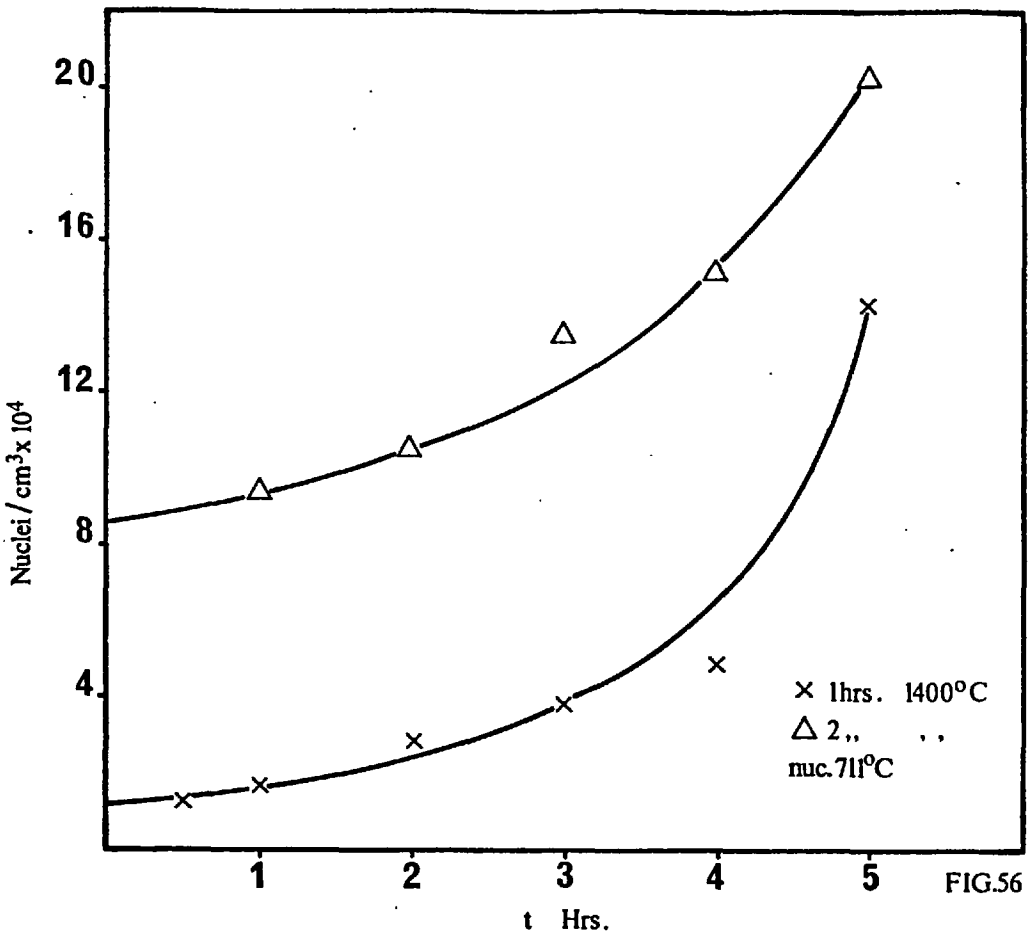

20
16
12
8
4
Nuclei / cm³ x 10⁴
× 1hrs. 1400°C
△ 2,, ,,
nuc. 711°C
1
2
3
4
5
t Hrs.

FIG.56

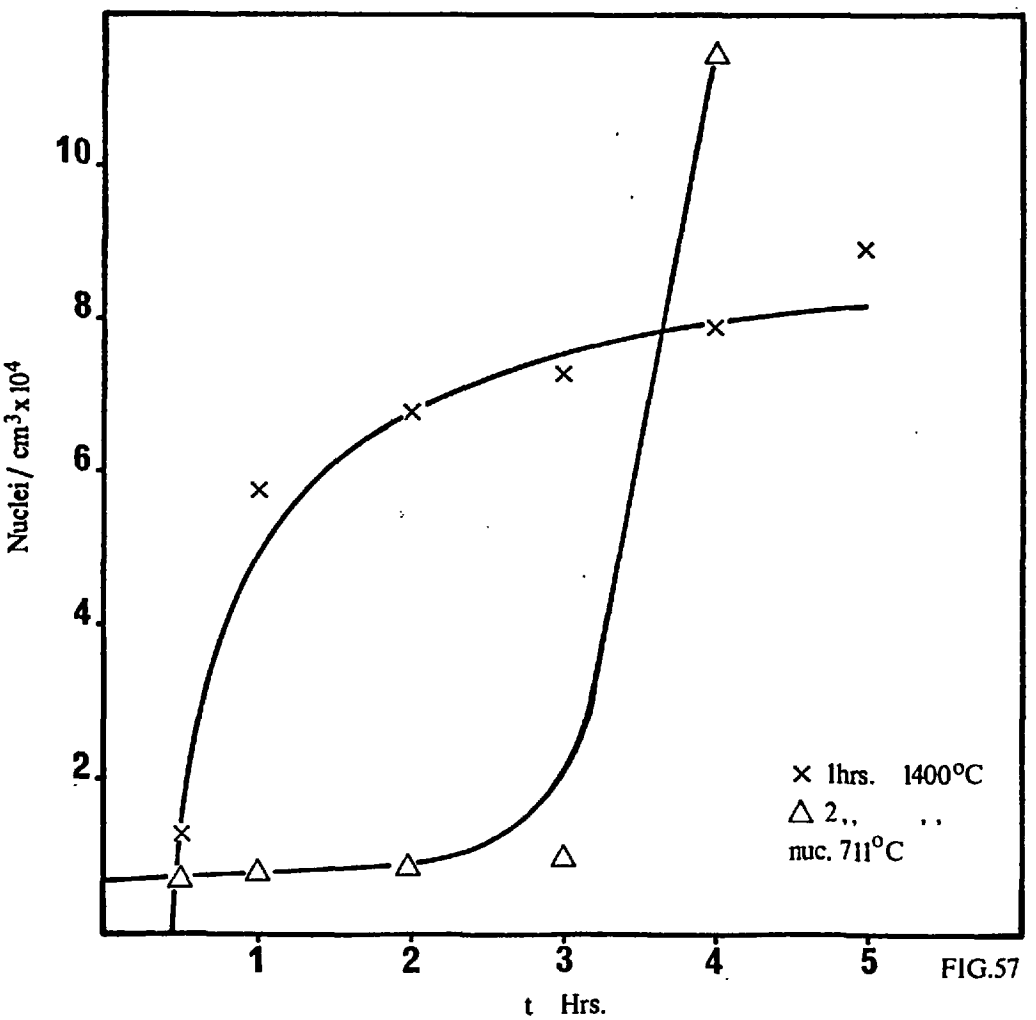

10
8
6
4
2
Nuclei / cm³ x 10⁴
× 1hrs. 1400°C
△ 2,, ,,
nuc. 711°C
1
2
3
4
5
t Hrs.

FIG.57

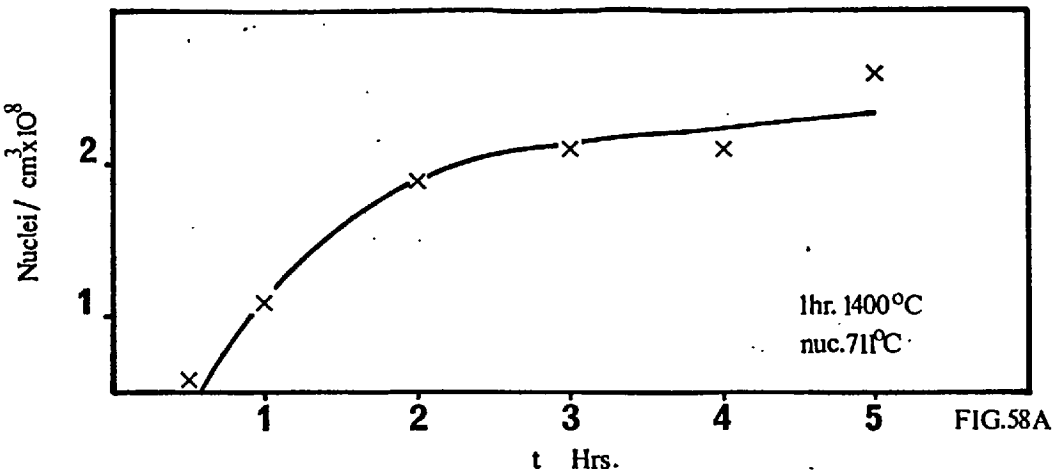


FIG.58A

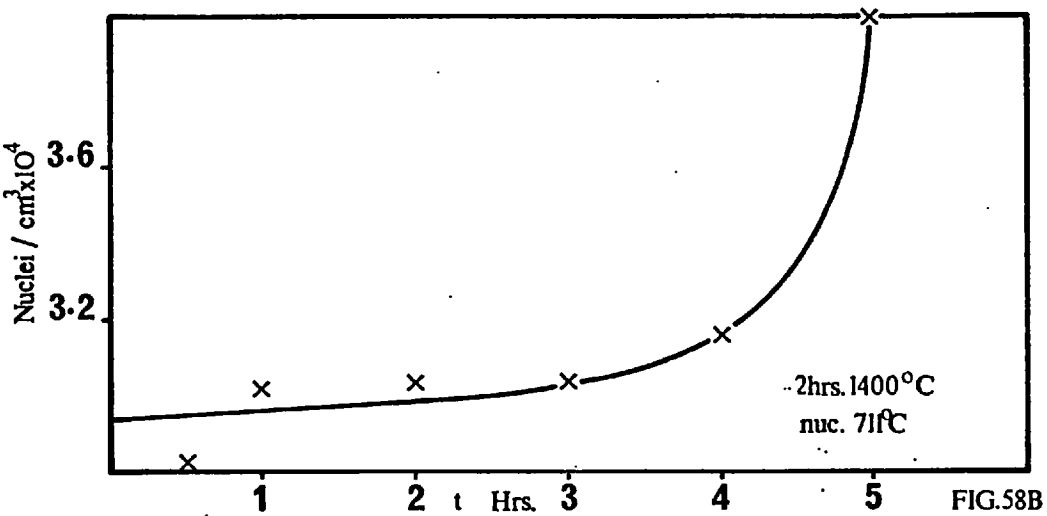


FIG.58B

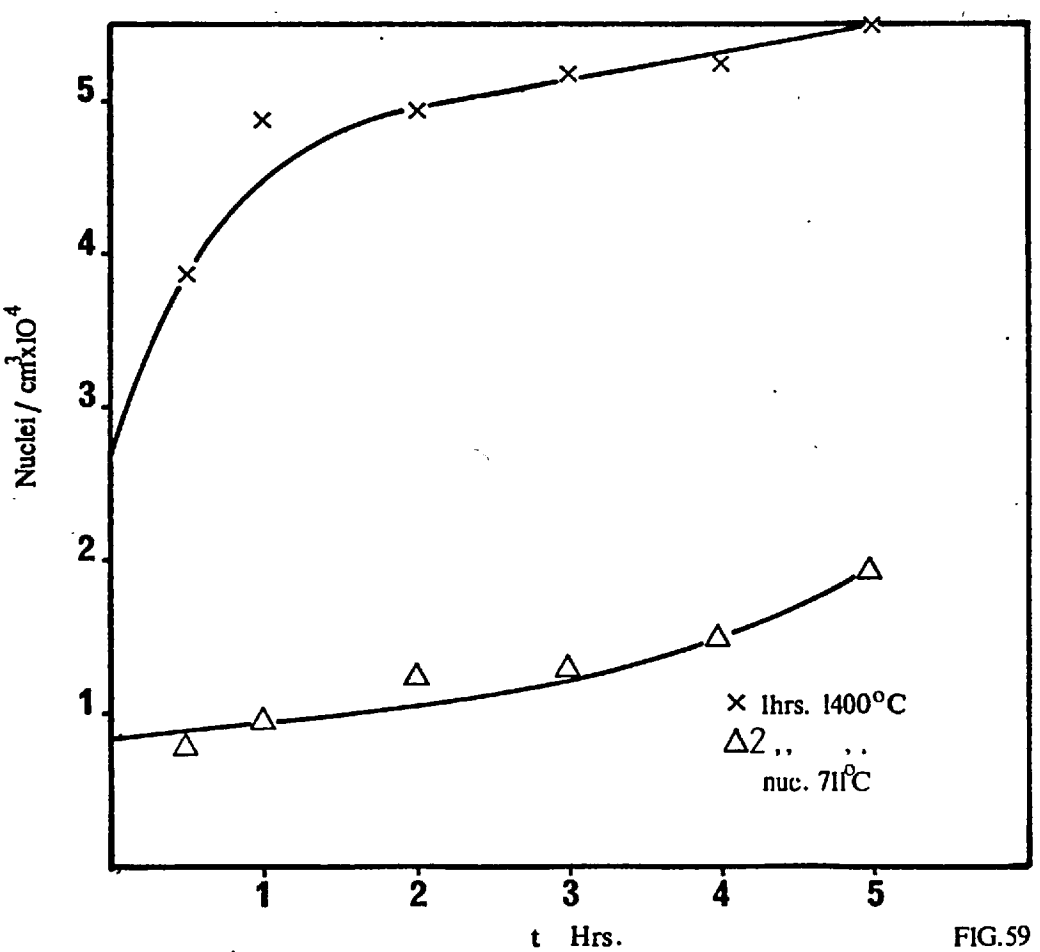


FIG.59

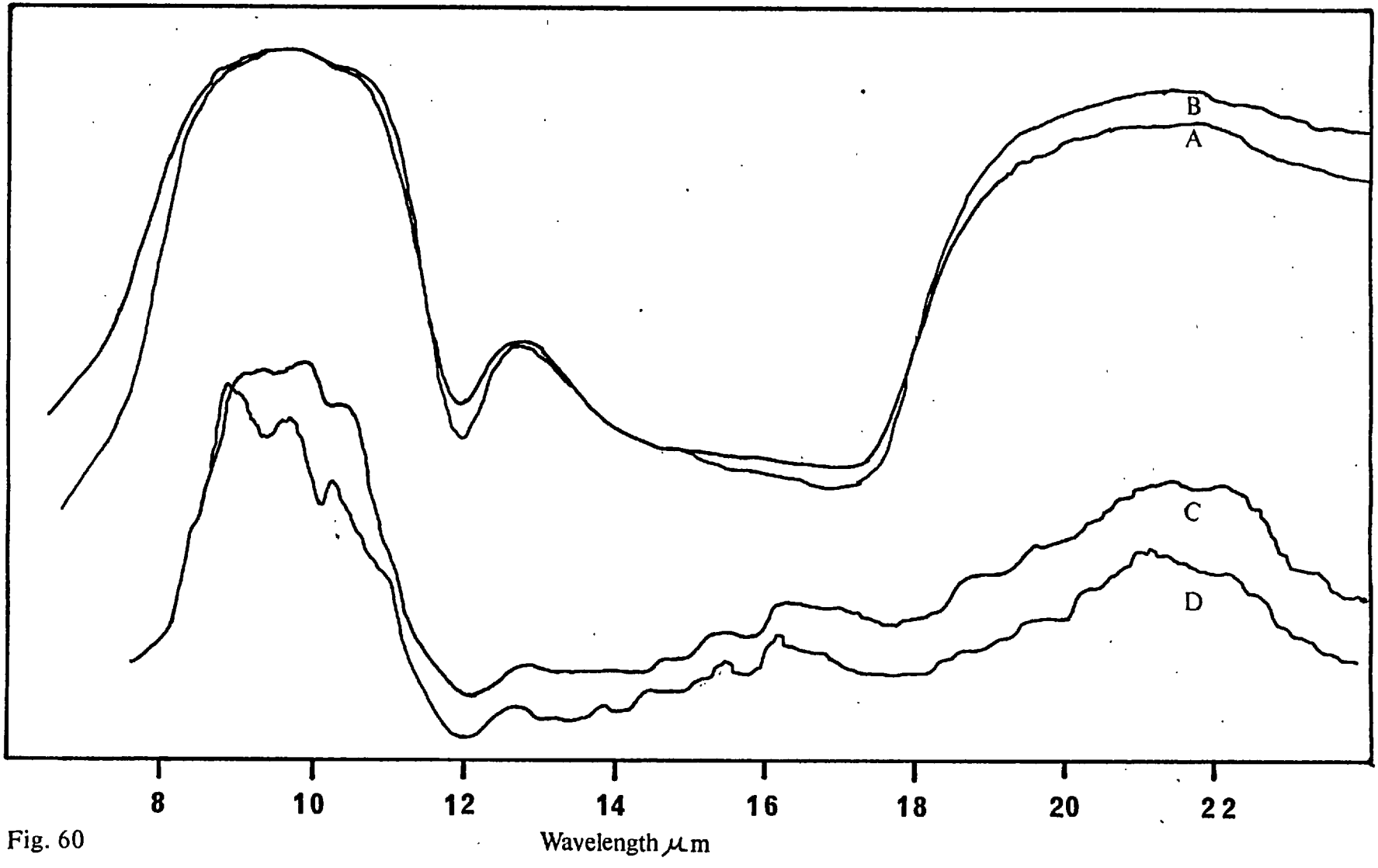


Fig. 60

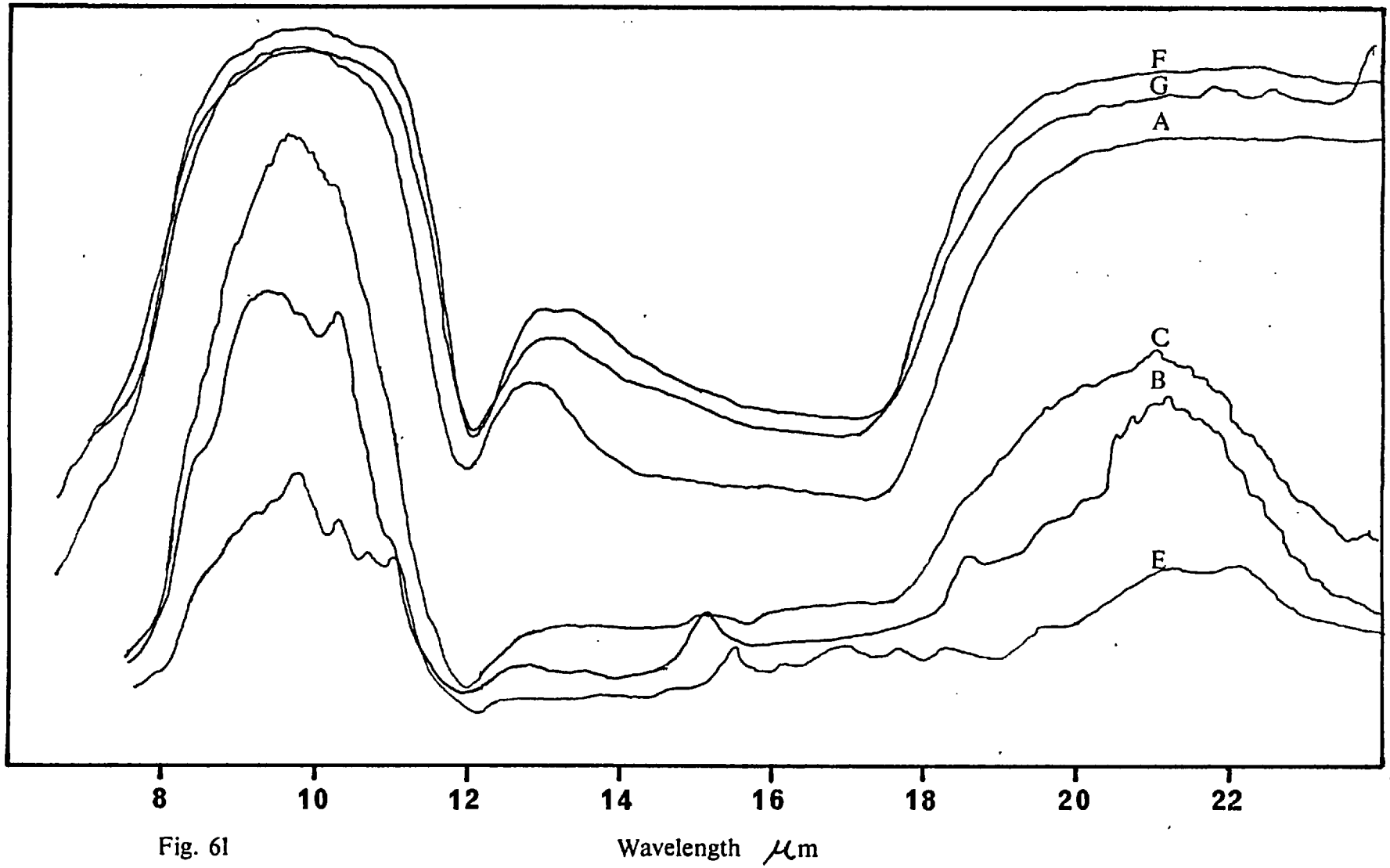


Fig. 61

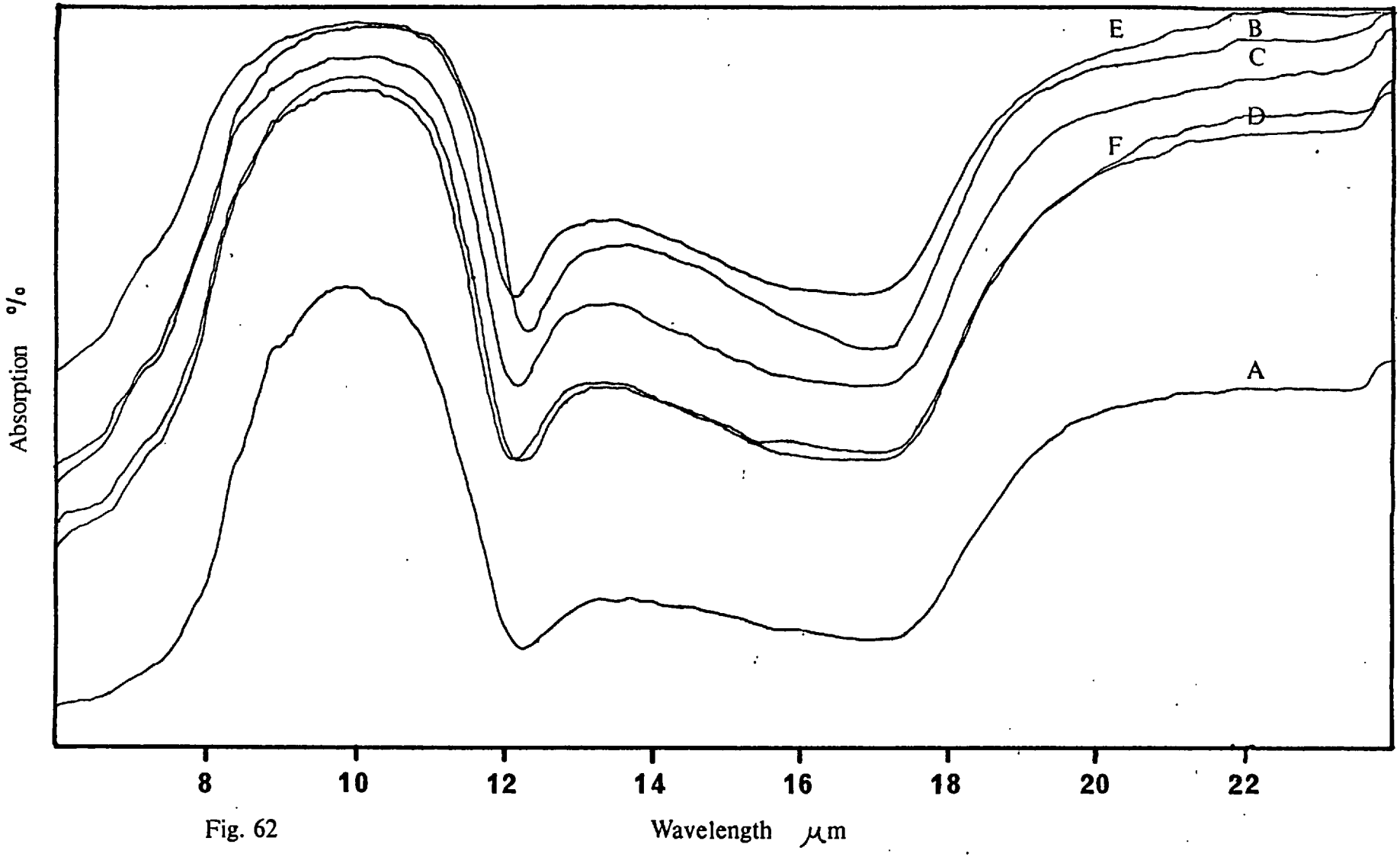


Fig. 62

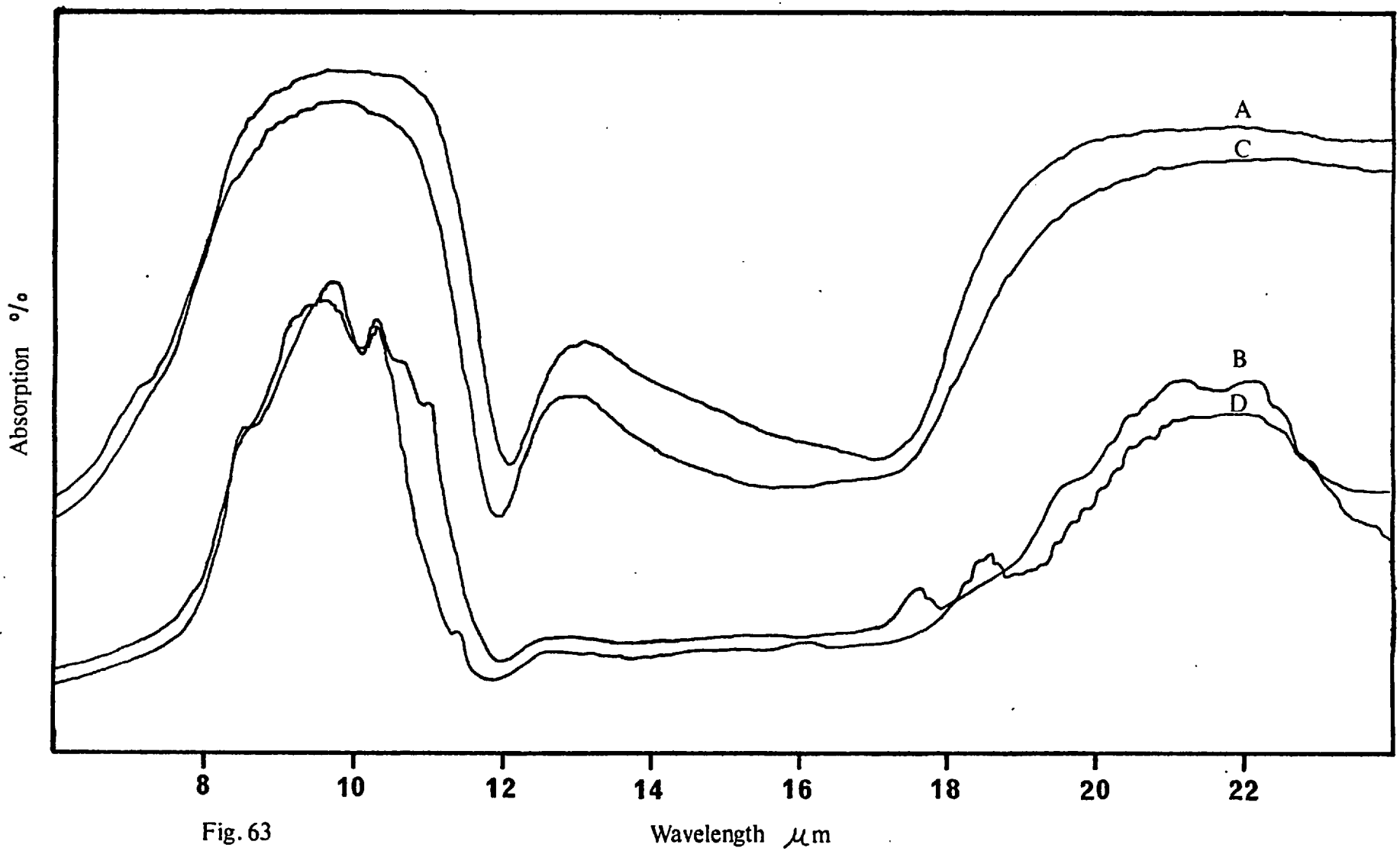


Fig. 63

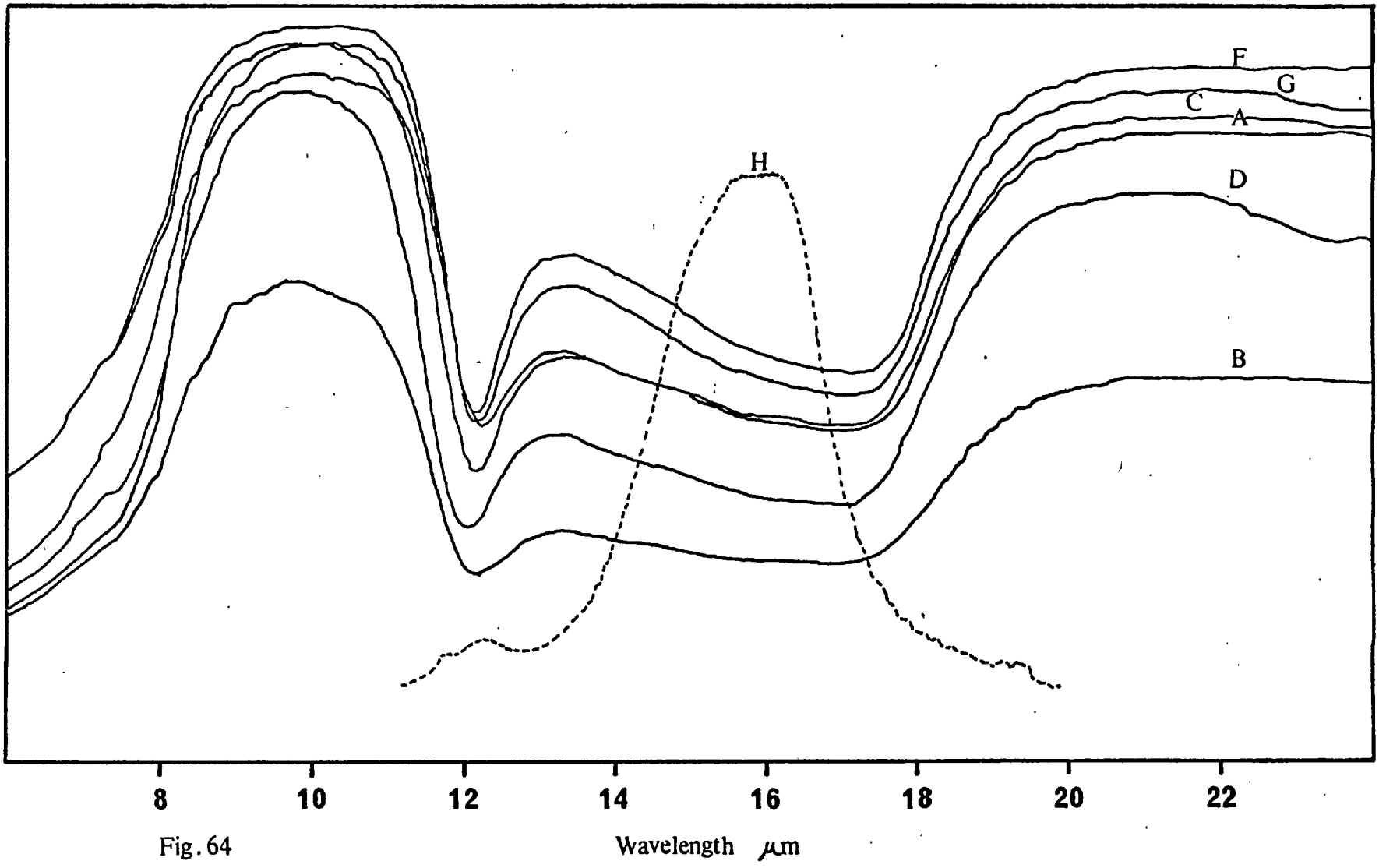


Fig. 64

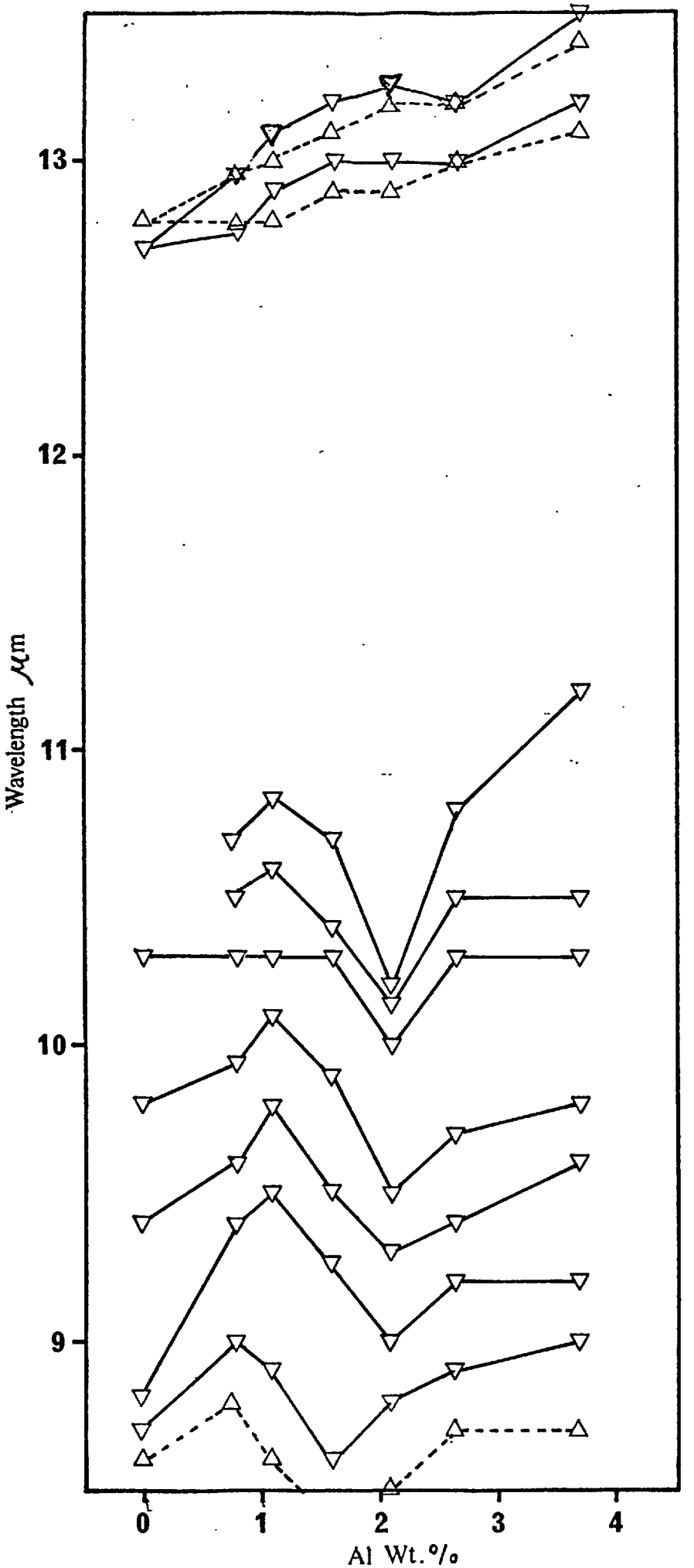


Fig. 65

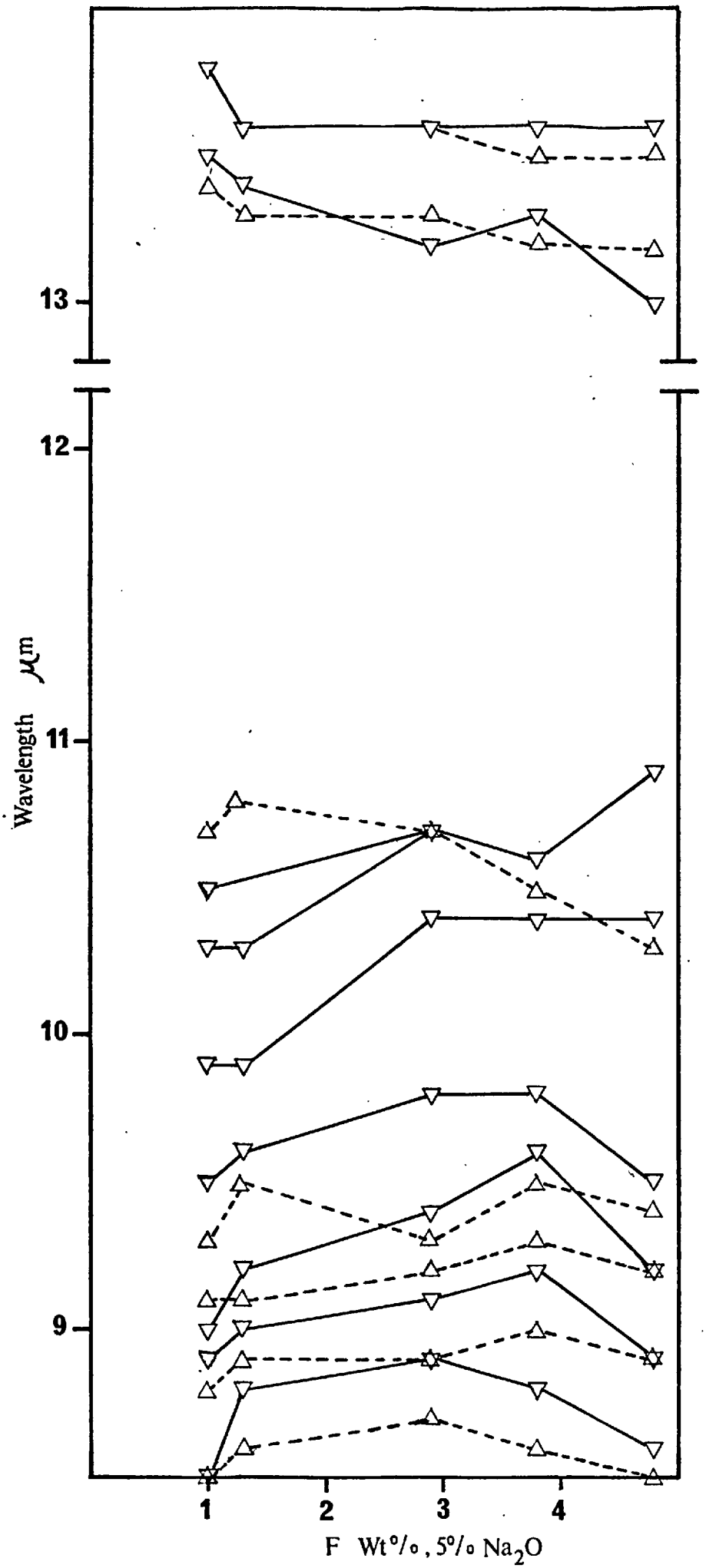


Fig . 66

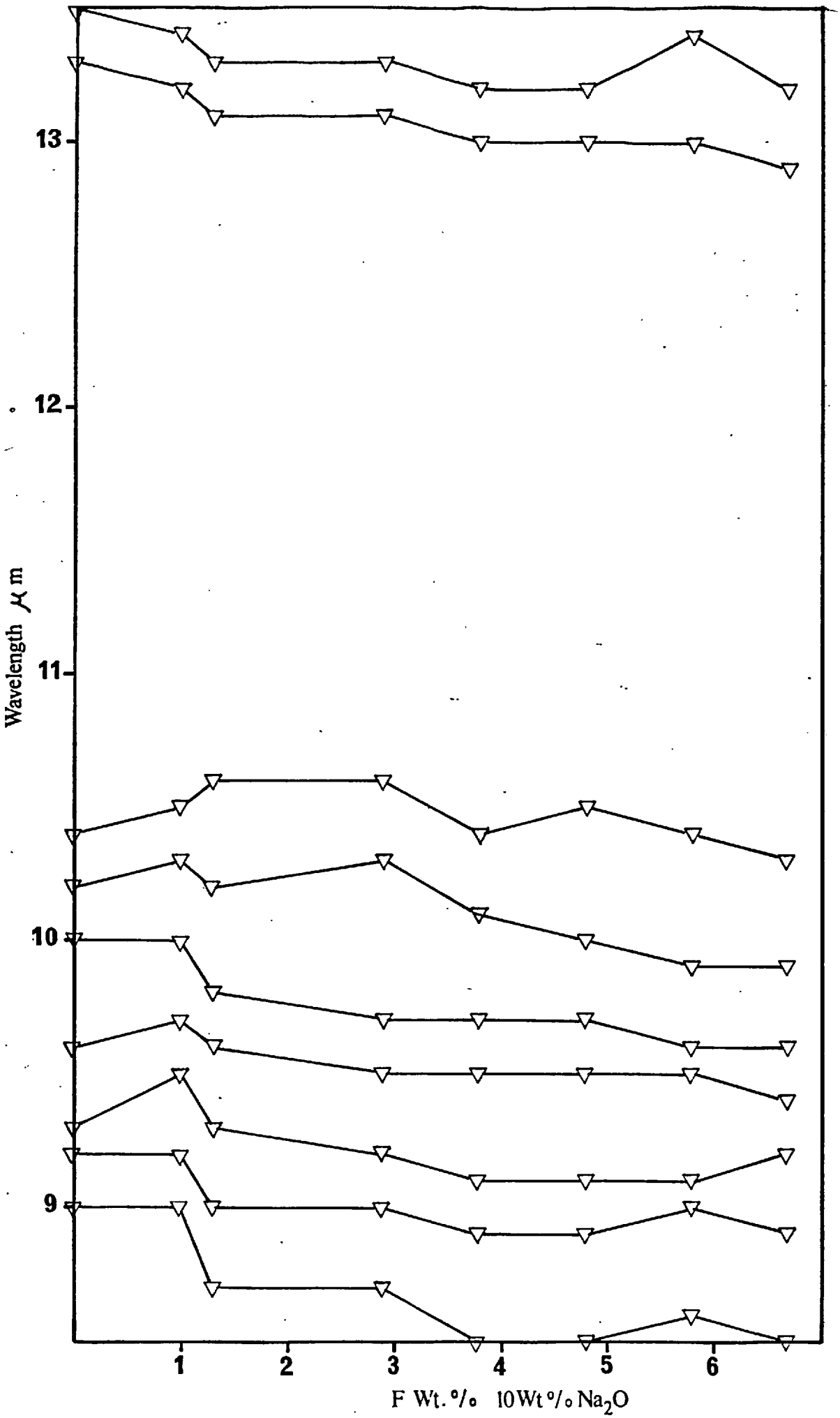


Fig. 67

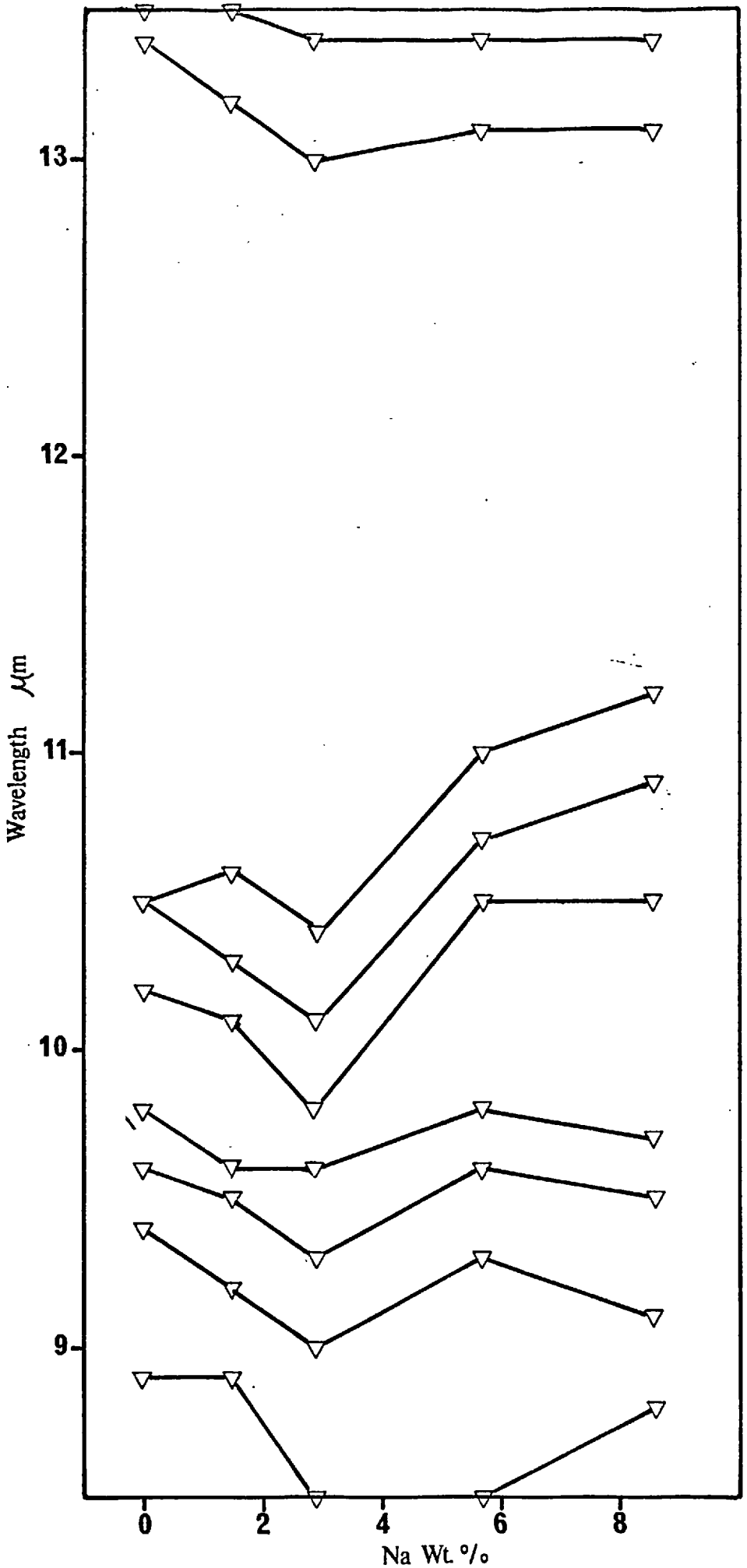


Fig. 68

References to Chapter 4

(1) J.E. Hillard, Trans. A.I.M.E., 224, 906, (1962).

(2) W.M. Tuddenham, R.J.P. Lyon, Analyt.Chem., 32, 1630, (1960).

(3) S.P. Mukherjee, P.S. Rogers, Phys.Chem., Glasses, 8, 81, (1967).

Chapter 5
Discussion and Elucidation of Results.

Before discussing the results obtained it would be well to point out that the kinetic equation 18 derived in Chapter 3 is a complex equation and experimental results cannot be fitted to it by the normal methods of regression analysis. The correct curve fitting procedures involve arduous and lengthy calculations and cannot readily be accomplished without the aid of a digital computer. As a consequence of this the log (N-A) plots were estimated. Because this undoubtedly introduced large errors into the calculation of I, no attempt was made towards a regression analysis for the plots of rate constant against temperature. A crude check, however, shows that the final errors in the activation energies and preexponential factors are at best about 10% and at worst 30-40%. It is hoped that this deficiency will be rectified in due course.

5.1. Phase separation and Crystallisation

Evidence of phase separation was found in all the glasses prepared as shown by Plates (21—28). However, glasses 2.1, 2.2, 3.0, 3.1, and 4.0 could not be induced to crystallise internally under any conditions. Therefore it can be concluded that although phase separation may be a necessary condition for nucleation it is certainly not a sufficient condition. Furthermore, the scanning electron micrographs Plates (29, 45) show spherulitic structures growing in extensive fields of droplet like structures and Plates (30, 32, 41) show bundles of needle-like crystals growing straight through droplets. These pictures show, quite dramatically, the enormous disparity between the extent of phase separation and the number of effective crystallisation centres. The suggestion that some of these droplets and not others may initiate crystallisation begs the question, for, without indicating some definitive, demonstrable characteristic of such droplets, nothing is thereby added to our knowledge of the process.

Indeed, calculations of the number of droplets from electron micrographs show that for glass 1.1. the number of droplets developed after 1hr at 620°C is about 10^{11} per cm^3 compared with a maximum number of nuclei of 10^4 per cm^3; for glass 1.5, 10^{11} droplets and 10^5 nuclei; for glass 1.7., 10^{10} droplets and 10^4 nuclei per cm^3. This means that, if the droplets are precursors to crystallisation, only one droplet in 10^6 or 10^7 is effective in this role. This does not seem to be a sufficiently good correlation to establish such a scheme as a suitable nucleation mechanism.

Therefore, it is reasonable to conclude that, in this part of this glass system, there is no evidence to support a nucleation mechanism causally related to phase separation.

5.2. The Kinetics of Nucleation

Although the general character of the nucleation has been described in Chapter 4 it is necessary to amplify some points.

No glasses could be induced to crystallise internally without a two-stage heat treatment. If the nuclei had been traditional heterogeneities this would have been unnecessary. This implies that the nuclei are homogeneous, which implication is strengthened by the observation that the number of nuclei for each glass is a strong function of composition.(Figs. 25,39,50).

The variation in the maximum number of nuclei with nucleation temperature is almost always within the experimental error for any determination and, in consequence, the experiments are not accurate enough to decide whether the maximum number of nuclei is a function of nucleation temperature.

If it is so it would seem to be a weak function of temperature but, even so, it would appear that the maximum number of nuclei is primarily a function of composition and possibly melt conditions as suggested in Chapter 3.

The mechanism proposed of nucleus growth by reversible steps is supported by the observation that in all glasses the overall rate of reaction rises with increasing nucleation temperature, passes through a maximum and falls at high temperatures (e.g. figs. 9-15)

The general, qualitative validity of the kinetic mechanism detailed in Chapter 3 has been demonstrated in Chapter 4 for all the glasses which displayed volume, as opposed to surface nucleation. Unfortunately, quantitative predictions from the theory of Absolute Reaction Rates, are difficult if not impossible to obtain. Activation energies have only been derived for the simplest processes and, even in these cases, the calculation of the partition function for the activated complex has presented some difficulty. Although the exact relationship of thermodynamic activities and statistical mechanical partition functions is obscure such a relation presumably exists and such activities could in fact be used in kinetic equations. However, it is difficult to conceive a more difficult system in which to measure activities than a silicate glass. The quantitative validity of the equations obtained in Chapter 3 must therefore be judged on the reasonableness of the parameters obtained by their application.

The significance of the pre-exponential terms shown in Figs. 24,42,53 is not clear both for the reasons outlined in the beginning of this chapter and because the mathematical analysis of Equations 18 (xxx) of Chapter 3 is not yet complete, however, a clue to their significance will be given later in this discourse. The activation energy thus stands out as the most easily discussed parameter determined in this work. The compositional variations of the activation energies for the forward and reverse reactions are illustrated in Figs. 23,41,52.

The range of variation and the absolute values of the activation energies illustrated in Figure 52 for increasing soda content should be compared to the activation energies for viscous flow found by

Bockris[1], who found, for the binary system Na_2O-SiO_2, a range of activation energy of 135 Kcals/mole at 0% Na_2O to 50 Kcals at 15 mole % Na_2O. Similarly Fig. 41 shows a variation of activation energy for increasing fluoride content which is in fair agreement with an activation energy calculated from Bills[2], although comparison is not easy because of the great difference in compositions being studied. Furthermore, the complex relationship between activation energy and alumina content is closely analogous to the complex relationship between alumina content and viscosity found by Kozakevitch[3]. There is therefore, nothing inconsistent between these results and the suggestion made in Chapter 3 that the activation energy discovered might bear a close relationship to the activation energy for viscous flow. This confirms the conclusions of Keyworth[4] regarding the activation energies for crystal growth in glasses containing chromium oxide. These energies were derived from a version of the Avrami treatment of phase changes, and the equivalence of this treatment and that derived in Chapter 3 is thus suggested [Ref. 39, Chap.3].

These results, however, are at considerable variance to the activation energy of 22 Kcals per mole found by Mukherjee and Rogers[5] for similar glasses. However, no relationship is really to be expected in the light of the theoretical approach outlined here and the value obtained in[5] probably represents an effective activation energy related to the difference in activation energy for the forward and reverse reactions.

5.3. The probable nature of the nucleus.

Although the nature and mechanism of the process preceeding crystallisation can be explained as shown above, the kinetic arguments are incapable of supplying information concerning the structural aspects of the transformation.

In Chapter 4 it was stated that the maximum number of nuclei was, most probably, a function of glass composition and melting temperature only. With this in mind the relationships are represented in Figs. 25, 39, 50. This dependence is particularly complex in the case of aluminium (Fig. 25) although the general trend is upward.

The variation with respect to fluorine content is particularly interesting (Fig. 39). The discontinuities in the otherwise smooth curves (full lines) are quite unreasonable and continuation of the lines to 0% fluorine shows, quite clearly, that nuclei exist in the absence of fluorine. This can only be explained if it is assumed that the nuclei do not consist of simple alkali halides. This can be explained, partially, by reference to Plates 1-20 which show the variation of crystal-growth habit as functions of composition. Plates 1-7 show that the structure of the 'spherulites' becomes more open as the percentage of alumina in the glass is increased. Plates 8-10 and 11-14 show that the texture of the spherulites becomes finer and the spherulites become more complete as the fluoride concentration increases. Plates 15 and 16 indicate that as the fluoride content is further increased the texture becomes more open again. The Plates 17-20 indicate that the spherulites become more complete and then more open again as the soda-content is increased.

These morphological changes can be understood by reference to the study of the morphology of spherulitic growth in poplypopylene [6,7]. It has been found that an increase in the concentration of impurities (sterioirregular molecules or molecules of low molecular weight) results in spherulites with an increasingly open texture. The non-crystallisable components are rejected by the growing crystal fronts and concentrate along the sides of the growing crystal. The presence of alumina in a glass will result in the formation of large, irregular aluminosilicate ions which would act as impurities in this sense. This would account for the changes in morphology shown in Plates 1-7. Fluoride additions to silicates are known to reduce the sizes of the silicate anions. This will result in a decrease in the concentration of large anions and the predicted morphological changes can be seen in Plates 8-10 and 11-14. However, Plates 15 and 16 show that a further reduction in the size of the anions results in the second type of impurity mentioned above and a consequent decrease in the perfection of spherulites. The addition of soda has a similar effect on the anion distribution of silicates and the effects on spherulite morphology (Plates 17-20) closely follow those observed for fluoride additions. Plots of maximum crystallinity, obtained by multiplying the volume

of a typical spherulite by the maximum number of nuclei developed (Figs 26,40,51), if taken as an indication of 'monomer' concentration, confirm these observations. The discontinuities in Fig. 39 are therefore due to the lack of suitable crystallisable species and not to the lack of suitable nuclei.

The crystallisation behaviour of glasses containing increasing amounts of alumina provides a clue to the probable nature of the nuclei. The non-random nature of the variation in nucleus number shown by all glass compositions rules out the possibility of heterogeneous nucleation. The nuclei have been shown to exist, at a reduced number, in the absence of fluorine and in consequence the nuclei cannot be simple alkali fluorides.

It is probable that increasing the aluminium content of a silicate glass increases the proportion of large silicate of aluminosilicate anions. The general increase in nucleation number with alumina shown in Fig. 25 indicates that the embryo nuclei are probably complex silicate or aluminosilicate anions. The other compositional variations observed and the low number of embryos found are not inconsistent with the implications of the theoretical studies of Bockris[8], Masson[9] and Lacy[10] indicating that large anions should be present in very low concentration at this sort of composition. Any geometric restraints will tend to reduce this small number even further, and it is easy to envisage a final concentration of suitable embryos of around 10^{-18} molar.

5.4. Infra-red spectra

Sample spectra are given in figures 60-64. It can be seen that the spectra are composed of between 5 and 7 bands in the region of 8-11 microns and 1 or 2 microns bands in the 13 micron region. The positions of these bands are summarised, as functions of composition in Figs 65-68. One very clear point emerges from an examination of Figs. 62, 63, 66 and 67, no new bands are observed on the introduction of fluorine. It may therefore be concluded that no silicon to fluorine or aluminium to

fluorine bonding occurs in these glasses. The reduction of viscocity due to fluorine must be due to a displacement of the equilibria controlling the melt structure towards the production of smaller units and to a sharpening of the molecular weight distributions in the melt. Unfortunately it is not possible to derive the relative proportions of the resonating species in the glass because of the overlap of the bands. It is hoped that the application of the technique of derivative spectroscopy, [11] mentioned in Chapter 2, may overcome this deficiency.

The discernable bands may be ascribed following Saksena [12] and Launer [13] to the following species, in descending order of wavelength;

8.5-9 microns silicate ring.
8.8 - 9.5 microns silicate chain.
9.3 - 9.8 microns silicate ring.
9.5 - 10.1 microns silicate chain.
10.0 - 10.3 microns silicate ring.
12.8 - 13.2 microns silicate ring.

The remaining three bands at 10.1-10.6, 10.2-11.2 and 13 to 13.5 may be ascribed to resonances involving aluminium in a zeolitic or feldspar structure. The positions of these bands are subject to complex alteration with changing composition and illustrate the unpredictable nature of environmental influences in infra-red spectra. However, if the position of the highest frequency (i.e. lowest wavelength) band as a function of composition is compared to the plots of pre-exponential factors against composition (Figs. 24, 42, 53) it can be seen that a close similarity of form exists. This may be coincidental but such a similarity can be explained if it is remembered that the preexponential factor contains a term due to the vibrational partition function of the species taking part in the reaction and the highest frequency mode would be expected to make the greatest contribution.

A tentative connection between the bandwidth at 8-10 microns and overall crystallisation behaviour can be seen by comparing Fig. 64 with Fig. 51. It can be seen that the narrowest band-width corresponds to the maximum crystallisation and vice-versa. This demonstrates that the relative structural diversity in a glass determines the crystallisation characteristics of that glass in that greater structural diversity leads to broad spectral bands on the one hand and low total crystallinity on the other.

Reference to Figs 60 to 64 and Figs 40 and 51 shows that, in general, those glasses which crystallise readily display a narrowing of the spectral bands on heating in the nucleation range whilst those which do not crystallise show a broadening. The broken lines in Figs. 65 and 66 show the effect of a nucleation heat treatment on the highest frequency band, it will be noticed that this moves to shorter wavelengths, which, according to Saksena[12] is indicative of increasing catenation. It would appear then, that silicate rings of some description are involved in the nucleation process. Figures 60 and 63 however, show that on crystallisation the 13 micron band almost completely disappears. This is inconsistent with the crystallisation of species containing a silicate ring, all of which have this band. However, the explanation may lie in a suggestion of Mukherjee and Rogers[5] that the primary crystallisation may involve fluor-xonotlite $Ca_6Si_6O_{17}F_2$. This would have a double chain structure containing important elements of ring symmetry and could arise by a rearrangement of primitive rings in the glass, this accounting for the disappearance of the characteristic ring band at 13 microns. Unfortunately, the infra-red spectrum of xonotlite $Ca_6Si_6O_{17}(OH)_2$ has not been reported.

5.5. Thermal History Effects

The great influence of melt structure and dynamics on the behaviour of the glass is well illustrated by the influence of melt conditions on nucleation kinetics. Figs. 54 to 59 illustrate the influence of increasing the melting time for several glass compositions. Invariably the increase in melting time results in an increase in the "induction" period. This induction period has been

explained in Chapter 3 as arising from the non-uniform distribution of monomers around the nucleus sites. A very short induction period is due to a very large concentration of "monomers" around the embryo and the results above would indicate that this concentration is very much reduced when the glass is melted for a long time, either through a polymerisation-depolymerisation relationship or by the diffusion of monomer units away from the embryo. Both of these mechanisms would be consistent with the establishment of conditions closer to the equilibrium configuration of the melt. The one surprising result is that for the glass heated for 1 hr at 1450°C (Fig 54) which shows that heating at a higher temperature results in an increase of monomer concentration around the nucleus coupled with an increase in nucleation number. This is not expected and can possibly be explained by the onset of platinum dissolution in the glass melt. This may give rise to large heterogeneous nuclei, a large particle would 'see' a greater concentration of monomers. In general however, the results are explicable as reasonable consequences of melt disequilibrium and confirm the importance of melt dynamics for glass crystallisation.

5.6 Miscellaneous Considerations.

An examination of Figs. 25,26,52,53,65 and 68 will reveal several minima in the properties illustrated. These minima always correspond to an alumina to soda ratio of about 1. This behaviour has been observed for several properties, (refractive index, density, infra red absorption) in aluminosilicate glasses containing lithia[14], potassia[15] and soda[16]. However, the changes involved with the present glass compositions are much greater than those observed in [14],[15] and [16]. The authors referred to have ascribed these discontinuities to the appearance of AlO_6 octahedra at alumina to soda ratios greater than one. Tarte has shown[17] that the infra red absorption bands for condensed (i.e. catenated) octahedra should occur at 14.7 to 20 microns and 19 to 25 microns for isolated octahedra. However, the spectra in Figs. 60 and 61 do not reveal any bands in this region. Furthermore this suggestion does not explain the other changes in the spectra. Figs. 65 and 68 show that all the main bands shift to higher frequencies

at this point. It has been stated before that such a shift is indicative of a tendency towards polymerisation. Figs. 25 and 26 show the effects of such a catenation reaction on the crystallisation behaviour of the glasses. The dramatic decrease in the maximum crystallisation of the glass and the less marked decrease in the upward trend for the number of nuclei are indicative of a major rearrangement of the glass structure at this point. This would seem to show that the general phenomenon is associated with the removal of a chain-breaking component from the glass which can only be soda. The compositional invariance of this point shows that the phenomenon involves soda and alumina only. The compound $LiAlO_2$ is known to exist and it is suggested that the observations detailed above may indicate the formation of an unstable compound or complex corresponding to the stoichiometry $NaAlO_2$. The existence of this would depend on the stochiometry being approached and it would be imagined not to exist outside a limited compositional variation. This would account for the apparent, temporary, removal of sodium from its network breaking role. The instability of the compound would preclude its use as a nucleating agent. The nature of this complex and its unusual, vitreous, environment could account for the difference between its main vibrational frequencies ($980\text{-}950cm^{-1}$) and those computed by Tarte[17] for condensed AlO_4 tetrahedra.

5.7. X-ray Diffraction Data.

The x-ray powder patterns of some representative glasses and some reference minerals are contained in the Appendix.

The powder patterns of most of the glasses are very complex and cannot be explained in terms of any one mineral. On the contrary most of the patterns have the appearance of more or less complex mixtures.

The glasses whose patterns are represented on page 130 all displayed both volume and surface crystallisation under the conditions indicated. The most persistent phase in all these glasses appears to be related to xonotlite, $Ca_6 Si_6 O_{17} (OH)_2$ and, if so, must be the fluorine containing analogue $Ca_6 Si_6 O_{17} F_2$. However, the match is by no means perfect. This is to be expected from the x-ray diffraction patterns of calcio-chondrodite and calcio-fluor-chodrodite (page 134., $Ca_5 (SiO_4)_2(OH)_2$ and $Ca_5(SiO_4)_2F_2$) which show that the substitution of fluorine for the hydroxyl radical does not result in a simple shift in d-spacing. If allowance is made for this and the presence of extra reflections, as indicated in the above comparison, the match is seen to be reasonable. Calcium fluoride may also be identified in these glasses, but, all the reflections from this compound are also contained in the proposed pattern for fluor-xonotlite. The possible presence of cuspidine, $Ca_4Si_2O_7F_2$, and $Ca_2 SiO_2 F_2$ is also indicated, and, for the glasses containing aluminium, pseudo-wollastonite, albite and cristobalite, arguing the existence of complex solid-solution series. Comparison of these results with the x-ray patterns of the same glasses heated for prolonged periods at high temperatures (page 132) displays the general stability of these phases and the appearance of a new phase, devitrite.

The glasses which did not display volume crystallisation (page 131) did not contain any detectable amounts of fluor-xonotlite. This shows that flour-xonotlite is probably the nucleating phase, or that it is specifically nucleated within the glass. Xonotlite is composed of a double pyroxene chain and contains pseudo-rings, in accordance with the spectroscipic evidence given above.

In view of the unpredictable nature of the consequences for the x-ray diffraction pattern of a hydrous-silicate mineral of fluorine substitution and the generally complex assemblages of phases within these glasses, the conclusions presented above are tentative and, in some part, speculative. With such complex patterns and the somewhat facile device of explaining differences between reference and observed patterns as the result of fluorine substitution in normally hydrous minerals, it is difficult to avoid the danger of establishing the presence of what is thought to be present rather than that which is present.

References Chapter 5

1. J.O'M Bockris, J.D. Mackenzie, J.A. Kitchener, Trans. Far. Soc., 51, 1734, (1955).
2. P.M. Bills, J. Iron and Steel Inst., 201, 133, (1963).
3. P. Kozakevitch, Physique et Chimie Des Laitiers, Berger Levrault, (1954).
4. B. Keyworth, Ph.D Thesis, University of London (1969).
5. S.P. Mukherjee and P.S. Rogers, Phys. Chem. Glasses, 8, 81-7, (1967).
6. F.J. Padden and H.D. Keith, J. Appl. Phys., 30, 1479, (1959).
7. F.J. Padden and H.D. Keith, J. Appl. Phys., 35, 1270, (1964).
8. J.O'M Bockris and D.C. Lowe, Proc. Roy. Soc., A.226, 423, (1954).
9. C.R. Masson, Proc. Roy. Soc., A.287, 201, (1964).
10. E.D. Lacy, Phys. Chem. Glasses, 6, 171, (1965).
11. G.L. Collier, F. Singleton, J. Appl. Chem., 6, 495, (1956).
12. B.D. Saksena, Trans. Far. Soc., 57 242-58, (1961).
13. P.J. Launer, Amer. Min., 37, 764, (1962).
14. H. Moore and P.W. McMillan, J. Soc. Glass Technol., 40, 97, (1956).
15. E.I. Galant, "Structure of Glass" Vol. 2. Proc. 3rd All Union Conference on Glassy State. Leningrad.
16. D.E. Day and G.E. Rindone, J. Am. Ceram. Soc., 45, 489, (1962).
17. P. Tarte, Spectrochim. Acta., 23A, 2127, (1967).

CHAPTER 6

Conclusions and Suggestions for Further Work

6.1. Conclusions

Despite the deficiencies in the treatment of the experimental results it is clear that the nucleation mechanism can be described by a series of reversible first and second order reactions

$$a_o + m \rightleftharpoons a_1$$

$$a_1 + m \rightleftharpoons a_2 \quad \text{etc.}$$

(a_o, a_1, a_2, being embryos of various sizes, and m representing one molecule of monomer), where the transition from a sub-critical to a critical nucleus is the rate determining step. This approximation was found to be good at low and high temperatures and at long times for all temperatures.

The number of embryos for each glass was shown to be a function of melt conditions and composition, and it has been suggested that these embryos may consist of large, complex silicate or alumino silicate anions. Infra-red spectra of the glasses can be interpreted as arising from a complex mixture of polymeric species and distinct structural elements can be thus identified. The investigation of changes in spectra and spherulite morphology have shown that fluoride additions result in changes in the distribution of the various polymeric species in the glass. These changes result in a reduction of the degree of disorder in the glass and facilitate crystallisation by imposing a more solid-like structure on the glass.

The activation energies for nucleation have been found to bear a close relationship to the activation energies for viscous flow in other, analogous, systems. This is consistent with the role

of fluorine as a network breaker and fluoride additions facilitate nucleation by reducing the average size of the flow unit in the glass and consequently, the activation energy for viscous flow.

No bands have been identified in the infra-red spectra which can be assigned to either Si-F or Al-F bonding. Fluorine must, therefore, displace the melt equilibria towards the production of smaller silicate anions by a mass action or electrostatic effect. This suggestion is closer to the conclusion of Baak and Olander [1] and Bills [2] than to that of Kozakevitch [3]. Electron microscopic examination has shown that there is no relationship between phase separation and nucleation in these glasses. Proof has been presented that suitable embryos exist in the glass in the absence of fluoride thus making it unlikely that the precipitation of a simple fluoride phase is the step initiating crystallisation.

The importance of melt structure and equilibria for crystallisation processes in glasses has been further demonstrated by the influence of melt history on nucleation kinetics. A tentative connection between pre-exponential factors calculated for the nucleation process and the positions of an absorption band in the infra-red spectra has been made. This, together with other spectroscopic evidence suggests that the primary crystallisation may involve a double pyroxene chain as in xonotlite, in accordance with the observations of Mukherjee and Rogers [4]

A discontinuity in properties for these glasses and other aluminosilicate glasses at an alumina to soda ratio of 1 has been explained by the temporary formation of a compound or complex corresponding to a stochiometry of $NaAlO_2$ analogous to the known compound $LiAlO_2$.

Finally, it is suggested that the theoretical treatment outlined in these pages represents a considerable advance on the classical nucleation theories normally used to explain nucleation phenomena in glasses. The theory makes the minimum number of assumptions and provides a reasonable mechanism for phase transformations in general. The theory also provides a reasonable definition of a critical nucleus

which does not rely on problematical considerations of the mechanical equilibria of surfaces. Furthermore the theory is capable of considerable development and, even in its present form, explains the appearance of the "induction period".

6.2. Suggestions for Further Work

It is clear that the necessary regression analyses must be undertaken in order to establish accurate values for the parameters involved in this transition.

The relationship between viscosity and crystallisation is not certain. It is therefore suggested that the activation energies for viscous flow must be determined for the glasses studied here.

The mathematical analysis of the theory must be completed and the theory must be expanded so that it can be applied to other systems. A great deal of work is obviously required concerning the lattice dynamics and other properties of small assemblages of atoms.

Infra red spectroscopy has proved itself to be a valuable tool for the investigation of glass structure. However, the correct application of the technique requires the establishment of a large body of the data concerning the spectra of silicates and siliceous polymers.

The relationship between bandwidth and crystallisation needs further investigation and the changes in the positions of spectral bands on nucleation need codification and explanation. It is also necessary that the relative proportions of the resonating species must be determined most probably by the application of the techniques of derivative spectroscopy (Ref 11 Chap 5). The latter is probably the clue to the successful application of infra-red spectroscopy to glasses and an attempt in this direction is most essential.

The establishment of the nucleation and crystallisation ranges presented some difficulty and it is suggested that these ranges may be better determined, in future work, by the use of a gradient furnace or by differential thermal analysis.

Difficulty was also experienced due to inhomogeneity in the glasses. The homogenisation process used is unsatisfactory and must be replaced.

References to Chapter 6

(1) Tr. Baak, A. Olander, Acta. Chem. Scand., 9, 1350, (1955).

(2) P.M. Bills, J. Iron and Steel Inst., 201, 133, (1963).

(3) P. Kozakevitch, Rev. Met., 51, 569, (1954).

(4) S.P. Mukherjee, P.S. Rogers, Phys.Chem.Glasses, 8, 81, (1967).

Key to Plates

(all transmitted light)

Plate1. Glass 1.0 crystallisation after 1 hr at 708°C and 1 hour at 864°C. Plain polarised light x 32.

Plate 2. Glass 1.1. Crystallisation after .5 hrs at 727°C and 1 hour at 864. Polarised light x 80.

Plate 3. Glass 1.2. 1 hour at 708°C and 1 hour at 864°C Polarised light x 80.

Plate 4. Glass 1.3. 5 hours at 708°C and 1 hour at 864°C Polarised light x 320.

Plate 5. Glass 1.4. 5 hours at 684°C and 1 hour at 864°C Polarised light x 504.

Plate 6. Glass 1.5 .5 hours at 708°C- 1 hr at 864°C. Polarised light x 320.

Plate 7. Glass 1.7 .5 hours at 708°C 1 hour at 864°C Polarised light x 320.

Plate 8, Glass 2.3 4 hrs at 706°C, 5 hrs at 879°C Polarised light X 320.

Plate 9. Glass 2.4. 5 hrs at 706°C, .5 hrs at 879°C. Polarised light x 320.

Plate 10. Glass 2.5. 5 hrs at 706°C, .5 hrs at 879°C. Crossed polars x 320.

Plate 11. Glass 3.2. 4 hrs at 706°C, .5 hrs at 915°C. Polarised light x 320.

Plate 12. Glass 3.3. 5 hrs at 706°C. 5 hrs at 915°C. Polarised light x 320.

Plate 13. Glass 3.4. .5 hrs at 607°C, .5 hrs at 915°C. Polarised light x 80.

Plate 14. Glass 3.5. 3 hrs at 706°C, .5 hrs at 915°C Polarised light x 80.

Plate 15. Glass 3.6. 3 hrs at 505°C, .5 hrs at 915°C Polarised light x 320.

Plate 16. Glass 3.7. .5 hrs at 505°C, .5 hrs at 915°C. Polarised light x 320.

Plate 17. Glass 4.1. 4 hrs at 741°C, .5 hrs at 915°C. Polarised light x 320.

Plate 18. Glass 4.2. 5 hrs at 741°C, .5 hrs at 917°C. Polarised light x 504.

Plate 19. Glass 4.4. 4 hrs at 660°C, .5 hrs at 917°C. Polarised light x 320.

Plate 20. Glass 4.6 .5 hrs at 660°C, .5 hrs at 917°C
Polarised light x 80.

Plate 21. Phase separation in glass 1.0. 11,500 X.

Plate 22. Phase separation in glass 1.1 after 1 hour at 620°C, 10,000X.

Plate 23. Phase separation in glass 1.5 after 1 hour at 720°C, 10,000X.

Plate 24. Phase separation in glass 1.7. 5,500X.

Plate 25. Phase separation in glass 3.0. 21,500X.

Plate 26. Phase separation in glass 3.7 after 1 hour at 620°C. 21,300X.

Plate 27. Phase separation in glass 4.0. 5,300X.

Plate 28. Phase separation in glass 4.1. 5,700X.

Plate 29. Droplets and crystals in glass 1.0 after 4 hrs at 603°C and 1 hour at 864°C. 2,400X.

Plate 30. Detail of Plate 29. 6,000X.

Plate 44. Detail from plate 43. 7,450X.

Plate 45. As for plate 43. 1,400X.

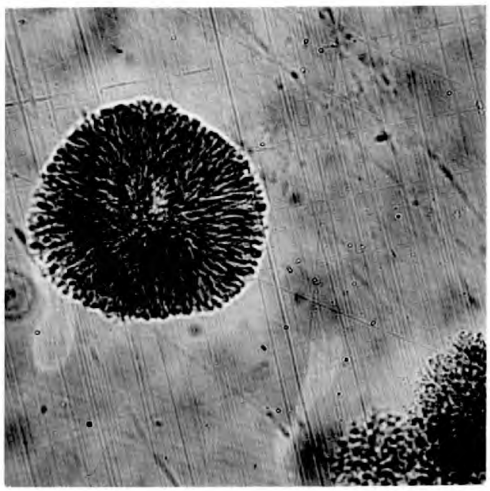
Plate 46. Surface crystallisation in glass 1.4 after 5 hrs at 708°C and 1 hr at 864°C. 2,300X.

Plate 47. As in plate 46. 2,300X.

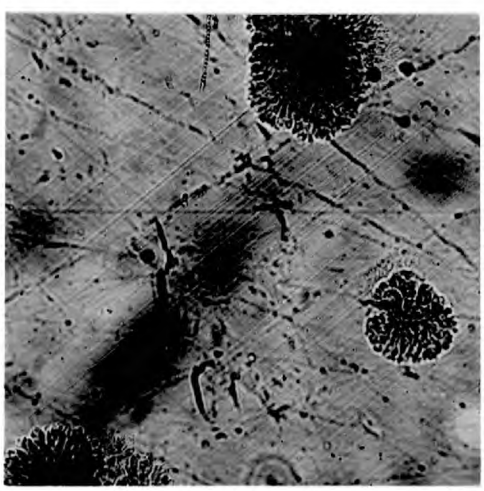
Plate 48. As for plate 46 but the glass was melted for 4 hrs at 1400°C instead of 1 hr. 2,300X.



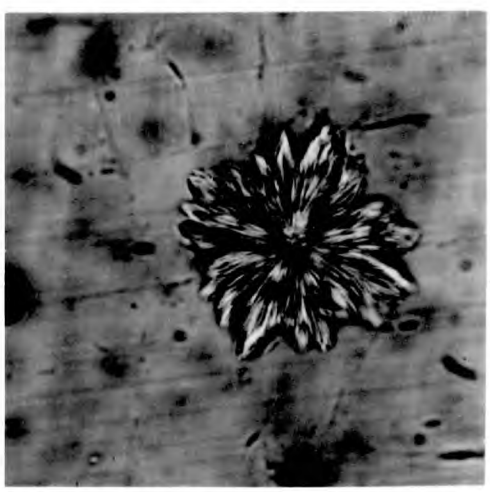
1



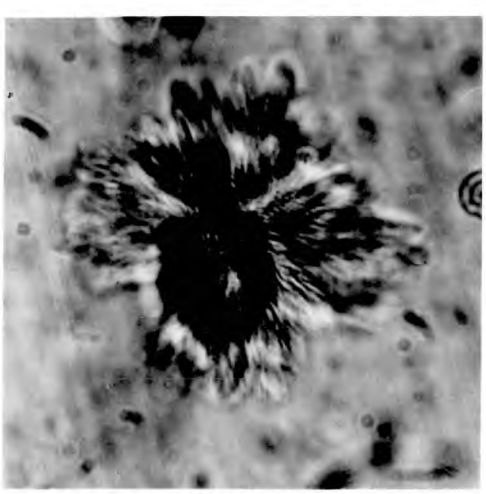
2



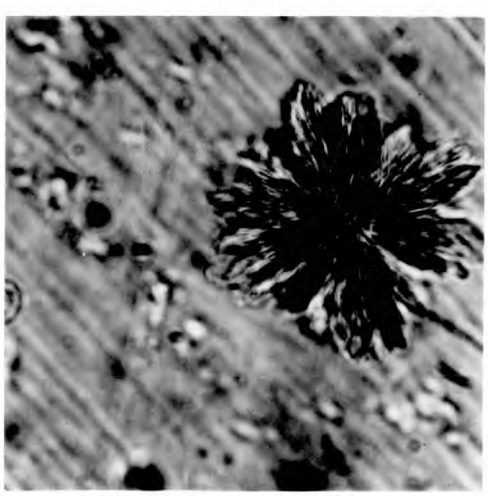
3



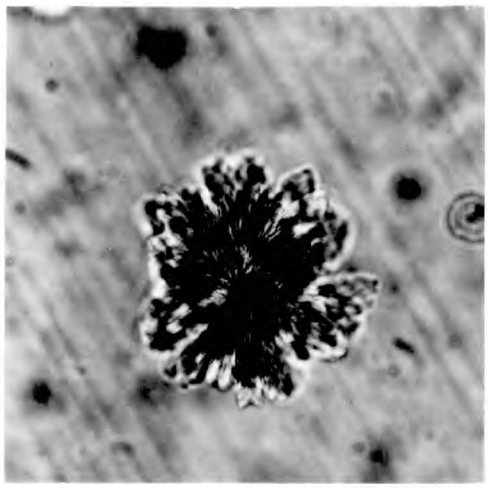
4



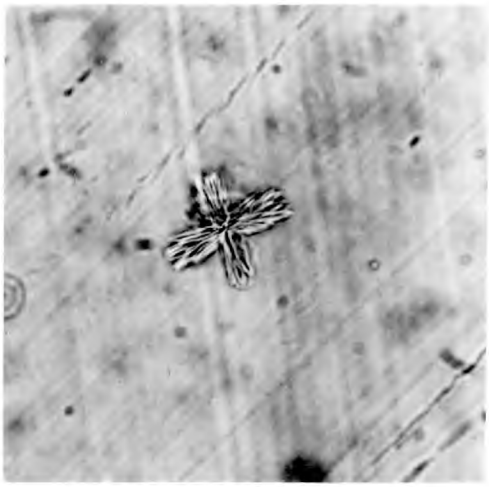
5



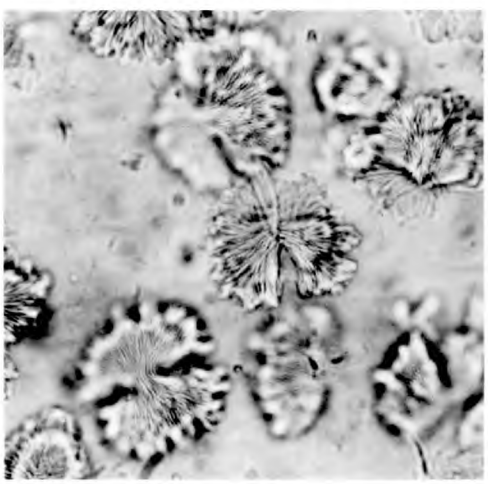
6



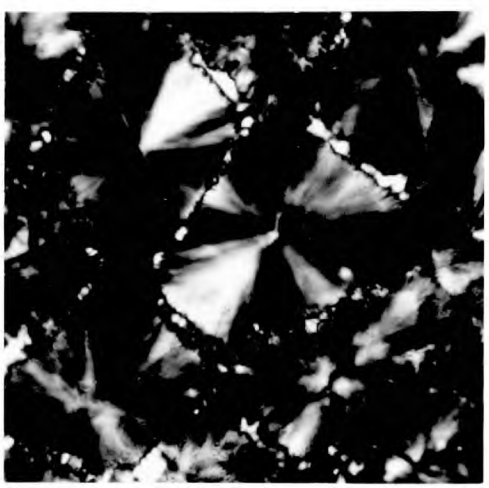
7



8



9



10



11



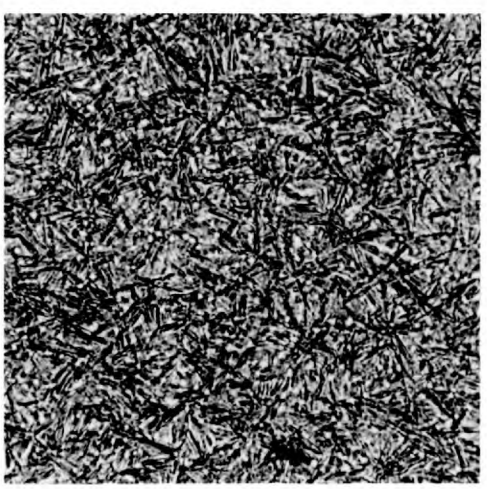
12



13



14



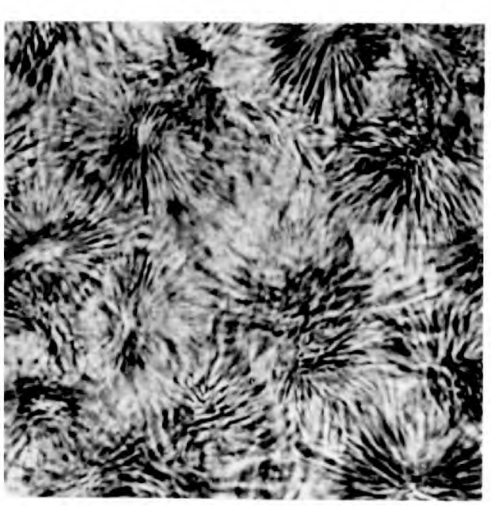
15



16



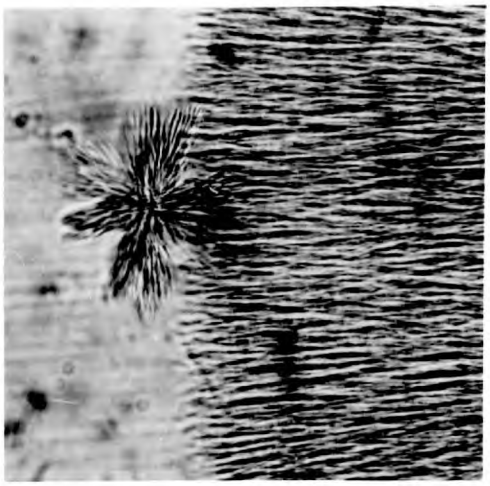
17



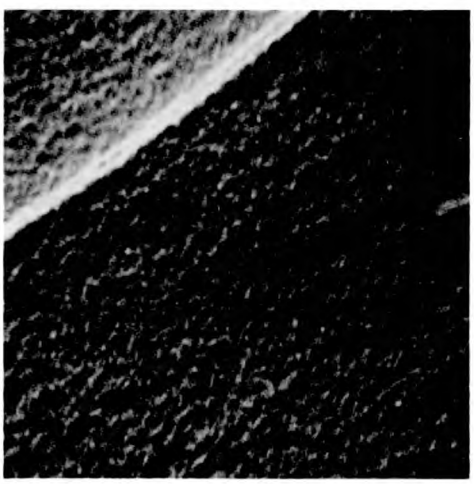
18



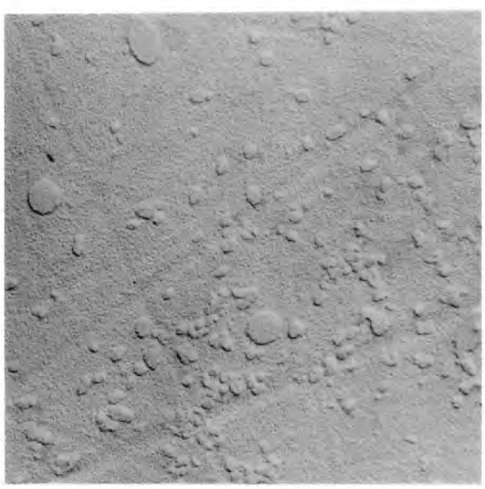
19



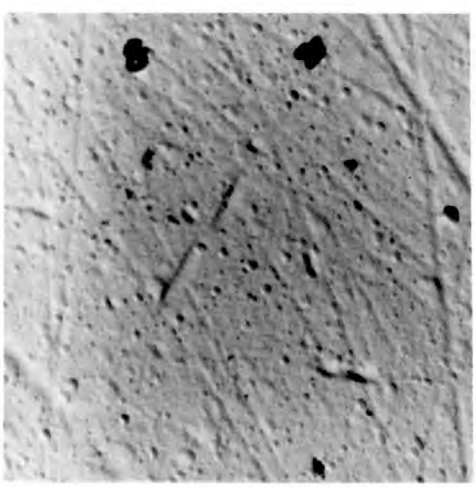
20



21



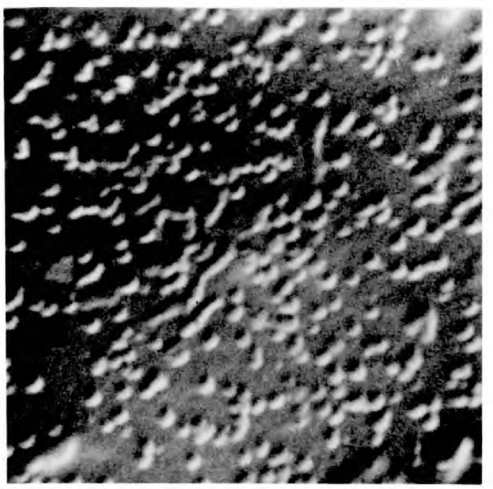
22



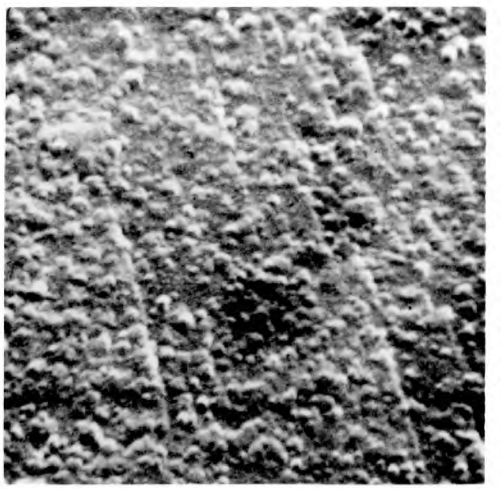
23



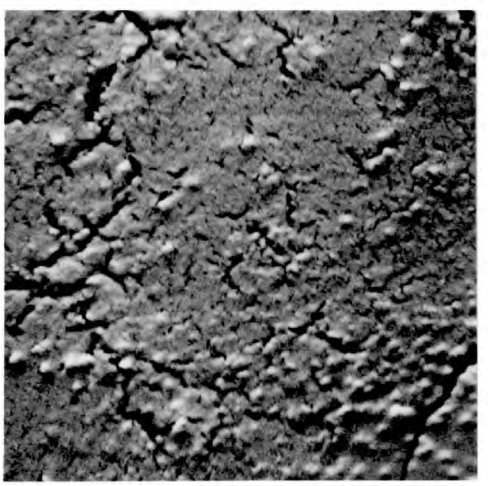
24



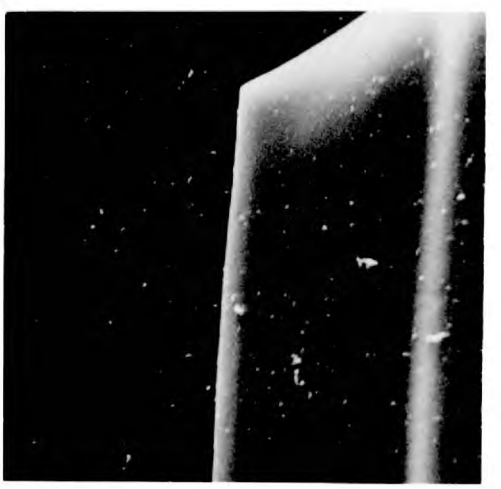
25



26



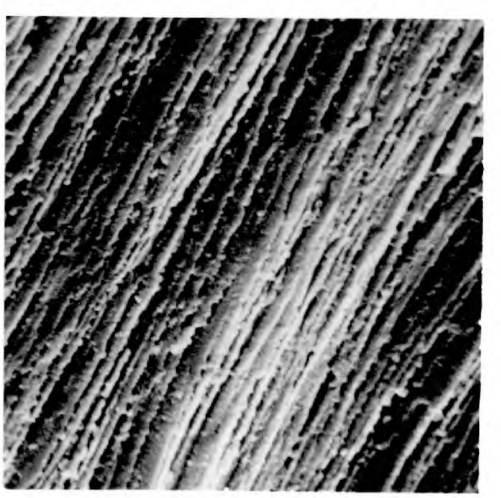
27



28



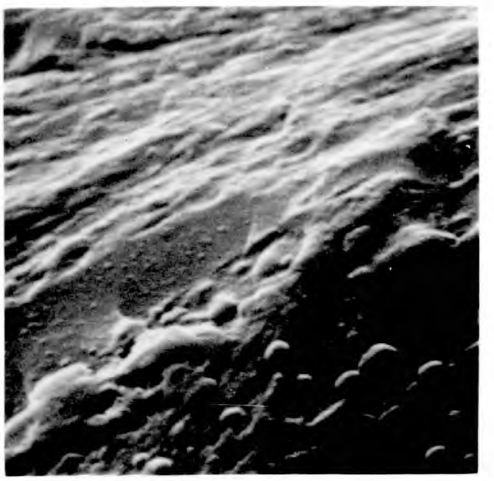
29



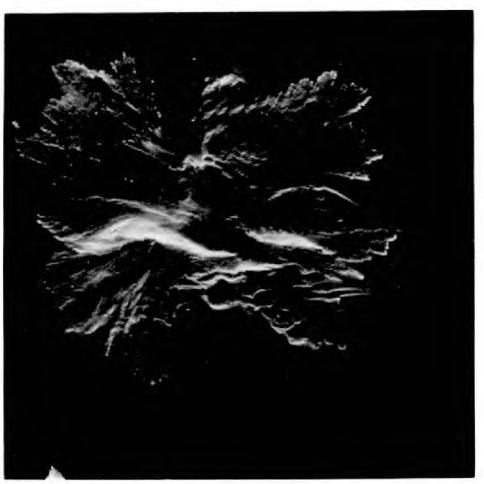
30



31



32



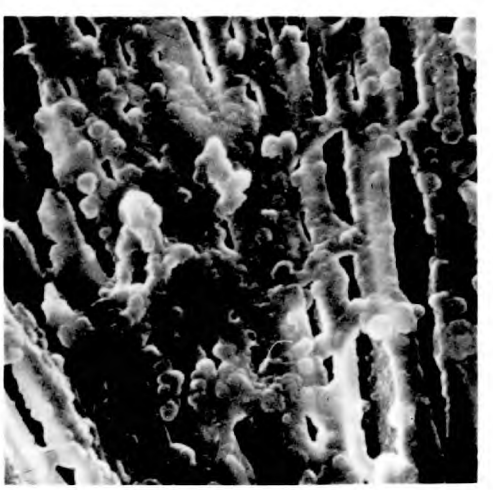
33



34



35



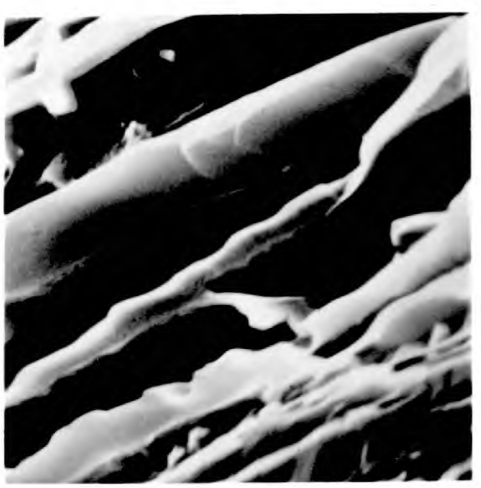
36



37



38



39



40



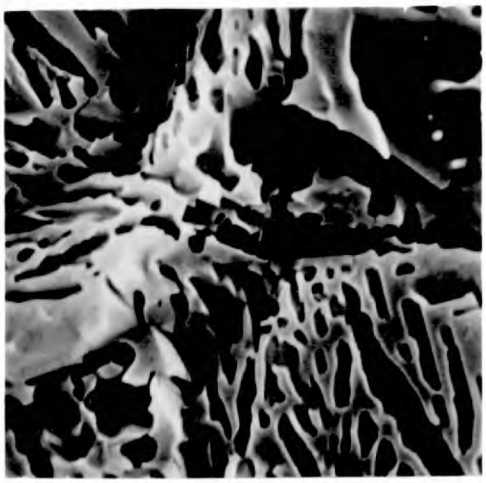
41



42



43



44



45



46



47



48

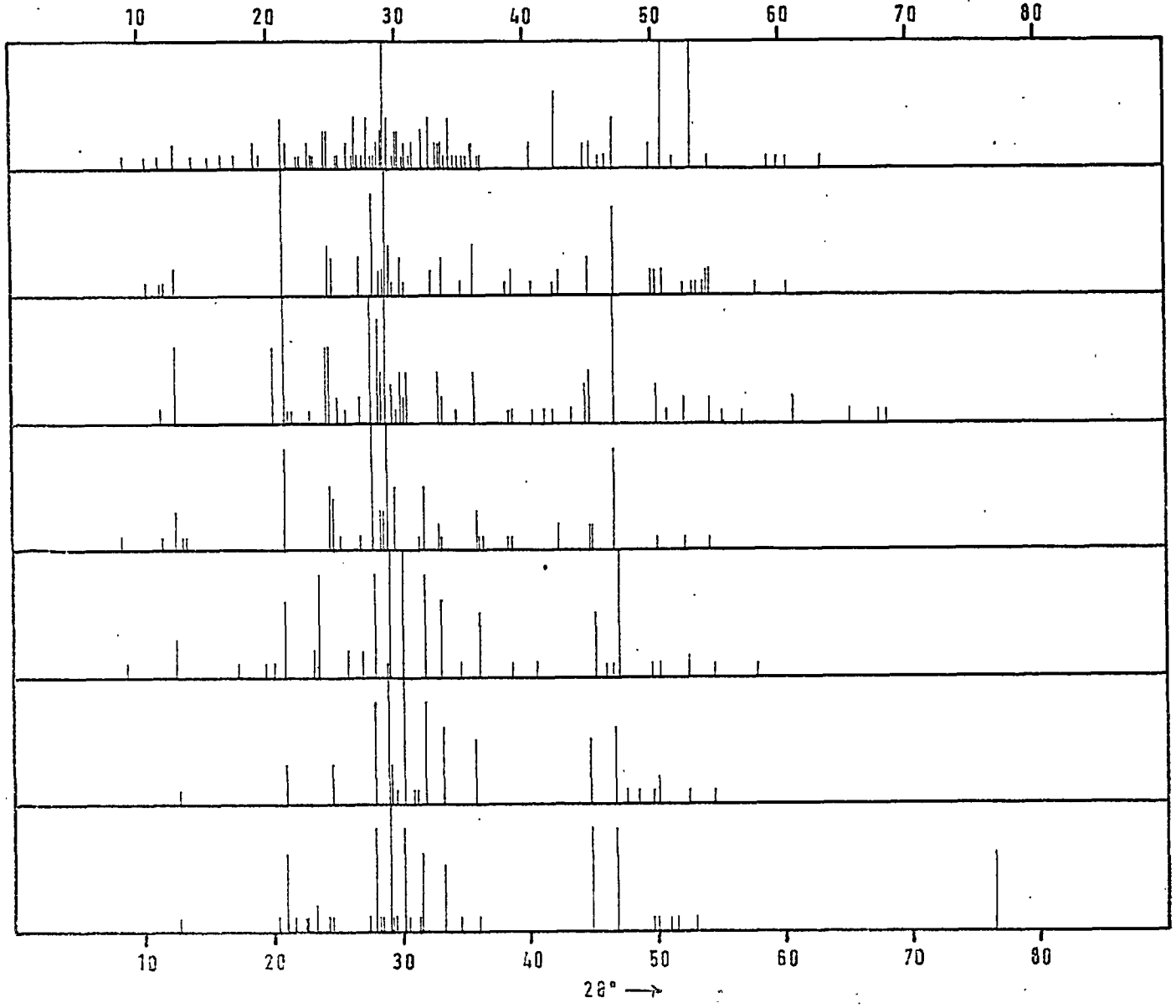
Appendix

This appendix contains X-ray powder diffraction patterns of some representative glasses and some reference crystalline phases.

The x-ray photographs from which the glass patterns were derived were taken on a Guinier de Wolff focusing x-ray camera using Cu $K\alpha$ radiation at 30 KV. and 20 mA. with exposure times of 2.5 to 3.5 hours.

The positions of the observed reflections are plotted as values of $2\theta^{\circ}$. The relative intensities of the reflections, I/I_o, were estimated visually.

The powder patterns for the reference crystalline phases were obtained from the A.S.T.M. Index and are similarly represented.



Glass 1.0 4 Hrs. 684°C/ 1 Hrs. 864°C

Glass 1.1 .. ..

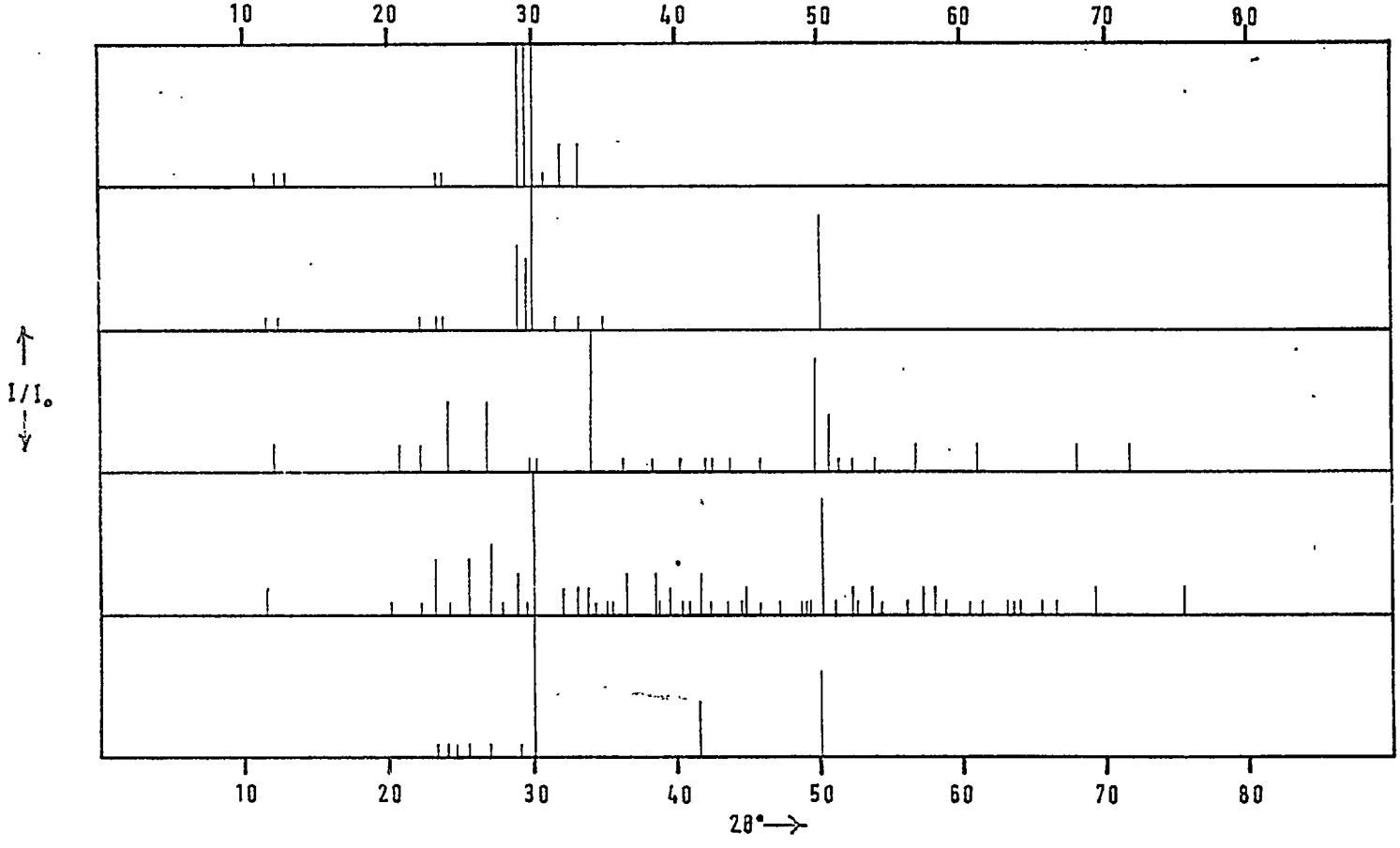
Glass 1.2 3 Hrs. .. ..

Glass 1.3 5 Hrs. .. ..

Glass 1.4 5 Hrs. 708°C/ 1 Hr. 864°C

Glass 1.5 5 Hrs. 708°C/ 1 Hr. 864°C

Glass 1.7 5 Hrs. 727°C/ 1 Hr. 864°C



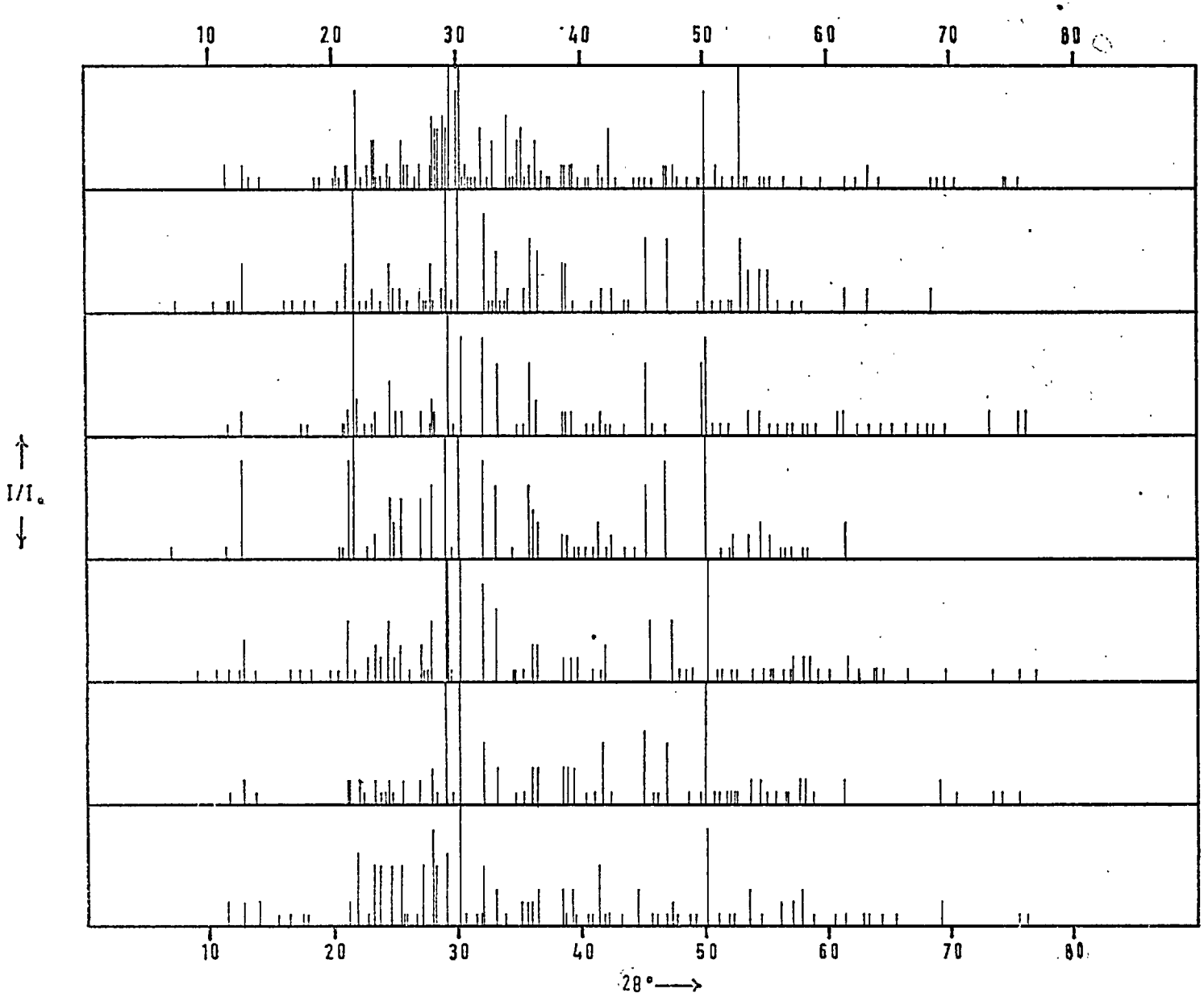
Glass 2.1 5Hrs.706°C/-5Hrs.879°C

Glass 2.2 ,, ,, ,, ,,

Glass 3.0 5Hrs.746°C/-5Hrs.915°C

Glass 3.1 ,, ,, ,, ,,

Glass 4.0 5Hrs.810°C/-5Hrs.917°C



Glass 1.0 10 Days at 900°C

Glass 1.1 .. ..

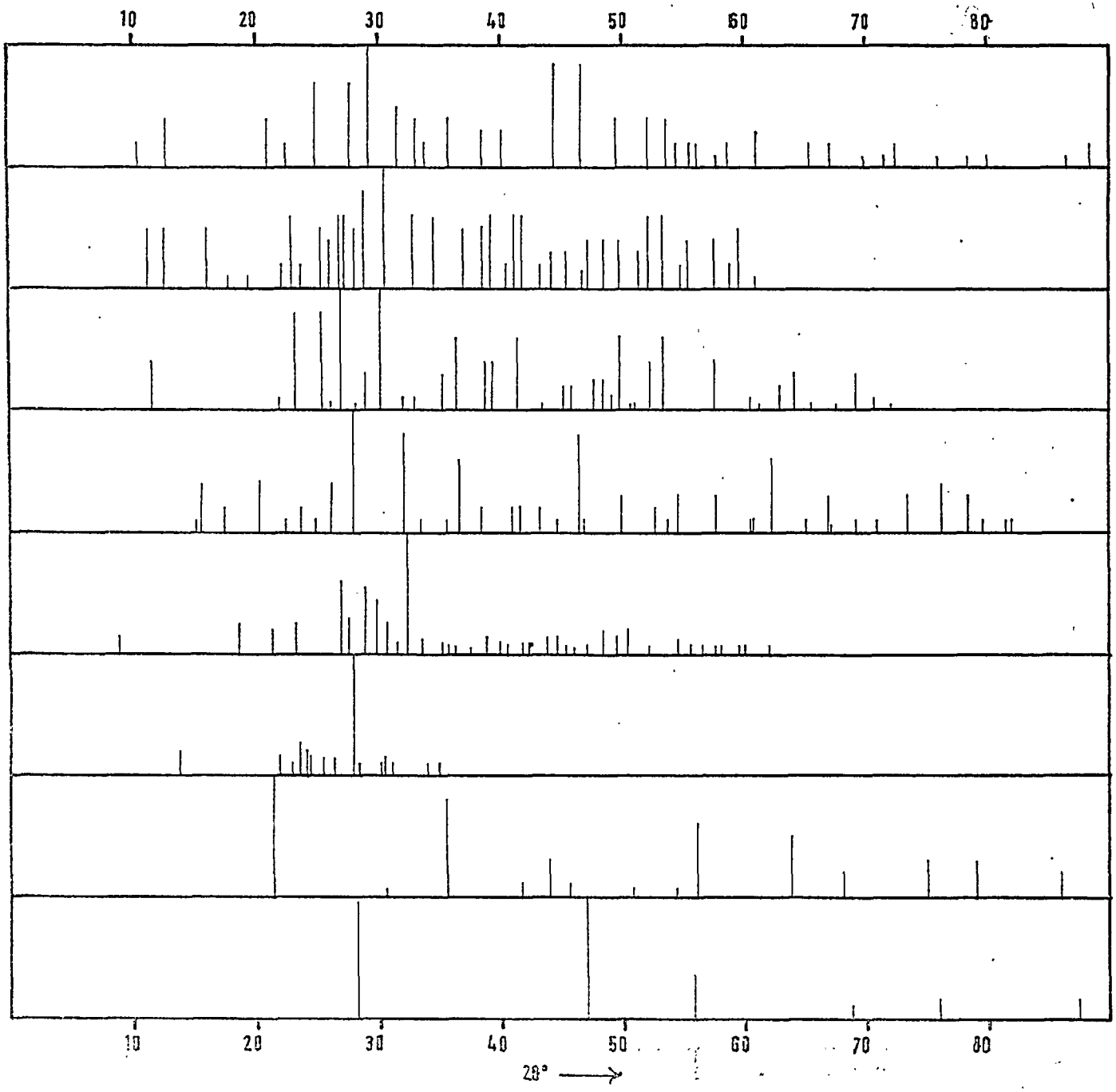
Glass 1.2 .. ..

Glass 1.3 .. ..

Glass 1.4 .. ..

Glass 1.5 .. ..

Glass 1.7 .. ..



Xonotlite A.S.T.M. 10–488
$Ca_6Si_6O_{17}(OH)_2$

Pectolite A.S.T.M. 12–238
$NaCa_2Si_3O_8OH$

Wollastonite A.S.T.M. 10–487
$CaSiO_3$

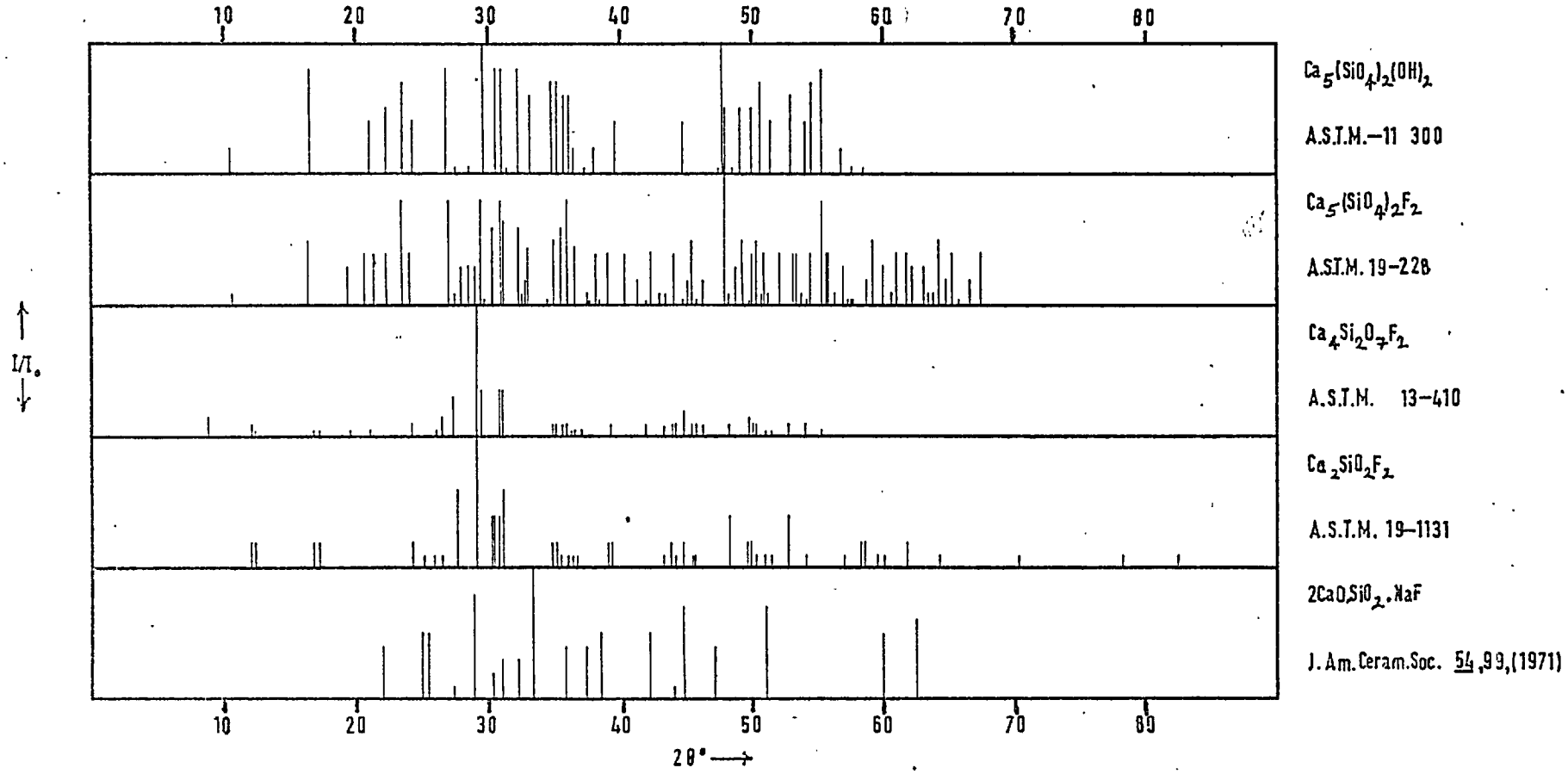
Pseudowollastonite A.S.T.M. 10–486

Devitrite A.S.T.M. 16–690
$Na_2Ca_3Si_6O_{16}$

Albite A.S.T.M. 10–393
$NaAlSi_3O_8$

Cristobalite A.S.T.M. 4–0359
SiO_2

CaF_2


10
20
30
40
50
60
70
80
I/I₀
2θ°
Ca5(SiO4)2(OH)2
A.S.T.M.—11 300
Ca5(SiO4)2F2
A.S.T.M. 19-228
Ca4Si2O7F2
A.S.T.M. 13-410
Ca2SiO2F2
A.S.T.M. 19-1131
2CaO.SiO2.NaF
J. Am. Ceram. Soc. 54,99,(1971)

Acknowledgement

I wish to express my thanks J.A. Joblings & Co Ltd., for their financial support during this work and, in particular, Mr.D.M.C. Thomas and Mr. S. Scholes for their kind and courteous treatment during my visits to the research unit of that company at Brancepeth Castle.

My greatest debt of gratitude is due to my supervisor Dr. P.S. Rogers for his help, encouragement, and guidance throughout this work.

I am greatly indebted to Dr. J.A. Kitchener of the Department of Mineral Technology for the use of the infra-red spectrometer and to the members of his research group for many entertaining discussions.

Thanks are due to Dr. J. Williamson, for his ready help and friendship, to Drs. Spencer, Fairweather and Keyworth, my erstwhile companions in adversity, and Mr. C.E. Taylor for their continual friendship and the pleasure of their company, and to all the members of the Nuffield Group who have eased my burden and expedited the completion of this work.

Finally, I am humbly thankful to my dear wife, Lynda, who has had so much to put up with and has born the stresses of the past years with such stoicism, for her support and for the preparation of all the illustrations in this volume.

P.E. Johnson.

P.E. Johnson,
February 1971.